DEALING WITH UNCERTAINTY IN ENGINEERING AND MANAGEMENT PRACTICES

A Thesis

Submitted to the Faculty of Graduate Studies and Research
in Partial Fulfillment of the Requirements
for the Degree of
Doctor of Philosophy
in Engineering
University of Regina

by
Wei Peng
Regina, Saskatchewan
July, 2011

UNIVERSITY OF REGINA

FACULTY OF GRADUATE STUDIES AND RESEARCH

SUPERVISORY AND EXAMINING COMMITTEE

Wei Peng, candidate for the degree of Doctor of Philosophy in Engineering**,** has presented a thesis titled, ***Dealing With Uncertainty in Engineering and Management Practices,*** in an oral examination held on March 11, 2011. The following committee members have found the thesis acceptable in form and content, and that the candidate demonstrated satisfactory knowledge of the subject material.

External Examiner:	Dr. Keith W. Hipel, University of Waterloo
Supervisor:	Dr. Rene V. Mayorga, Industrial Systems Engineering
Committee Member:	Dr. Mehran Mehrandezh, Industrial Systems Engineering
Committee Member:	Dr. Amr Henni, Industrial Systems Engineering
Committee Member:	Dr. Dianliang Deng, Department of Mathematics & Statistics
Chair of Defense:	Dr. Phillip Hansen, Department of Philosophy & Classics

*Not present at defense

ABSTRACT

A set of methodologies is proposed for dealing with uncertainties in five fields. These fields are: (1) traffic noise impact assessment, (2) hydraulic reliability assessment and reliability based optimization, (3) binary linear programming, (4) real-time multiple source water blending optimization, and (5) process control of an industrial rotary kiln. The proposed methods are applied to several engineering and management cases to demonstrate their explicabilities and advantages.

In the field (1), an integrated approach is presented to assess traffic noise impact under uncertainty (Peng and Mayorga, 2008). Three uncertain inputs, namely, traffic flow, traffic speed and traffic components, are represented by probability distributions. Monte Carlo simulation is performed to generate these noise distributions. Further, fuzzy sets and binary fuzzy relations are employed in the qualitative assessment. Finally, the quantification of noise impact is evaluated using the probability analysis.

In the field (2), two innovative approaches are developed under uncertainty (Peng and Mayorga, 2010e). One is to assess hydraulic reliability that accounting for the deterioration of both structural integrity and hydraulic capacity of each pipe; another is to design a reliability-based optimal rehabilitation/upgrade schedule that considering both hydraulic failure potential and mechanical failure potential. In these two approaches, all uncertain hydraulic parameters are treated as random values. The main methodologies used are: Monte Carlo simulation, EPANET simulation, genetic algorithms, Shamir and Howard's exponential model, threshold break rate model, and two-stage optimization model. Eventually, two universal codes, the hydraulic reliability assessment code and the long-term schedule code, were written in MATLAB and linked with EPANET.

In the field (3), an interval coefficient fuzzy binary linear programming (IFBLP) and its solution are built under uncertainty (Peng and Mayorga, 2010c, 2010d). In the IFBLP, the parameter uncertainties are represented by the interval coefficients, and the model structure uncertainties are reflected by the fuzzy constraints and a fuzzy goal. The solution includes a defuzzification process and a crisping process. An alpha-cut technique is utilized for the defuzzification process, and an interval linear programming algorithm is used to the crisping process. One mixed technique (links the alpha-cut technique and min-operator technique) is used to determine a single optimal alpha value on a defuzzified crisp-coefficient BLP. Finally, the IFBLP is converted into two extreme crisping BLP models: a best optimum model and a worst optimum model**.**

Uncertainties in the field (4) include the modeling uncertainty and dynamic input uncertainty (Peng et al, 2010a, 2010b). This dissertation provides a fuzzy multiple response surface methodology (FMRSM) to deal with these kinds of uncertainties. In the FMRSM, the experimental data sets are fitted into the first quadratic models and their residuals are fitted into the second quadratic models; the multiple objectives are optimized using a fuzzy optimization method. Six scenarios are designed based on a real-time operation. The results show the FMRSM is a robust, computational efficient and overall optimization approach for the real-time multi-objective nonlinear optimization problems.

In the field (5), a dual-response-surface-based process control (DRSPC) programming is developed to address the uncertainty and dynamic calcination process (Peng, et al, 2010f). Several response surface models are appropriately fitted for an industrial rotary kiln. The proposed approach is applied on a real case. The application shows that the proposed approach can rapidly provide the optimal and robust outputs to the industrial rotary kiln. Other properties of the proposed approach include a solution for the time delay problem and a statistical elimination of measurement errors.

ACKNOWLEDGEMENTS

I want to express my sincere appreciation to my supervisor, Dr. Rene V. Mayorga. I would like to thank him for his extremely helpful guidance, support, and encouragement and for lending his wisdom, knowledge, and experience. The countless hours he spent guiding both my writing and research efforts have been extremely helpful for the successful completion of this dissertation as well as for my future career ambitions.

I would also like to express my gratitude to my committee members, Drs. A. Henni, M. Mehandezh, and D. Deng, for their insightful suggestions, which were helpful for improving this dissertation.

I gratefully acknowledge the Faculty of Graduate Studies and Research and the Faculty of Engineering and Applied Science at the University of Regina, for providing research scholarships and teaching fellowships for my Ph.D. study.

My further appreciation goes to my friends for their assistance in various aspects of my research and for their support with constant friendship. They include Dr. Syed Imran, Dr. Ming Zhong, Dr. Yuefei Huang, Dr. Yafei Hu and many others.

Finally, I would particularly like to express my gratitude to my entire family for their affection and moral support. My parents in China, Peng Guangmin and Zhang Fanxiang, have always been supportive of my ambitions and have encouraged me to chase my dreams. I would like to thank my wife, Ting Hu, for always pressing me to perform to the best of my abilities. Her sacrifices, love, and steadfast support have brought about all of my success. I am also grateful to my sons, Arthur Peng and Allen Hu, for bringing me many joys during the course of my Ph.D. study.

POST-DEFENCE ACKNOWLEDGEMENTS

I want to express my appreciation to External Examiner, Dr. Keith W. Hipel. I would like to thank him for his insightful suggestions that were helped to improve my dissertation work, and for lending his wisdom, knowledge, and experience.

I would like to thank Chair, Dr. Philip Hansen, for his guidance during my oral examination.

TABLE CONTENTS

ABSTRACT I

ACKNOWLEDGEMENTS III

POST-DEFENCE ACKNOWLEDGEMENTS IV

LIST OF FIGURES XII

LIST OF TABLES XIV

CHAPTER 1 ..... …..1

Introduction 1

1.1. Background 1

1.2. Challenges of dealing with uncertainty in environmental impact assessment 3

1.3. Challenges of dealing with uncertainty in hydraulic reliability analysis and reliability based optimization 5

1.4. Challenges of dealing with uncertainty in binary linear programming 6

1.5. Challenges of dealing with uncertainty in real-time multiple source water blending optimization 8

1.6. Challenges of dealing with uncertainty in the process control of industrial rotary kilns 10

1.7. Objectives 11

CHAPTER 2 14

Literature Review 14

2.1. Uncertainty expression 14

2.1.1. Probability distribution 14

2.1.2. Fuzzy set and fuzzy number 17

2.1.3. Interval value 18

2.2. Modeling under uncertainty 18

2.2.1. Linear model 19

2.2.1.1. Binary linear model 19

2.2.2. Response surface model 20

2.2.3. Nonlinear model 21

2.2.3.1. Traffic noise prediction model 22

2.2.3.2. Hydraulic Empirical model 22

2.2.3.3. Water quality models for water blends 24

2.2.3.4. Phenomenological models for the process control of rotary kiln 24

2.3. Mathematical approaches for dealing with uncertainty 26

2.3.1. Monte Carlo simulation 26

2.3.2. Fuzzy mathematical programming 27

2.3.3. Interval programming 30

2.3.4. Dual response surface optimization 32

2.3.5. Genetic algorithm 34

2.4. Summary 35

CHAPTER 3 38

Assessing Traffic Noise Impact Based on Probabilistic and Fuzzy Approaches under Uncertainty 38

3.1. Statement of problems 38

3.2. Methodology 41

3.2.1. Traffic noise prediction model 41

3.2.2. Stochastic simulation 47

3.2.3. Integrated fuzzy theory assessment 50

3.2.3.1. Fuzzy sets and binary fuzzy relations 52

3.2.3.2 Application of fuzzy theory for qualitative analysis 54

3.2.4. Quantification of noise impact 61

3.3. Case study 62

3.4. Summary 70

CHAPTER 4 70

Hydraulic Reliability Assessment and Optimal Schedule of Rehabilitation and Upgrading in Water Distribution Systems under Uncertainty 72

4.1. Statement of problems 72

4.2. Methodology 75

4.2.1. Hydraulic reliability assessment 75

4.2.1.1. Nodal hydraulic failure probability 76

4.2.1.2. Mechanical failure probability 79

4.2.1.3. System hydraulic reliability assessment 80

4.2.2. Optimal rehabilitation & upgrade schedule 80

4.2.2.1. Rehabilitation optimization model 82

4.2.2.2. Upgrade optimization model 83

4.2.2.3. Optimization procedure 86

4.3. Example 93

4.4. Summary 95

CHAPTER 5 104

A Mixed Approach to Settle Uncertainties in Binary Linear Programming 104

5.1. Statement of problems 104

5.2. Methodology 107

5.2.1. Defuzzification process 108

5.2.1.1. α-cut technique approach 109

5.2.1.2. Min-operator approach 110

5.2.1.3. The link of two methods 111

5.2.2. Crisping process 114

5.2.2.1. Value range of α^* 115

5.2.2.2. Solution for interval-coefficient BLP 117

5.2.2.3. Monte Carlo simulation for boundary values of α^* 119

5.2.2.4. A mathematical approach for boundary values of α^* 120

5.2.2.5. The best and the worst optimum models 124

5.3. Application 132

5.3.1. Site information 132

5.3.2. Traffic noise control techniques 132
5.3.2.1. Three traffic noise control methods 132
5.3.2.2. Noise Abatement Criteria (NAC) 133
5.3.2.3. Traffic noise prediction 133
5.3.3 Build the IFBLP model 134
5.3.4 Solve the IFBLP model 136
5.3.5. Results 138
5.4. Summary 139
CHAPTER 6 145
A Robust Optimization Approach for Real-time Multiple Source Water Blending Problem under Uncertainty 145
6.1. Statement of problems 145
6.2. Methodology 148
6.2.1. Dual-RSM 148
6.2.2. Min-operator 149
6.2.3. FMRSM programming 151
6.3. Modeling 153
6.3.1. Quadratic polynomial models 154
6.3.2. Membership function design 159
6.3.2.1. Corrosion models 159
6.3.2.2. Residual models 160
6.3.3. Scenario design 167
6.4. Results and Discussion 170

6.4.1. FMRSM vs. Fuzzy RSOP 170
6.4.2. Nonlinear model based optimization 172
6.4.3. Fuzzy RSOP vs. weighted-objective RSOP 173
6.5. Summary 174
CHAPTER 7 181
Dual-Response-Surface-Based Process Control to an Industrial Rotary Kiln under Uncertainty 181
7.1. Statement of problems 181
7.2. Methodology 185
7.2.1. Data acquisition 185
7.2.2. Fitting response surface models 189
7.2.3. Optimization control 191
7.3. Proposed approach application 193
7.3.1. Overview of the study rotary kiln 193
7.3.2. Variable design 194
7.3.3. Response surface models 196
7.3.4. Results and discussion 198
7.4. Summary 199
CHAPTER 8 208
Conclusions and Recommendations 208
8.1. Summary 208
8.2. Research achievements 211
8.3. Recommendations for future research 214

REFERENCES..... 216

APPENDIX 1..... 240

MATLAB Code for Hydraulic Reliability 240

APPENDIX 2..... 247

MATLAB Code for Repair Schedule 247

LIST OF FIGURES

Figure 1-1 Key uncertainties of the five studying fields..... 13

Figure 2-1 Prevous studies to uncertainty..... 37

Figure 3-1 The FHWA highway traffic noise prediction model 43

Figure 3-2 The fuzzy noise abatement criteria..... 57

Figure 3-3 The comparison of the probability distribution and fuzzy noise abatement criteria..... 58

Figure 3-4 The noise impact assessment procedure..... 59

Figure 3-5 The cumulated hourly traffic flow 64

Figure 3-6 The histogram result of scenario 1 65

Figure 3-7 The histogram result of scenario 2 66

Figure 3-8 The histogram result of scenario 3 67

Figure 4-1 The flowchart of system hydraulic reliability 89

Figure 4-2 the procedure of system hydraulic reliability assessment 90

Figure 4-3 The flowchart of two-stage method 91

Figure 4-4 Example of the distribution system..... 92

Figure 5-1 The study road sketch..... 125

Figure 5-2 The predicted noise level at the zone #11 141

Figure 5-3 The predicted noise level for the future 10th year 142

Figure 6-1 The membership function of corrosion model 162

Figure 6-2 The membership function of the corrosion model with L = 0 163

Figure 6-3 The normal distributions for the residuals of iron, copper and lead 164

Figure 6-4 The membership function of residual model 165

Figure 6-5 The column chart of the ratio of optimal metal corrosion and permitted level --the weighted-objective RSOP 179
Figure 6-6 The column chart of the ratio of optimal metal corrosion and permitted level--the fuzzy RSOP 180
Figure 7-1 Sketch of an industrial rotary kiln 184

LIST OF TABLES

Table 3-1 Noise abatement criteria (NAC)—hourly A-weighted sound level in dBA 51
Table 3-2 Example of the use of noise zones (day/night) 56
Table 3-3 Traffic record on the study site (May 17, 2004) 63
Table 4-1 Node information 96
Table 4-2 Pipe information 97
Table 4-3 Tank information 98
Table 4-4 Weighting coefficients 99
Table 4-5 Results of the reliability assessment 100
Table 4-6 Costs of different pipe diameters 101
Table 4-7 Threshold break rate and replacement timing (discount rate =0.06) 102
Table 4-8 The optimal repair schedule 103
Table 5-1 Noise correction factors of pavements (dBA) 126
Table 5-2 Noise reduction deterioration of OGA 127
Table 5-3 The Interval values of NAC (dBA) 128
Table 5-4 26 study zones identification 129
Table 5-5 Five sections information 130
Table 5-6 The pavement repaving and maintenance costs (1000 Dollar) 131
Table 5-7 Results of the IFBLP 143
Table 5-8 Solution of the IBLP 144
Table 6-1 Water quality of the source waters 166
Table 6-2 Results of the FMRSP in various scenarios 176

Table 6-3 Results of the fuzzy RSOP in various scenarios 177

Table 6-4 Results of the weighted-objective RSOP 178

Table 7-1 A portion of the recorded data 101

Table 7-2 Statistical results of the recorded data 102

Table 7-3 Results for variations of the weighted coefficients 203

Table 7-4 Results for a variety of scenarios when w_1=1000, w_2=*1*, and w_3 =*1* 204

Table 7-5 Results for a variety of scenarios when w_1=100, w_2=*1*, and w_3 =*1*. 205

Table 7-6 Results for a variety of scenarios when w_1=10, w_2=*1*, and w_3 =*1*. 206

Table 7-7 Results for a variety of scenarios when w_1=1, w_2=*1*, and w_3 =*1*. 207

CHAPTER 1

Introduction

1.1. Background

To scientists and engineers, dealing with uncertainty is almost second nature. They would not report an experimental result without an associated estimate of uncertainty, nor would they design a new product without giving careful attention to uncertainties (Morgan and Henrion, 1990).

Uncertainty is a capacious term, used to encompass a multiplicity of concepts. It might arise because of incomplete information: how much water will this city's inhabitants demand in the year 2020? It might arise from imprecision information: the traffic flow on this road is from 200 to 600 per hour; the water demand of this city is about 10,000 tons per day. It might arise from the variability of impact factors: the water quality in this river changes with temperature fluctuations.

In academic research and engineering application, uncertainty exists in various forms:

(1) It exists in parameters. Impact factor is one type of parameter, for example, in which the values of the major traffic noise impact factors are uncertain. In practice, parameter uncertainty can be previously measured and quantified and then steadily used in mathematical models. For instance, the uncertain traffic speed can be expressed as a beta distribution; the uncertain vehicle components can be represented by a normal distribution (Lam and Tam, 1998). Parameter uncertainty includes inherence uncertainty

and measurement uncertainty. Noise generated from a vehicle has inherence uncertainty; noise measured at one reception point has measurement uncertainty. The inherence uncertainty can be quantified by a continued probability distribution; it is non-reducible. The measurement parameter uncertainty can be quantified by a discrete probability distribution. It might arise from random error in direct measurements and from the systematic error of biases in the measuring apparatus and experimental procedure. For the random error, the resulting uncertainty depends on the size of the variations between observations and the number of observations taken. A variety of techniques are provided for quantifying this measurement parameter uncertainty, such as standard deviation, confidential intervals, and fuzzy membership values. For the systematic error, the uncertainty may be reduced by careful pre-design, careful calibration of the measurement apparatus and procedure, and careful analysis.

(2) Uncertainty might arise from modeling. This is because a model is only a simplified version of the real-world system being modeled. For example, there is a discrepancy between the modeled traffic noise and measured traffic noise. Modeling uncertainty can be reduced by a more precise model, e.g., a nonlinear model or differential model, or by some mathematical programming, e.g., a flexible linear programming.

(3) Uncertainty exists in dynamic input. For example, in a real-time water blending optimization, the dynamic inputs of water quality are uncertain due to the fluctuation of ambient temperature. This type of uncertainty cannot be directly reduced through a mathematical method, but can be reflected dynamically by a rapid responding mathematical model and then to be fast treated. It is worth mentioning that some

researchers believe that dynamic input will result in variability not uncertainty (EPA, 1997). However, a number of academic debates exist on it (Kaplan and Garrick, 1981; Morgan and Henrion, 1990). This dissertation treats dynamic input as an uncertain value.

Therefore, this dissertation focuses on three types of uncertainty: parameter uncertainty, modeling uncertainty and dynamic input uncertainty. It is found that (1) the major uncertainties in environmental impact assessment and hydraulic reliability assessment and reliability based optimization are parameter uncertainty and modeling uncertainty, (2) both parameter uncertainty and modeling uncertainty profoundly affect the result of a binary linear programming, and (3) dynamic uncertainty, parameter uncertainty, and modeling uncertainty make it extremely difficult to solve a real-time multiple source water blending optimization problem and the process control problem in an industrial rotary kiln. This dissertation develops several integrated approaches and cross-sectional plans to deal with these types of uncertainties in environmental impact assessment, hydraulic reliability assessment and reliability based optimization, binary linear programming, real-time multiple source water blending optimization and process control of an industrial rotary kiln.

1.2. Challenges of dealing with uncertainty in environmental impact assessment

The International Association for Impact Assessment (IAIA) defines environmental impact assessment (EIA) as "the process of identifying, predicting, evaluating and mitigating the biophysical, social, and other relevant effects of development proposals prior to major decisions being taken and commitments made"

(IAIA, 1999). EIA is often viewed in terms of four elements: (1) impact factor identification, which is to determine what factors can cause adverse environmental effects and to collect relative data, (2) modeling, which is to characterize the relationship between the impact factors and the incidence of environmental effects, (3) implementing simulation (or prediction), which is to do forecasting in some cases that may support the operational decisions to be made, and (4) evaluation, which is to estimate the incidence of environmental effects under various conditions.

Uncertainties of environmental impact assessment contain parameter uncertainty and modeling uncertainty. As mentioned above, the modeling uncertainty can be reduced by a precise model, such as a differential or exponential model. However, the parameter uncertainty might not be reducible if it is inherent (the inherent uncertainty). In a traffic noise impact study, for example, the impact factors (including traffic flow, traffic speed, and vehicle components.) have, by nature, uncertainties that cannot be expressed by certain values, even if their measurement uncertainties were reduced to zero. Moreover, their uncertain values have different numerical expressions. The previous studies identified the traffic speed as being subjected to a Beta distribution, and the traffic composition, which in terms of the percentage of heavy vehicles, was subjected to a normal distribution (Lam and Tam, 1998). Additionally, uncertainty exists in the degree of noise impact on human beings since different individuals have different noise perception levels.

Many problems might arise from these uncertainties (Peng and Mayorga, 2008). For example, in order to obtain the distribution of vehicle speed (or traffic flow, vehicle components), how much data do we need to measure on the road? How do we handle

those different types of distributions in the prediction model? How do we judge the predicted traffic noise emission that is expressed by a probabilistic distribution? How do we define the uncertainty of the different noise perception levels?

Generally, the approaches to account for uncertainties in the EIA include probabilistic analysis and fuzzy set theory (Li et al., 2003). Probabilistic methodologies have been widely used in environmental modeling during recent decades and have been regarded as an effective framework for tackling uncertainties (Li et al., 2003; Chen et al., 2003). The fuzzy approach has also been employed in many fields to describe the uncertainties in a non-probabilistic framework (Klir, 1997). It can handle the uncertainties in a direct way without requiring a large number of realizations. Two separate approaches have been used successfully in many environmental fields, but combining these two techniques to deal with uncertainty still is very rare in the field of EIA, especially for traffic noise impact assessment.

1.3. Challenges of dealing with uncertainty in hydraulic reliability analysis and reliability based optimization

Uncertainty can directly cause a reliability problem (Peng and Mayorga, 2010e). In the engineering field, reliability is defined as the ability of a system or component to perform its required functions under stated conditions for a specified period of time. In statistics, reliability is the consistency of a set of measurements or of a measuring instrument. Two definitions lead to people using different methods to deal with a same reliability problem.

Hydraulic reliability assessment is to study mechanical failure and hydraulic

failure in water distribution systems. A hydraulic failure occurs when a demand node does not receive sufficient flow and/or adequate pressure due to old pipes with low roughness arising from corrosion and deposition, increases of demand and pressure head requirements, inadequate pipe sizes, and insufficient pumping or/and storage capabilities. The reliability analysis of hydraulic failure is in the engineering field. Mechanical failures involve pipe breakages, pump failures, power outages, and control valve failures. The reliability analysis of mechanical failure is in the statistic field due to it being based on the historical records. Moreover, mechanical failure is integrally linked with hydraulic failure. For instance, pipe breakage is a mechanical failure, but the occurrence of a pipe break will eventually result in an insufficient flow rate and/or inadequate pressure head on the demand nodes.

The literature shows that the previous hydraulic studies only address either hydraulic failure problems, or mechanical failure problems (Mays, 1996; Prasad and Park, 2004). That is, there is no current methodology to deal with overall uncertainties of all aspects of hydraulic reliability assessments and hydraulic-reliability-based optimizations in the engineering and research fields.

1.4. Challenges of dealing with uncertainty in binary linear programming

Binary linear programming (BLP), also called Boolean linear programming or 0-1 integer linear programming, plays a significant role in many fields such as location and candidate selection in management studies, assignment and assembly line balance in operation researches and representing & reasoning in artificial intelligence (Yu and Li,

2001). Similar to EIA, the major uncertainties in a BLP are parameter uncertainty and modeling uncertainty (Peng and Mayorga, 2010c, d).

The major methods to deal with uncertainty in the linear programming (LP) area can be roughly categorized into two groups: parameter-based approaches and model-structure (or stipulation)-based approaches. The parameter based approaches include stochastic linear programming (SLP), fuzzy-coefficient linear programming (FLP), and interval-coefficient linear programming (ILP). These methodologies are based on the assumption of knowing the probability distributions (or fuzzy membership functions/boundary values) of parameters. However, in practice, we often do not know this information. Moreover, any non-deterministic value in a model can cause a complex optimization computation, especially in the SLP model. Compared to the probability distribution value, an interval value has the simplest mathematical expression, which reflects uncertainty using only two bound values with a uniform distribution. One of the model-structure-based approach is flexible fuzzy linear programming (FFLP), in which the objective can be fuzzy and the constraints may allow some violations.

Obviously, a model integrating parameter-based approach with model structure based approach can efficiently solve uncertainty in LP. However, no such study has been found in the BLP area, though such attempts have been successful in other areas such as in the mixed-integer linear programming (Liu and Sahinidis, 1997; Huang et al., 2001). This is because some extreme difficulties might arise from the application of the FFLP model in BLP. For instance, applying the min-operator (one operator of fuzzy optimization approach) might result in a nonlinear programming problem (see Zimmermann, 1987, pp.100-108 and 254; Herrera et al., 1993). Therefore, overall dealing

with uncertainties in the BLP still is a challenge for researchers and engineers.

1.5. Challenges of dealing with uncertainty in real-time multiple source water blending optimization

One major uncertainty of a mathematical optimization arises from the deviation between the predicted outcome and measured data. It is called "modeling uncertainty" in this dissertation. A precise mathematical model can reduce this modeling uncertainty efficiently. If the system is complex, a nonlinear model could describe the real-world system more accurately than a linear model. However, nonlinear optimization may require very large computational efforts. So, there is a trade-off between the accuracy and the computational effort (Peng et al., 2010a, b).

Because real-time optimization is a time-series process, the input variables vary with time. The dynamic input variables would bring another uncertainty, called "dynamic input uncertainty" here, which is non-reducible. The best way of settling dynamic input uncertainty is to set up an optimization model that could rapidly respond to the dynamic change of the input variables and expeditiously treat it. In the manufacturing field, this uncertainty can be minimized by maintaining the consistency of feeding material quality, but that is beyond the scope of this study. Generally, either increasing computation capacity or simplifying the simulation model could achieve the target of rapid response.

Dealing with these two types of uncertainties will cause conflicting requirements in real-time nonlinear optimization. Decreasing the modeling uncertainty requires a complex and nonlinear mathematical model for accurately reflecting the true system, but the dynamic input uncertainty requires a simple and linear mathematical model for

achieving a rapid optimization computation. In the industrial and environmental fields, real-time optimization is related to a dynamic process control. The previous approaches with regard to this field are intelligent control/optimization, model predictive control/optimization and nonlinear optimization that contributed to improving product quality, optimizing production rate, reducing production costs, and minimizing pollution(Miller et al., 1990; Willis, 1992; Khalid, 1993; Tan, 1996; Ferrer et al., 1998; Rao and Rawlings, 2000; Cannas et al., 2001; Das et al., 2001; Lee et al., 2001; Jamishidi, 2002; Zhou et al., 2002; Guh, 2003; Cano and Odloak, 2003). However, intelligent control/optimization has a high requirement of prior operation knowledge that highly depends on expert experience that may not be available (Huang et al. 2008). Model predictive control/optimization is capable of dealing with simple nonlinear systems or used in applications with slow dynamics (Wang and Boyd 2010). Conventional nonlinear optimization methodologies such as gradient-based algorithms and genetic algorithms (Mehrez et al. 1992, Ostfeld et al. 1996, Yang et al. 2000, Tu et al. 2005) cannot rapidly produce a robust optimum objective. For example, gradient-based algorithms may only find local optimums and genetic algorithms are time-consuming when used to solve a large-scale nonlinear problem. Therefore, it is a challenge for researchers and engineers to solve real-time optimization problems.

In practice, many real-time nonlinear optimizations have multiple objectives. For example, a multiple source water blending problem in a drinking water treatment plant reflects a need to minimize several adverse material releases synchronously, such as copper release, lead release, and iron release. However, previous research about drinking water blends only focused on steady state optimization technologies such as gradient-

based algorithms and genetic algorithms (Mehrez et al., 1992; Ostfeld et al., 1996; Yang et al., 2000; Tu et al., 2005; Imran et al., 2006). Real-time multi-objective nonlinear optimization problems still lack a suitable method that can deal with the modeling and dynamic input uncertainties as well as simultaneously optimizing multiple objectives.

1.6. Challenges of dealing with uncertainty in the process control of industrial rotary kiln

An industrial rotary kiln is a large scale piece of sintering equipment widely used in chemical, metallurgical, cement and environmental protection industries (Peng et al, 2010f). Similar to the real-time multi-objective nonlinear optimization problems, the uncertainty in the process control of an industrial rotary kiln includes "modeling uncertainty" and "dynamic input uncertainty". The high uncertainty and complex dynamics natures of the calcination process, with its nonlinear reaction kinetics, long time delays and variable raw material feed characteristics, make the rotary kiln process inherently difficult to model and control. Moreover, due to the high combustion temperature environment and the uncertainty of operational conditions, it is very hard to measure some key quality parameters in a rotary kiln, such as the flame temperature and composition of raw material.

The existing control techniques in this field include proportional integral-derivative (PID), intelligent, model predictive controls, as well as their hybrid approaches, which contribute to improving product quality, maintaining stable operations, reducing production costs and minimizing exhaust pollution (McIlwain, 1992; Wang, 1996; Valiquette and Savoie, 1999; Zanovello and Budman, 1999; Jarvensivu et al., 2001; Chen,

2002; Li and Zhu, 2004). However, in PID control, decoupling is a steady-state process and the constraints are not handled explicitly, leading to a suboptimal result. Intelligent controls have a high demand for prior operational knowledge that depends on expert experience, which may not be available (Huang et al., 2008). Model predictive control is capable of dealing with simple nonlinear systems or it may be used in applications with slow dynamics (Wang and Boyd, 2010). Therefore, research needs on dealing with uncertainty in the process control of rotary kiln are still substantial.

1.7. Objectives

In this dissertation, hybrid impact assessment technologies, numerical modeling methodologies, and mixed optimization approaches will be developed as attempts to deal with uncertainties and mitigate a number of the shortcomings that exist in the previous studies. The developed methodologies will be employed to real case studies in order to provide more realistic decision support and bring enormous environmental and economic benefits. The specific objectives of this research include the following aspects:

(i) Develop a novel integrated fuzzy-stochastic approach to qualitatively and quantitatively assess the predicted noise levels, and apply this approach to a case of traffic noise impact assessment.

(ii) Develop a novel hybrid stochastic method for hydraulic reliability assessment, and build a novel reliability-based simulation-optimization approach for long-term rehabilitation and upgrade schedule in a water distribution system.

(iii) Formulate a novel interval-parameter binary linear programming to represent

uncertainties in binary linear problems, and develop a novel mixed fuzzy-interval-stochastic approach to solve the problem. The proposed problem formulation and the novel solution approach are applied to a long-term traffic noise control plan.

(iv) Set up a fuzzy multiple response surface methodology in a novel manner to deal with uncertainties in real-time multi-objective nonlinear optimization problems, and apply the approach to a multiple source water blend in water distribution systems.

(v) Establish a Dual-Response-Surface-Based process control (DRSPC) programming in a novel manner to address uncertainties in the process control of the industrial rotary kiln, and apply it to a case of a rotary alumina kiln in China.

This dissertation is structured as follows. Chapter 2 contains a review of the previous studies of dealing with uncertainty in traffic noise impact assessment, hydraulic reliability analysis, reliability based optimization, binary linear programming, and real-time multiple source water blending optimization. Chapter 3 presents the development of an integrated fuzzy-stochastic approach for the traffic noise impact assessment and its application to a highway site in Canada. Chapter 4 presents the development of a hybrid stochastic method and a reliability-based simulation-optimization approach, as well as an example of a benchmark water distribution network. Chapter 5 gives the development of a mixed fuzzy-interval-stochastic approach for the binary linear programming and its application to a traffic noise control plan in Canada. Chapter 6 presents the development of a fuzzy multiple response surface methodology for real-time multiple source water blending optimization as well as its application. Chapter 7 presents the development of a Dual-Response-Surface-Based process control (DRSPC) programming for a rotary kiln and its application to a rotary alumina kiln in China. Chapter 8 presents the conclusions.

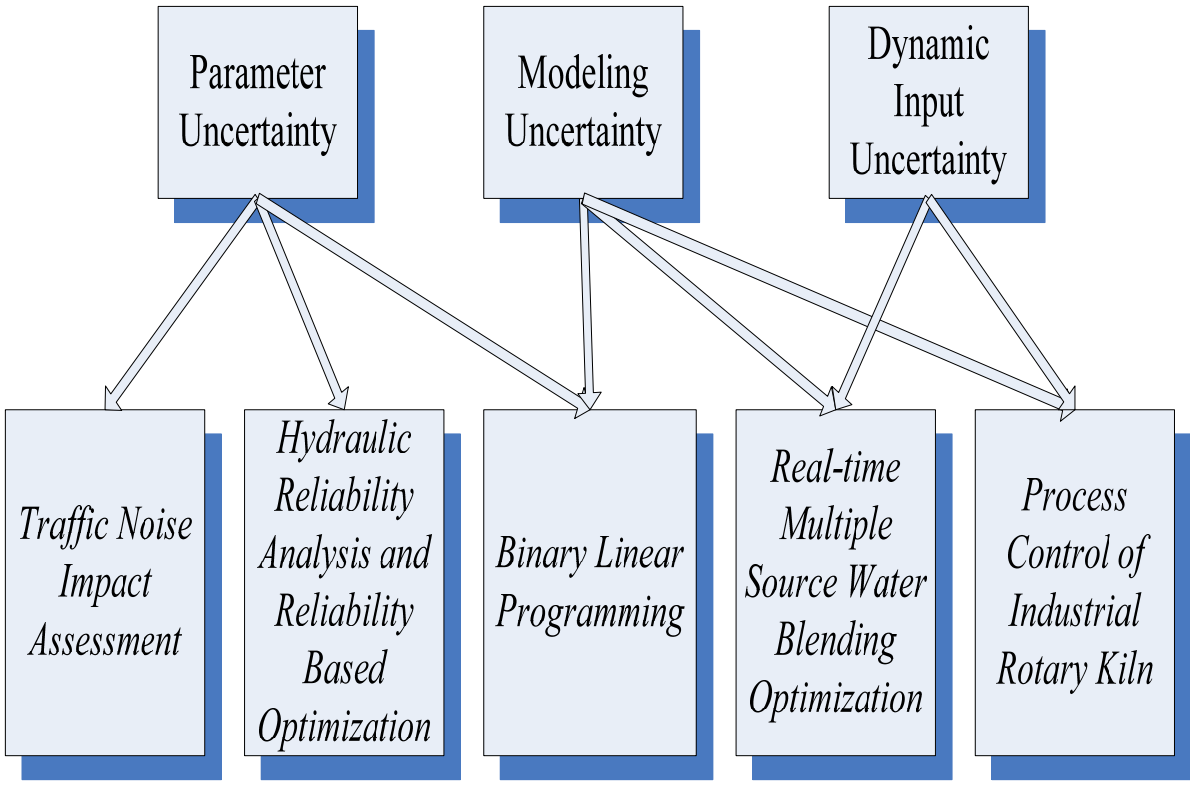

Figure 1-1 Key uncertainties of the five studying fields

CHAPTER 2

Literature Review

For engineering applications, dealing with uncertainty is not an ultimate goal but a necessary means to achieve the goal. In the past decades, many such methodologies were developed in the engineering and management fields. These approaches identified desired management strategies and optimized operation processes through accounting for uncertainties in complex systems. The results from these studies have contributed to economic improvement, product quality, production rate, and environmental efficiency. This chapter will review the previous research on the traffic noise impact assessment, hydraulic reliability assessment and reliability based optimization, binary linear programming, real-time fuzzy multiple response surface methodology and Dual-Response-Surface-Based process control, as well as their applications.

2.1. Uncertainty expression

2.1.1. Probability distribution

In a traditional view, uncertainty tends to be determined for the maximum, the average, or the minimum of a value. It is obvious that this calculation will result in an overestimate or an underestimate. Probability is certainly the best-known and most widely used formalism for quantifying uncertainty (Morgan and Henrion, 1990).

In probability theory and statistics, a probability distribution identifies either the

probability of each value of a random variable (when the variable is discrete), or the probability of a value falling within a particular interval (when the variable is continuous). However, there is often confusion and controversy about which kind of probability notion it is. For example, traffic noise is a continuous distribution value from a source (e.g., vehicle). Meanwhile, traffic noise is also believed as a discrete distribution value on a receiving point, in which each vehicle through this point will generate one discrete noise value. Considering both continuous probability distribution and discrete probability distribution are defined by a theoretically infinite sequence of discrete measured values, and both used cumulative distribution function in practices, the difference between them is negligible in this dissertation. The continuous probability distribution is considered as a special type of the discrete probability distribution. It doesn't matter that a probability density function is for a continuous random variable or that a probability mess function is for a discrete random variable.

There are many probability distribution functions, such as normal distribution functions and log-normal distribution functions. Uncertainty can be quantified into its specific probability distribution function. In the traffic noise field, for example, many investigators of traffic noise assume that histograms of noise levels, especially for freely moving traffic with a rate exceeding 100 vehicles per hour, approximate closely to a Gaussian distribution (Skarlatos, 1993). Some published papers proposed other non-Gaussian density functions for traffic noise. For instance, Kurze (1971) described a density function based on a Pearson type II1 distribution for the intensity ratio. Miedema and Oudshoorn (2001) presented a model that involves normal distributions for the distribution of noise annoyance with the mean varying with a function of the noise

exposure. There is a variety of research that used probability distribution to describe the traffic noise impact factors. Skarlatos (1993) used a Poisson distribution to describe light traffic flow and applied a beta model to depict heavy traffic flow. Lam and Tam (1998) identified that the probability distribution of the traffic speed as being subjected to a beta function and the traffic composition, which in terms of percentage of heavy vehicles, is subject to a normal distribution.

In the hydraulic field, uncertainties exist in required demands, required pressure heads, and pipe roughness coefficients. A great number of previous studies treated these uncertain parameters as random variables, and modeled them by means of probability density functions (Germanopoulos et al., 1986; Lansey et al., 1989; Quimpo and Shamsi, 1991; Mays, 1993; Calvin et al., 1996; Ostfeld, 2001; Shinstine et al., 2002; Kapelan et al., 2005; Giustolisi et al., 2009). According to the literature, the normal probability distribution function is the most popular probability density function that has been used for these parameters. Some might use other types of functions. For example, Kapelan et al. (2005) formulated pipe roughness coefficients to follow a uniform probability density function.

In the water quality field, the parameter values of water quality were formulated as various probability density functions to deal with their inherent uncertainty (Radovanovic and Koelmans, 1998; Castillo et al., 1999; Mecray and ten Brink, 2000; Lee et al., 2003; Sanchez et al., 2004; Rogevich et al., 2008). However, if using the maximum likelihood estimation, the estimated parameter values should follow a normal distribution. Some regulations of water quality parameters were also designed into probability density functions. For example, the Lead and Copper Rule action level for copper stipulates that

90% of samples have a copper concentration of less than 1.3 mg/L and a lead concentration of less than 15 μ g/L (Imran et al., 2006).

2.1.2. Fuzzy set and fuzzy number

A fuzzy set is a class of objects with a continuum of grades of membership. Such a set is characterized by a membership function that assigns to each object a grade of membership ranging between zero and one (Zedeh, 1965). A fuzzy number is a convex, normalized fuzzy set whose membership function is at least segmentally continuous and has a functional value equal to 1 at precisely one element. Fuzzy sets and fuzzy numbers are widely used to reflect uncertainties due to the fact that structures (e.g., the linear membership function's fuzzy sets) are simpler than those of the probability distribution and are consequently integrated into simulation models earlier. Scherm (2000) developed a climate change impact assessment in which the inputs (i.e., climate projections) are expressed as fuzzy numbers to represent the uncertainties. Dahab et al. (1994) developed a nitrate risk-assessment methodology to assist decision makers in estimating human health risks because of a nitrate water quality problem, and the uncertainty associated with assessing the health risks of nitrate and its impact on results are represented using a fuzzy-set approach and incorporated into the nitrate risk assessment methodology. Cammarata et al. (1995) presented a fuzzy model for predicting acoustical noise. They used fuzzy sets to represent the uncertain parameters. The reported results showed that the fuzzy models contribute to an improvement in the capacity to approximate real data.

2.1.3. Interval value

An interval value is a set of real numbers with the property that any number lays between two boundaries (which are also included in the set). It can be seen as a uniform probability distribution. It is usually used when parameters lack enough information but their boundary values are known. An interval value is the simplest expression for uncertain data, so it can be easily incorporated into mathematical models. Bass et al. (1997) quantified uncertainty based on interval numbers in their mathematical programming model. Peng and Mayorga (2008) used interval numbers to quantify the vehicle flows in their traffic noise impact assessment model. Two paper's results showed that the interval values could help for improving the capacity to deal with uncertainties.

2.2. Modeling under uncertainty

It is necessary to construct a mathematical model to simulate or predict the consequences of various possible events or decisions. The identified uncertain inputs can then be propagated through the model to discover the uncertainty in the simulated consequences. A considerable variety of such mathematical models have been developed with wide differences in conception, purpose, and computational effort required. This section contains a review of previous research on the linear model (first order model), response surface model (second order model), and nonlinear models (high order model or exponential model).

2.2.1. Linear model

The linear model is a simple and important mathematical model. It may be written as:

$Y = BX + \varepsilon$,

where Y is a matrix of responses, X is a matrix of input variables, B is a matrix of vectors or parameters, and ε is a matrix of errors. Because of its simplicity, the linear model is easily integrated with other mathematical analysis and inference methodologies, such as fuzzy linear model and stochastic linear model, to enhance the capability of dealing with uncertainty.

2.2.1.1. Binary linear model

If the input variables are binary (0-1variables or Boolean variables), the linear model becomes a binary linear model. The binary linear model plays a significant role in many fields such as location and candidate selection in management studies, assignment and assembly line balance in operation research, and representing and reasoning in artificial intelligence (Yu and Li, 2001). Bitran (1979) developed an algorithm for linear multiple objective programming with zero-one variables. He presented theoretical results to explore the strong and weak efficient points as well as an extension of the main problem in this algorithm. Zahedi (1987) applied a 0-1 integer linear programming to selection decisions in which the decision variables were 0-1 integers. Malakooti (1994) set up a multiple criteria optimization method to design the optimal allocation of different work elements to various workstations. Gokcen and Erel (1997) developed a binary goal programming model for the mixed-model assembly line balancing. A considerable

amount of flexibility could be provided to the decision maker due to the fact that several conflicting goals can be simultaneously considered in this model. In the artificial intelligence field, Jaumard et al. (1988) compiled an artificial intelligence bibliography specifically addressed to a binary operations research audience. This bibliography includes approximately 450 references from the areas of search, automatic deductions, planning, learning, and knowledge-based systems. Wilson (1990) developed an alternative linear time algorithm for achieving a clausal form equivalent to a given logical proposition, which established a connection between logical propositions and mixed integer programs.

The common difficulty in solving a binary linear model problem is the uncertainty related to its 0-1 decision environment (Yu and Li, 2001). For example, applying the min-operator in a binary linear programming may result in a nonlinear problem (see Zimmermann, 1987, pp.100-108 and 254). This dissertation will solve such difficulty in the following content.

2.2.2. Response surface model

A response surface model is a second order model. It can be written as:

$C = b_o + S'b + S'BS$,

where $b_0 = \beta_0$, $b = (\beta_1, \beta_2, ...\beta_k)'$, and

$$B = \frac{1}{2}\begin{bmatrix} 2\beta_{11} & \beta_{12} & \cdots & \beta_{1k} \\ \beta_{12} & 2\beta_{22} & \cdots & \\ \vdots & \vdots & \ddots & \vdots \\ \beta_{1k} & \beta_{2k} & \cdots & \beta_{kk} \end{bmatrix}$$

b_0 and b are the appropriate vectors of the estimates for the coefficients, B is a diagonal ($k \times k$) matrix of the estimates for the coefficients, C is a matrix of responses, and S and $S^{'}$ are a ($k \times 1$) vector of the input variables and its transverse, respectively.

For large and computationally expensive systems, it is useful to build a simple response surface model, which is an approximate version of the full model (Myers, 1971; Downing et al., 1985). Because of this model's rapid response to the variability of input variables, it may be particularly useful for real time tasks, such as the real time control of a complex system, a manufacturing process or aerospace vehicle (Morgan and Henrion, 1990). The response surface model has been developed for uncertainty analysis of some very large computer codes for simulation of the liquid metal fast breeder reactor (Vaurio, 1982). It has been set up for a regional photochemical air pollution system (Milford et al., 1989). It has also been developed for surfactant enhanced remediation at a petroleum contaminated site (Huang et al., 2003).

2.2.3. Nonlinear model

In practice, the study systems are often complex and a simple linear model might not work so well for such large uncertainties. One way to improve the accuracy of simulation is to use a nonlinear model such as exponential models, cubic models, or higher order models. However, the algebraic complexity increases rapidly with the complexity of the model (Morgan and Henrion, 1990). For example, the exact expression of a cubic model for the product of four independent variables contains 68 terms. Consequently, the computing time of a nonlinear model is increased exponentially. It

should be noted that another name of quadratic model is response surface model that was aforementioned.

2.2.3.1. Traffic noise prediction model

Traffic noise prediction models are nonlinear models because they contain one or more logarithmic equations of the sound pressure level (SPL):

$$SPL = 10Log\left(pres^2 / refpres^2\right)$$

where SPL = the sound pressure level in decibels, *pres* = the measured pressured amplitude in N/m^2, and *refpres* = reference sound pressure amplitude in N/m^2. In applied acoustics, several models are widely used in modeling road noise. These are: the CRTN model in the UK, the FHWA model in the US, the RLS90 model in Germany, the OAL model in Austria, the Statens Planverk 48 model in Scandinavia, the EMPA model in Switzerland, and the ASJ model in Japan (Li et al., 2002). Peng and Mayorga (2008) developed a modified FHWA model to assess traffic noise level in Canadian traffic conditions.

2.2.3.2. Hydraulic Empirical model

There are many factors that may cause pipe breaks, for instance, aging, physical bending stress, chemical and biological corrosion. Among these factors, aging, material type, dimension, and bedding quality are important factors in predicting pipe breakage. Shamir and Howard's (1979) exponential break rate model describes an exponential relationship between aging and breakage:

$$P(t)_j^p = P(t_0)_j^p e^{A_j (t-t_0)_j} \qquad j = 1, 2, ..., M$$

where A_j is the growth rate coefficient of the pipe j, $P(t)_j^p$ is the number of breaks per 1000 ft. length of pipe j in year t, t is time in years, t_0 is base year for the analysis (pipe installation year, or the first year for which data are available), and M is total number of pipes.

Pipe roughness directly affects the capacity of pipe. The magnitude of the pipe roughness increases at a rate. This roughness growth rate varies with pipe type, water quality, and operation and maintenance practices. The equation of Sharp and Walsli (1988) is used to model the aging effect on the capacity of pipes:

$$C(t) = 18.0 - 37.2 \log[\frac{e_o + a(age)}{R}]$$

where $C(t)$ is the Hazen-Williams coefficient in year t, e_o is the roughness at the time of installation (mm), a is the roughness growth rate (mm/year), and R is the pipe diameter (mm).

Dandy et al. (1985) developed a model to predict nodal water demands:

$$D_i = D_{0i}(1 + \frac{DGR}{100})^t (\frac{P_t}{P_0})^{PREL}$$

where D_{0j} is the base year water demand for the node j , DGR is the annual percentage rate of increase in the base demand (DGR was assumed to follow demographic data patterns closely, and so it was taken as the population growth rate with typical values of about 2 to 5), t is the time in years, P_t and P_0 are the price per unit volume of water for year t and the base year, respectively, and PREL is the price elasticity of demand (A typical range of PREL values is -0.2 to -0.5).

2.2.3.3. Water quality models for water blends

A number of water quality models have been developed for water pollution control and water quality management (Beck, 1985; Beck, 1987; Ambrose et al., 1988; Reckhow, 1994; Cox, 2003). But only a few were set up for the drink water blending problem in which several nonlinear models based on the data of a pilot distribution system were developed for the releases of copper, lead, and color (iron) (Imran et al. 2006, Imran et al. 2005b, Taylor et al. 2005; Xiao 2004), and the nonlinear kinetic models for the decay of mono-chloramine have been developed based on the same data of the pilot distribution system (Taylor et al. 2005; Arevalo, 2003). They used those nonlinear models to optimize multiple source water blending problems. However, the nonlinearity of those models greatly increased the computational time during the optimization processes that could not be utilized to solve dynamic uncertainty in a real time operation. This weakness is solved in this dissertation.

2.2.3.4. Phenomenological models for the process control of rotary kiln

The process control of rotary kiln has been studied since the early 1960s. These applications were model-based process controls that studying the uncertainty / dynamics of solids phase, the fundamental principles of heat transfer mechanisms, the kinetics of reaction processes and the formation of pollutant. These phenomenological models have provided useful insights into the rotary kiln process.

Imber and Paschkis (1962) used a mathematical model to calculate the optimum kiln length for a heat process. Sass (1967) developed the differential models to simulate the temperatures in cement kiln and iron ore preheating kiln. Brown and Rastogi (1983)

developed a steady-state mathematical process model to estimate the peak refractory temperature and predict the residual carbonate in the product. Barr et al. (1989) set up a heat transfer model for the rotary kiln. In the 1990s, after the emergence of the new intelligent control methods, the phenomenological models were developed to simulate the calcination process of rotary kilns by a variety of methods. Yakimow et al. (1994) used a constant heat rate thermogravimetric analysis to study the kinetics of the reaction. The rate of the reaction is described by an equation of the temperature. Boating and Barr (1996) developed a thermal model for the rotary kiln to study heat transfer in the calcination process. Ramakrishnan and Sai (1999) integrated the kinetics of heat exchange with the experience equation to established one-dimensional steady mathematical models for the calcination process and refining process in the imenite and ferric oxide rotary kiln. Mastorakos et al. (1999) modeled the clinker formation in coal-fired rotary cement kilns under realistic operation conditions. In which, a commercial axisymmetric CFD code was used for generating the gaseous phase model, a Monte Carlo method is used for radiation, a finite-volume code is used for the energy equation in the kiln walls, and a novel code is used for the species and energy conservation equations.

However, the existing phenomenological models are still not accurate enough to describe the rotary kiln process, because the kiln process involves high uncertainty, complex dynamics, non-linear reaction kinetics, long time delays, and variable raw material feed characteristics and is multi-variable in nature. Research needs on the process control of rotary kilns are still substantial. This dissertation provides a new way to solve the difficulties in the process control of rotary kiln.

2.3. Mathematical approaches for dealing with uncertainty

2.3.1. Monte Carlo simulation

In practice, uncertain quantities are naturally thought as continuous such as the environmental concentration of a toxic chemical, or as a set of discrete samples such as the measured noise levels of a reception point on a highway. However, the inputs of a mathematical model should be deterministic values rather than probability distributions (or fuzzy sets, interval values). Therefore, it is necessary to find a method that can convert probability distributions into deterministic values. Monte Carlo simulation is such a method.

Monte Carlo simulation involves the repeated generation of pseudo-values for uncertain inputs drawn from known probability distributions, so as to produce probability and cumulative distribution curves for the modeling outputs (Hoogeweg, 1999). It is the most common stochastic technique for linking the various uncertain inputs and the designed model. Eschenroeder and Faeder (1988) used Monte Carlo technology to perform statistical sampling from each uncertain risk parameter, which was used to generate the corresponding exposure estimation of human intake of polychlorinated dibenzofurans, and was eventually used to conduct the analysis of health risks from PCB-contaminated mineral oil transformer fires. Similarly, Burmaster and von Stackelberg (1991) used Monte Carlo simulation to estimate full distributions of public health risk. Lam and Tam (1998) examined the reliability of traffic noise measurement techniques and the noise estimates in Hong Kong. In their study, the probability distribution of each key factor was derived from the survey data, and the Monte Carlo technique was used to

incorporate these distributions into a simulation model for traffic noise estimation. In the water industry, Bao and Mays (1990) developed a methodology that was based upon a Monte Carlo simulation to define the hydraulic reliability of a water distribution system as a probability distribution. In this methodology, Monte Carlo simulation was used to generate the random numbers of future water demands, required pressure heads, and pipe roughness.

In a typical application, analysts used very large numbers of Monte Carlo runs. For example, Jackson et al. (1981) used over 18,000 runs in a reliability analysis for nuclear power plants. However, such an extreme number of Monte Carlo runs might not be required. It was reported that the optimal number of Monte Carlo runs is between 500 times and 3000 times for the system reliability assessment of a water network because the fact that results had only tiny differences after 2000 runs (Bao and Mays, 1990; Xu and Goulter, 1998). Additionally, the computation of Monte Carlo simulation is getting more efficient with the development of computer technology.

2.3.2. Fuzzy mathematical programming

A fuzzy mathematical programming (FMP) is derived through the incorporation of fuzzy set theory within ordinary mathematical programming frameworks. The FMP methods contain two major categories: fuzzy flexible programming (FFP) and fuzzy possibilistic programming (FPP) (Inuiguchi, 1990). In the FFP methods, the flexibility in the constraints and fuzziness in the system objective, which are presented by fuzzy sets and denoted as “fuzzy constraints” and “fuzzy goals” respectively, are introduced into

ordinary mathematical programming models (Zimmermann, 1985). In the FPP methods, fuzzy parameters are introduced into ordinary mathematical programming frameworks, where various intermediate models could be formulated based on the problem interpretation (Zadeh, 1978).

There were a number of extensions of fuzzy set theory to other mathematical programming frameworks, such as fuzzy binary linear programming (FBLP) and fuzzy multi-objective programming (FMOP). For example, Ignizio and Daniels (1983) formulated a network model for zero-one or mixed integer mathematical programming models, with the utilization of fuzzy programming techniques as well as a hybrid solution approach. Zimmermann and Pollatschek (1984) provided two equivalent formulations for a linear zero-one programming with a fuzzy right-hand side. Castro et al. (1994) discussed the applications of FBLP problems for representing and reasoning with propositional knowledge. The use of the models provided by the fuzzy binary problems was proposed to answer imprecise questions in precisely stated knowledge-based systems. Herrera et al. (1994) provided a fuzzy method that was based on a α-cut technology to solve the structure uncertainties of the constraints in a binary linear model. Herrera and Verdegay (1996) developed and linked the different approaches to deal with Boolean linear programming problems involving coefficients in the objective function as fuzzy numbers. Yu and Li (2001) developed an algorithm that can simultaneously solve a binary linear programming problem with fuzzy coefficients in the objective function, fuzzy coefficients in the constraint matrix, and fuzzy numbers in the right-hand side of constraints. Van Hop N (2006) formulated a FBLP model to heuristically address the mixed-model line balancing problem with fuzzy processing time. Chang (2010) proposed

a piecewise-linear approach to formulate an S-shaped membership function (MF) for improving the efficiency of fuzzy-linear programming with binary variables in solving decision/management problems.

Fuzzy multi-objective programming (FMOP) was first introduced by Zimmermann (1976) when he applied fuzzy linear programming approaches to a linear vector maximization problem for finding a compromise solution. The method was then extended to a number of other approaches. Sakawa and Yano (1990) contributed significantly to the further development of the FMOP approaches. They proposed interactive fuzzy satisfying methods for solving multi-objective LP problems with fuzzy parameters through a combined use of a bisection method and a LP formulation, as well as five types of membership functions: linear, exponential, hyperbolic, hyperbolic-inverse, and piecewise-linear functions (Sakawa, 1983; Sakawa and Yano, 1990). Sakawa and Yano (1991) extended the method for solving multi-objective linear fractional programming and nonlinear programming problems and introduced four types of feasibility for multi-objective linear and linear fractional programming problems with fuzzy parameters by making use of the four indices for ranking fuzzy numbers proposed by Dubois and Prade (1980). More recent research of the FMOP can be found in Bit et al. (1993) and Lee and Li (1993). The effectiveness of solution algorithms and computational requirements are two major concerns when the FMOP is applied to large-scale problems (Lee and Li, 1993). Shih and Wangsawidjaja (1996) developed a mixed fuzzy-probabilistic programming for multi-objective engineering optimization through introducing fuzzy parameters and random variables into the model. Gen et al. (1997) applied a genetic algorithm to solve the developed fuzzy nonlinear goal programming.

Sakawa and Kato (1998), Sakawa et al. (2000), and Chakraborty and Gupta (2002) formulated multi-objective linear fractional programming problems. Different problem solving procedures, such as an interactive decision-making method with decomposition procedures, were proposed to derive a satisfying solution for decision makers. Guu and Wu (1999) introduced a two-phase approach to solve fuzzy linear programming problems. The result indicated that the two-phase method not only pursued the highest membership degree in the objective, but also pursued a better utilization of each constrained resource. Wang and Liao (2001) proposed a heuristic algorithm to analyze a differentiable nonlinear integer programming when the fuzzy inequality constraint was considered. Stanciulescu et al. (2003) developed a multi-objective fuzzy linear programming problem and introduced a method that used fuzzy decision variables with a joint membership function instead of crisp decision variables. Liang (2009) presented a two-phase fuzzy programming methodology to solve the real-world PM decision problems with multiple objectives. Wu et al. (2010) used a possibility approach to develop a fuzzy multi-objective programming to decide on the supplier selection while taking risk factors into consideration.

2.3.3. Interval programming

In interval analysis, the only available information on model parameters is the upper and lower bounds that are insufficient for creating distribution functions and/or membership functions. The interval programming used from the 1960s to 1980s dealt with models in which the constraints can be upper and lower bounded. For example, Ben-

Israel and Robers (1970) proposed a decomposition method for an interval linear program. After that, the study focused on solving linear programming problems with interval coefficients / variables. Jansson (1988) developed a self-validating method to solve linear programming (LP) problems with interval input data. Inuiguchi and Sakawa (1995) dealt with linear programming models in which interval coefficients were involved in the objective function. Tong (1994) solved an interval coefficient linear programming problem by transforming the original interval linear programming model into two specific linear programming models according to the boundary values of interval coefficients. Chinneck and Ramadan (2000) gave an approach to solve linear programming in which some or all of the coefficients are specified as intervals.

On the other hand, some researchers attempted to combine interval programming with flexible fuzzy programming, which can deal with uncertainties in both the parameter and the structure in a model. For example, Liu and Sahinidis (1997) presented such an approach using interval theory and fuzzy optimization for the process planning in an uncertain environment. Huang and his colleagues (Huang, 1994; Huang et al., 1994; Huang, 1998) proposed several interval-parameter mathematical programming (IMP) methods as a special group of interval programming and applied them to a number of environmental decision analysis problems in Canada, USA, Japan, Taiwan and China. Examples include environmental planning for the Great Lakes - St. Lawrence Basin, the Lake Erhai Basin, the Mackenzie Basin, the Region of Hamilton-Wentworth, and the city of Regina (Huang et al., 1993a, b, 1994, 1995, 1997, 2001). However, their successes are only limited to the mixed-integer linear programming area; other fields, such as binary linear programming, have not been involved.

2.3.4. Dual response surface optimization

Dual response surface optimization (DRSO) is based on response surface methodology. The response surface methodology (Box and Wilson, 1951) was designed for empirical studies to research the relationship between the responses and the mean value of observations. It works well when the variances of observations are relatively small or equal. However, it can be misleading due to the fact that these variances are not equal in practice. The DRSO was then designed to tackle such non-equal variance situation based on the dual response approach (Myers and Carter, 1993). Vining and Myers (1990) first fitted second order models to both primary and secondary response surfaces and then applied the dual response approach to optimize the primary response subject to an appropriate constraint on the value of the secondary response.

The DRSO has received great attention. Del Castillo and Montgomery (1993) optimized the dual response system based on the generalized reduced gradient algorithm. They further used a more advanced computational algorithm to avoid the dimensionality problem. The algorithm consists of computing confidence regions for the stationary points of quadratic responses and confidence cones for the direction of maximum improvement for linear responses (Del Castillo, 1996). Lin and Tu (1995) developed a mean squared error objective function for DRSO to avoid the misleading circumstances that arose from the unrealistic restriction of forcing the estimated mean to a specific value. Copeland and Nelson (1996) suggested a direct function minimization method for DRSO and demonstrated this using the Nelder-Mead simplex procedure. Kim and Lin (1998) applied a fuzzy modeling approach for DRSO. The approach aimed to identify a set of

process parameter conditions to simultaneously maximize the degree of satisfaction with respect to the mean and the standard deviation responses. Tang and Xu (2002) proposed a goal programming approach to optimize a dual response system. Koksoy (2003) used a joint optimization method to generate more alternative solutions for the decision-makers. This method graphically examines how the controllable variables simultaneously impact the mean and standard deviation. Fen et al. (2009) presented a study on a response surface-based optimization approach for a soil vapour extraction system (SVES) design. The SVES design involves extraction rate determination for a number of wells at fixed locations. Two optimization problems were investigated in this study: (1) minimizing total cost while achieving the required cleanup goal, and (2) maximizing percentage of contaminant mass removal under the constraint of total extraction rate. Lee et al. (2010) proposed a posterior preference articulation approach to DRSO. This method initially finds a set of non-dominated solutions without the decision maker's preference information, and then allows the decision maker to select the best solution among the non-dominated solutions.

This technology has also been widely used in the industrial area. For example, it is used in grinding operations (Dhavlikar et al., 2003), in the inspection process of aero-engine components (Wong et al., 2006), in the deep-drawing process of sheet metal (Li et al., 2006), in the design of helicopter vibration reduction (Viswamurthy and Ganguli, 2007), in the heater control of thermoforming preheating (Li et al., 2008), in a biological wastewater treatment plant (kim et al., 2009); for soil vapor extraction system design (Fen et al., 2009), and in the drawbead design of sheet metal forming (Sun et al., 2010).

2.3.5. Genetic algorithm

The genetic algorithm (GA) was developed through the imitation of the principle of natural evolution (Holland, 1975). It can effectively deal with the problems inherent in non-convexities and uncertainty (Borkowski and Grabska, 2001). It is applicable for solving the discrete and nonlinear optimization model with high nonlinearity (Holland, 1975, Chipperfield, 1994).

GA differs from other optimization and search procedures in four main ways: (1) it uses a coding of the decision variable set rather than the decision variables themselves, (2) it searches for optimal solutions in a population of decision variable sets rather than a single decision variable set, (3) it uses the objective function itself rather than derivative information of the objective function and constraints, and (4) it uses probabilistic transition rules for the realization perturbation rather than deterministic rules (Goldberg, 1989; Davis, 1991).

Thus, the advantage of using GA is that the implementation procedure is independent of the cluster tree (interrelationship between system performance and operating conditions) and the objective function. With these characteristics, GA is computationally simple, but powerful in its optimal-solution search procedure in large and complex decision spaces.

2.4. Summary

The literature review indicated that many research efforts have been made for dealing with uncertainty in traffic noise impact assessment, hydraulic reliability assessment and reliability based optimization, binary linear programming, and real-time fuzzy multiple response surface methodology during recent decades. However, further improvements in the following areas are necessary:

(1) The dominant methods reflecting uncertainties in the previous studies of traffic noise impact assessment mainly included fuzzy sets/numbers, probability distributions and interval values. Due to the difficulties inherent in the solution algorithm, computational requirements, and result interpretation, it was common in their practical applications that they treated various types of uncertainty using a same mathematical formulation. Indeed, when the characteristics of the uncertain input are quite different from their mathematical expression, the proposed methodology can be misleading. Therefore, it is desirable to present an uncertainty using a suitable distribution according to its inherent attribute and data availability.

(2) The literature shows that the previous hydraulic studies only address either hydraulic failure problems or mechanical failure problems (Mays, 1996; Prasad and Park, 2004). It is desirable to develop a method to deal with uncertainties in these two areas simultaneously.

(3) Assuming that uncertainties could be categorized into parameter uncertainty and model structure uncertainty in binary linear programming problems, all previous research has persisted in work done in only one of these two classes. Obviously, it is desirable to integrate these two types of methods for addressing uncertainties in both

coefficients and model structure.

(4) The quadratic model and dual surface response optimization have been applied more widely in real-time operations / process control from the 1990s. However, most of the previous studies have focused on single objective problems. Moreover, there are only a few applications for large and complex systems. It is desirable to expand their application to new areas such as the real time multiple source water blending optimization and the process control of rotary kilns.

In the next chapter, a novel methodology is proposed to assess traffic noise impact under uncertainty. It is based on integrating the probabilistic approach with the fuzzy logic method.

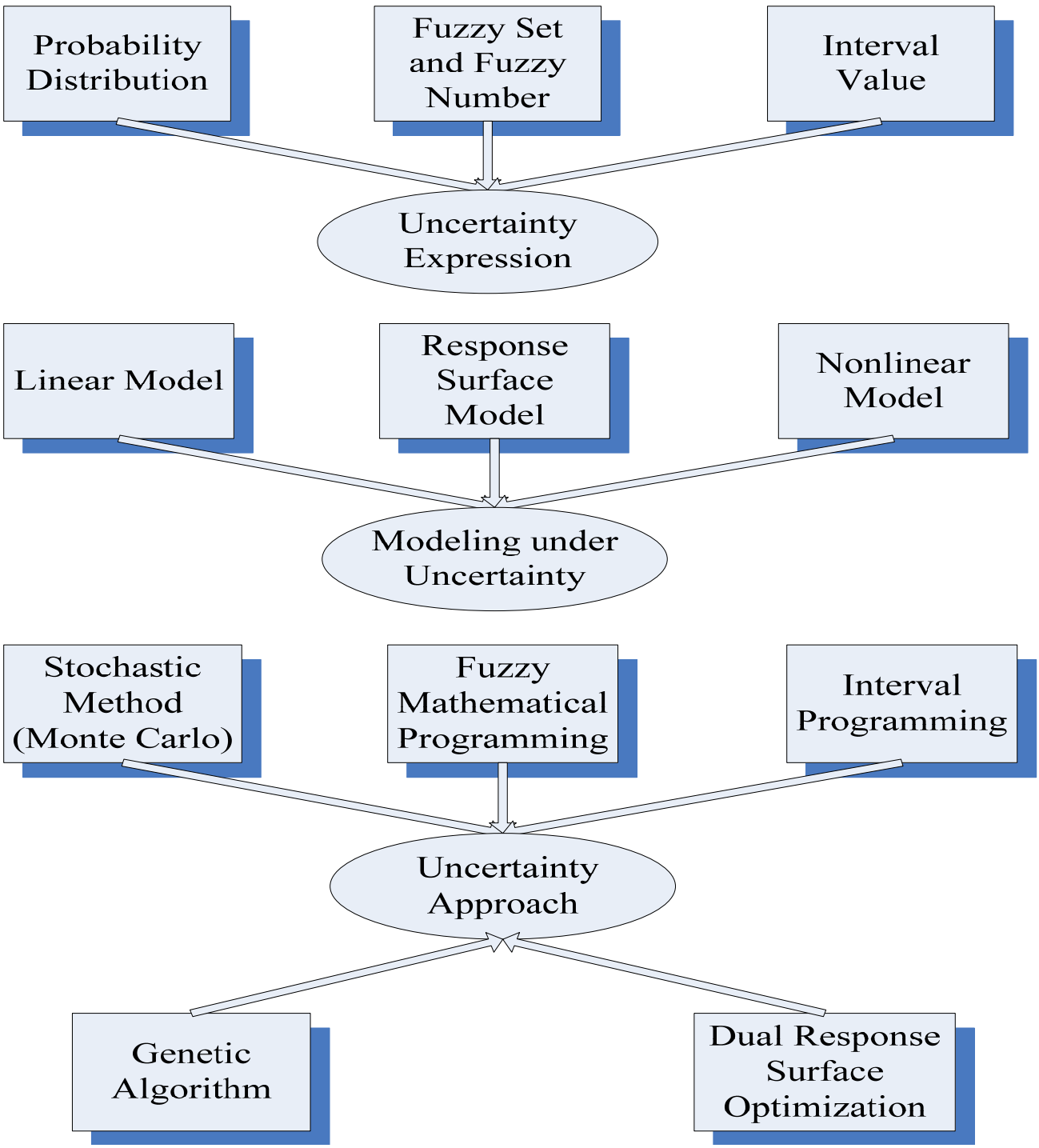

Figure 2-1 Previous studies to uncertainty

CHAPTER 3

Assessing Traffic Noise Impact Based on Probabilistic and Fuzzy Approaches under Uncertainty

3.1. Statement of problems

Exposure to noise is potentially hazardous and can cause hearing loss and other physical or psychological stress (Peng and Mayorga, 2008). The Canadian Compensation Board estimated the average cost per hearing loss claim to be Can$14,000 in 1989 (Alleyne et al., 1989). In the United States, compensation was estimated as US$200 million for the calendar year of 1990 (US Army Environmental Hygiene Agency, 1990). Noise pollution could also result in adverse socio-economic impacts. For instance, houses values might diminish when they are located in a noisy area.

The standard noise descriptor is L_{eq} using the decibel scale, a logarithmic scale denoted as dBA. It is the equivalent continuous sound level containing the same quantity of sound energy over a unit time-period as the actual time-varying sound level. Studies showed that traffic noise tends to be a dominant noise source in urban areas as well as rural environments (Calixto et al., 2003; Lam and Tam, 1998; Li et al., 2002; Ruedi, 2004). For example, the World Health Organization (WHO, 2001) recommends a maximum noise level of 45 dBA at night in a bedroom and a maximum of 55 dBA outside during the day. However, the Canada Government Report (2004) reported that the average sound volume recorded within a radius equal to the distance of the first row of houses alongside urban and suburban expressways was 70 to 75 dBA, a level that is

clearly harmful for human health and well-being. To assess noise level, especially for traffic noise, researchers have to face the high complexity and variability that exists in traffic flow, traffic speed, vehicle components and roads. Moreover, uncertainties exist not only in noise emission but also in the degree of noise impact on human beings since different individuals have different noise perception levels.

There have been a number of studies on noise measurement and noise impact assessment (Chien et al., 2003; Raimbault et al., 2003; Hardy, 2000; Davies and Holland, 1999; Schulte-Werning et al., 2003; Li et al., 2002, Hume, et al. 2003). Ahmed et al. (2000) used a cross-section study method and interview questionnaire to determine the prevalence of hearing loss associated with occupational noise exposure and other risk factors. Franssen et al. (2000) proposed a comprehensive approach to quantitatively estimate the effect of aircraft-related pollution in term of the number of affected people for aircraft noise annoyance. Kluijver and Stoter (2003) suggested and illustrated the essence of standardized noise mapping tools combined with GIS. However, extensive applications of these methods were limited due to limitations in addressing the uncertainty of noise and its impacts. The qualitative analysis of the output in these studies is based only on the mean value of the noise distribution that would generate an unreasonable result.

Generally, applied approaches to account for uncertainties in environmental simulations include probabilistic analysis and fuzzy set theory (Li et al., 2003). Probabilistic methodologies have been widely used in environmental modeling during recent decades and have been regarded as effective frameworks for tackling uncertainties (Li et al., 2003; Chen et al., 2003). In this approach, uncertainties associated with the

modeling inputs are described using probability distributions, such that the modeling outputs can be characterized as probabilistic information. The Monte Carlo technique is one such simulation method that involves repeated generation of pseudovalues for uncertain input parameters drawn from known probability distributions, so as to produce probability and cumulative distribution curves for modeling outputs. Such probability information can then be interpreted into an indicator of uncertainties (Lam and Tam, 1998). The fuzzy set approach has been applied successfully in many fields to describe the uncertainties in nonprobabilistic frameworks (Klir, 1997). It can handle the uncertainties in a direct way without requiring a large number of realizations. Both above approaches and their combination have been widely used in the environmental field, but very few attempts dealt with uncertainties in assessing noise impacts.

This chapter contains an integrated (combining statistical and fuzzy methodologies) approach to assess traffic noise impact under uncertainty. Three uncertain inputs, namely, traffic flow, traffic speed, and traffic components, are represented by probability distributions; Monte Carlo simulations are performed to generate a noise distribution. Furthermore, fuzzy set and binary fuzzy relations are applied to this assessment process for qualitative analysis, to identify which abatement criteria the noise distribution has exceeded. Finally, the quantification of noise impact is produced using probability analysis. A case study is provided to demonstrate the applicability of this proposed technique.

3.2. Methodology

3.2.1. Traffic noise prediction model

In general, a traffic noise impact assessment includes two parts: an accurate simulation model for traffic noise and a suitable noise criterion. The simulation model consists of mathematical equations and is used to predict traffic noise level according to traffic factors (such as traffic speed) and corrections (such as road surface condition). In applied acoustics, several models are widely used in modeling road noise. These are: the CRTN model in the UK, the FHWA model in the US, the RLS90 model in Germany, the OAL model in Austria, the Statens Planverk 48 model in Scandinavia, the EMPA model in Switzerland, and the ASJ model in Japan (Li et al., 2002). No specific model is consistently used for Canadian traffic conditions. However, based on the similarity of Canadian traffic conditions to that of US, FHWA is used in this chapter to assess traffic noise level for Canadian highways. The FHWA model can be formulated as:

$$L_{eq} = L_O + C_D + C_G + C_B + C_S + C_C + C_R \quad (3\text{-}1)$$

where L_{eq} = the A-weighted hourly energy equivalent noise level dBA, L_O = the reference energy mean emission level dBA, C_D = the distance correction dBA, C_G = the road surface gradient correction dBA, C_B = the noise barrier correction, C_S = the road surface condition correction, C_C = the ground absorption correction, and C_R = the noise reflection and obstruction correction.

To compute the reference energy mean emission in the FHWA model, the

correction terms in the right hand side of Equation 3-1 should be set as constants, which is based on following assumptions: (1) the whole study road has been separated into finite and straight segments, (2) various vehicles are represented by heavy vehicles (or other types of vehicles) and are running on the road at a constant speed and flow, (3) assuming that longitudinal inclination is zero, (4) assuming that road surface is a certain type, such as smooth asphalt, (5) the noise receiving point is perpendicular to and 1.5m from the centerline of the closest traffic lane on both sides of the road, and (6) there are no barriers along the two sides of the study road, and the nearby terrain between the edge of the road segment and the reception point is even, where noise is absorbed by natural materials (e.g., grass land and cultivated land).

For the purpose of highway traffic noise analysis, motor vehicles fall into one of three categories: (l) automobiles - vehicles with two axles and four wheels, generally having a gross vehicle weight of less than 4500 kg, (2) medium trucks - vehicles with two axles and six wheels, generally having a gross vehicle weight of greater than 4500 kg but less than 11800 kg, and (3) heavy trucks - vehicles with three or more axles, generally having a gross vehicle weight of greater than 11,800 kg. The noise emission levels of all three-vehicle types increase as a function of the logarithm of their speed. A heavy vehicle emits louder noise than a light vehicle and dominates the noise production. Therefore, the actual vehicle flow (Q_A) could be transposed into an equivalent heavy vehicle flow (Q_E). Using a regression method, three curves (Figure 3-1) could be fitted to the collected data, and they can be expressed as:

$$L_{eq(L)} = a_L + b_L LogV \tag{3-2}$$

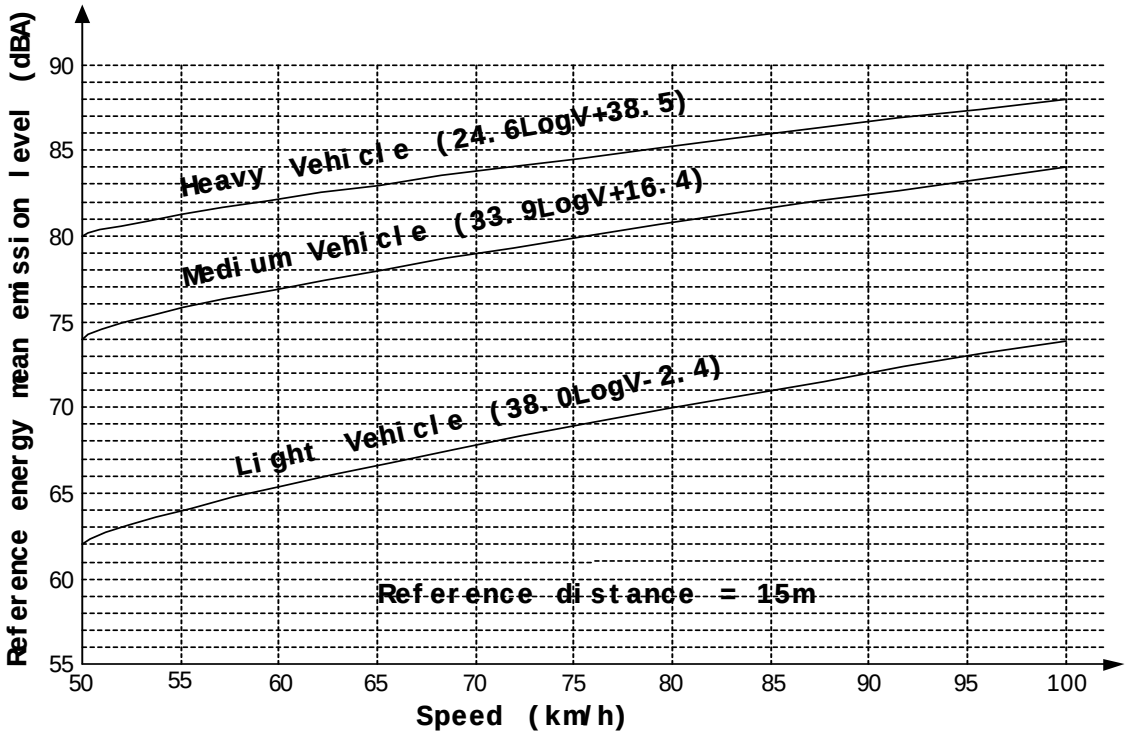

Source: FHWA-RD-77-108

Legend:
1. **Light Vehicle: Two axles and four wheels**
2. **Medium Vehicle: Two axles and six wheels**
3. **Heavy Vehicle: Three or more axles**

Figure 3-1 The FHWA highway traffic noise prediction model

$$L_{eq(M)} = a_M + b_M LogV \tag{3-3}$$

$$L_{eq(H)} = a_H + b_H LogV \tag{3-4}$$

where Log(*) = $\log_{10}$(*), a_L, b_L = coefficients of light vehicle or automobile, a_M, b_M = coefficients of middle vehicle, a_H, b_H = coefficients of heavy vehicle, and V = the velocity of vehicle. According to the definition of the sound pressure level (SPL):

$$SPL = 10Log\left(pres^2 / refpres^2\right) \tag{3-5}$$

where SPL = the sound pressure level in decibels, *pres* = the measured pressured amplitude in N/m^2, and *refpres* = reference sound pressure amplitude in N/m^2 (the threshold of hearing = 2×10^{-5} N/m^2). So, the measured sound pressure can be described as:

$$pres = 10^{0.05SPL} \times refpres \tag{3-6}$$

The measured noise pressure rate n ($n < 1$) between two kinds of vehicles can then be shown as:

$$n_{L/H} = 10^{0.05(a_L + b_L LogV - a_H - b_H LogV)} = 10^{0.05(a_L - a_H)} \times V^{0.05(b_L - b_H)} \tag{3-7}$$

$$n_{M/H} = 10^{0.05(a_M + b_M LogV - a_H - b_H LogV)} = 10^{0.05(a_M - a_H)} \times V^{0.05(b_M - b_H)} \tag{3-8}$$

For instance, $n_{L/H}$ = 0.04 and $n_{M/H}$ = 0.4 when V = 100 *km/h* and the reference mean energy emission level for the FHWA model in Figure 3-1 is used. Thus, the equivalent heavy vehicle noise emission flow is represented by:

$$Q_E = Q_A(p_L \times n_{L/H} + p_M \times n_{M/H} + p_H) \tag{3-9}$$

where p_L, p_M and p_H = the percentage distribution of the three types of vehicle in traffic flow. The basic noise level of highway traffic depends on three factors: (l) the volume of the traffic Q_A, (2) the speed of the traffic V, and (3) the percentage distribution of vehicles p. Q_E can be represented by Q_A and p as described in Equation 3-7. Thus, the reference main energy emission level in the FHWA model can be converted as a function of speed and equivalent heavy vehicle flow:

$$L_o = cLogQ_E + dLogV + e \tag{3-10}$$

where c and d = coefficients of logarithmic traffic flow of equivalent heavy vehicle and logarithmic vehicles speed, and e = the bias.

The uncertain factors in Equation 3-1, which involve V, Q_A and p, are temporal data and should be treated using suitable methods. The factors of other terms are spatial data that depend on road conditions, traffic behavior, and topographic information. For example, traffic noise levels are affected by the gradient of a road. The impact of gradient critically depends upon the percentage of heavy vehicles, and the traffic noise can be increased up to 12 dBA for a gradient of 1 in 8 (Lam and Tam, 1998). Road surface

conditions also affect the noise generated by the interaction between a tire and the road surface. The noise produced from a concrete surface can be 2 to 3 dBA higher than that from an open-textured material surface.

According to the study by Lam and Tam (1998), the scheme of this modified FHWA model also can be decomposed into three steps:

1. Basic noise evaluation
2. Noise propagation
3. Noise modification

Basic noise evaluation involves the calculation of the reference energy main emission L_O, longitudinal gradient correction, C_G, and the road surface condition, C_S, in which C_G is an important factor that should be applied on each segment; but C_S is only applied where the road surface has more than 5 mm of deep random grooving (Lam and Tam, 1998). The second step involves the distance correction, C_D, the noise barrier correction, C_B, and the ground absorption correction, C_C. The distance correction should be conducted when the distance between the noise reception point and the centerline of the travel is greater than the design distance (e.g., 15 m). This distance correction is subjected to the noise drop-off rate, and expressed as decibels per doubling distance (dBA/DD) (Li et al., 2002). The most suitable drop-off rate is about 4.5 dBA/DD in traffic noise analysis (U.S. Department of Transportation, 1995) where sound from a highway propagates close to "soft" ground (e.g., ploughed farmland, grass, and crops). The distance correction can be expressed by the following equation:

$$C_D = a_D Log(D_o / D) \tag{3-11}$$

where D_o = the design distance, and D = the actual distance from the centre of the road to the noise reception point.

The third step is to determine the reflection and obstruction correction, C_R. This is because the noise reflected or obstructed by buildings is an important factor that affects the magnitude of noise measured at any given point.

The FHWA model modified above is used to predict the noise level at a certain reception point along the entire roadside in each calculation. It is known that different reception points have different ground conditions, different site topography and different populations. In order to deal with those differences, a geographical information system (GIS) might be used to generate a user-friendly, two-dimension noise distribution map with contour lines (Kluijver and Stoter, 2003; Li et al., 2002).

3.2.2. Stochastic simulation

The modified FHWA model for predicting noise impact levels requires inputs of various traffic information and road conditions. However, some fundamental parameters, such as traffic flow, traffic speed, and vehicle components vary with time and are generally hard to acquire with accurate and deterministic values. Some researchers used statistical techniques to deal with uncertainty (Sopasakis, 2004; Diehl, 1998; Ohta, 1980). For example, previous studies identified that the probability distribution of the traffic speed can be subjected to a beta function, and the traffic composition, which is drawn out in terms of the percentage of heavy vehicles, can be subjected to a normal distribution

(Lam and Tam, 1998). The probability distribution of the traffic speed is expressed as:

$$V \sim Beta(\alpha, \beta) \qquad \alpha > 0, \quad \beta > 0 \tag{3-12}$$

where *Beta* (*) is the beta distribution, and α and β are the shape parameters to determine the shape of the probability density function (PDF) or the cumulative distribution function (CDF). The general formula for the PDF of the beta distribution is

$$f(v, \alpha, \beta) = \frac{(v-a)^{\alpha-1}(b-v)^{\beta-1}}{B(\alpha, \beta)(b-a)^{\alpha+\beta-1}} \qquad a \le v \le b; \quad \alpha, \beta > 0 \tag{3-13}$$

where v is the variable of velocity, a and b are the lower and upper bounds of traffic speed to determine the range of the distribution and $B(\alpha, \beta)$ is the beta function, which has the formula:

$$B(\alpha, \beta) = \int_0^1 t^{\alpha-1}(1-t)^{\beta-1} dt \qquad \alpha, \beta > 0 \tag{3-14}$$

The probability distribution of the vehicle component can be expressed as

$$p \sim N(\mu, \sigma^2) \tag{3-15}$$

where N (*) is the normal distribution, μ is the mean, and σ^2 is the variance. Both the mean and variance determine the shape and the range of the PDF. The general formula for

the PDF of the normal distribution is:

$$f(p;\mu,\sigma^2) = \frac{1}{\sigma\sqrt{2\pi}} \exp\left(-\frac{(p-\mu)^2}{2\sigma^2} \right) \tag{3-16}$$

where p is the vehicle component variable.

Traffic flow is another uncertain input represented by empirical distribution in the literature (Lam and Tam, 1998). Different traffic locations have different flow distributions. Moreover, there are different traffic patterns during daytime and nighttime at a given location. In this study, the traffic flow distributions are assumed to be continuous uniform distributions in each scenario. The traffic flow distributions can be generally expressed as:

$$Q \sim U(a,b) \tag{3-17}$$

where U (*) is the traffic flow, and a and b are the lower and upper bounds of traffic flow. The PDF formula of the continuous uniform distribution is:

$$f(Q) = \frac{1}{b-a} \qquad for \quad a \le Q \le b \tag{3-18}$$

where Q is the variable of traffic flow.

A Monte Carlo simulation involves repeated generation of pseudovalues for the modeling inputs, drawn from known probability distributions within the ranges of

possible values. In this study, three random values for the uncertain factors (traffic flow, traffic speed and vehicle components) are produced synchronously at each time. The generated pseudovalues are then used as inputs for the modified FHWA model. The Monte Carlo simulation includes the following steps: (1) the development of the representative probability distribution functions for selected model input parameters, (2) the generation of the pseudovalues for each of the selected input parameters from the distribution developed in the previous step, (3) the implementation of the modified FHWA model with the pseudovalues, (4) repeat steps 2 and 3, (5) the representation of the results in the probability distribution function, and (6) the analysis of the probability distribution function of the model output for decision making (Hoogeweg, 1999).

3.2.3. Integrated fuzzy theory assessment

The noise abatement criteria (NAC), issued by FHWA, categorizes sound into 5 levels (shown in Table 3-1). The assessment of traffic noise impact is carried out by comparing the predicted noise level or the measured noise level with the regulated values in the NAC. The limitation of this straightforward method is that only the deterministic value (or the certain value) of noise could be used in this comparison. The sound level, however, actually should be reflected by a range of values, and usually could be demonstrated by a kind of possibility distribution as discussed above.

Previous studies (Calixto et al., 2003; Diehl, 1998; Lam and Tam, 1998; Ohta et al., 1980; Sopasakis, 2004) applied the mean value of the possibility distribution to represent the noise level without considering the variance. When the variance of the

Table 3-1 Noise abatement criteria (NAC)—hourly A-weighted sound level in dBA

Activity Category	L_{eq}	Description of Activity Category
A	57 (Exterior)	Lands on which serenity and quiet are of extraordinary significance and serve an important public need and where the preservation of those qualities is essential if the area is to continue to serve its intended purpose.
B	67 (Exterior)	Picnic areas, recreation areas, playgrounds, active sports areas, parks, residences, motels, hotels, schools, churches, libraries, and hospitals.
C	72 (Exterior)	Developed lands, properties, or activities not included in Categories A or B above.
D	--	Undeveloped lands.
E	52 (Interior)	Residences, motels, hotels, public meeting rooms, schools, churches, libraries, hospital, and auditoriums.

Source: 23 Code of Federal Regulations (CFR) Part 772, FHWA

distribution is small enough, the result might be acceptable in this case, but if the variance were large, the result might be wrong. For instance, the measured noise level in a residential area follows the normal distribution with a mean value of 65 dBA and a variance of 10^2. The mean falls in category B of the NAC that represents a good residential noise level even though there might be many complaints about the noise due to annoyance. This is because the noise level exceeded 65 dBA for a few hours a day, which is reflected by the large variance.

In order to solve this contradiction, fuzzy set and binary fuzzy relations theory is introduced in the noise impact assessment. A brief introduction to the concept of fuzzy set and binary fuzzy relations is presented as follows.

3.2.3.1. Fuzzy sets and binary fuzzy relations

According to Zadeh (1965), if X is a collection of objects denoted by x, a fuzzy set A in X is then a set of ordered pairs defined as follows:

$$\underset{\sim}{A} = \left\langle \left(x, \mu_{\underset{\sim}{A}}(x) \right) \middle| x \in X \right\rangle \tag{3-19}$$

where $\mu_{\underset{\sim}{A}}(x)$ is the membership function of x in $\underset{\sim}{A}$ that maps X to an evaluation set [0,1]. The closer the membership value of $\mu_{\underset{\sim}{A}}(x)$ to unity, the more certain it is that x belongs to $\underset{\sim}{A}$. For fuzzy sets $\underset{\sim}{A}$ and $\underset{\sim}{B}$, some of their basic operations can be summarized as follows (Bellman and Zadeh, 1970):

Inclusion: $\underset{\sim}{A}$ *is included in* $\underset{\sim}{B}$ *iff* $\mu_{\underset{\sim}{A}}(x) \le \mu_{\underset{\sim}{B}}(x)$*;* (3-20)

Equality: $\underset{\sim}{A}$ *is equal to* $\underset{\sim}{B}$ *iff* $\mu_{\underset{\sim}{A}}(x) = \mu_{\underset{\sim}{B}}(x)$*;* (3-21)

Complementation: $\underset{\sim}{A}$ *and* $\underset{\sim}{B}$ *are complementary iff* $\mu_{\underset{\sim}{A}}(x) = 1 - \mu_{\underset{\sim}{B}}(x)$*;* (3-22)

Intersection: $\underset{\sim}{A} \cap \underset{\sim}{B}$*;* $\mu_{\underset{\sim}{A}\cap\underset{\sim}{B}}(x) = Min\left\{\mu_{\underset{\sim}{A}}(x), \mu_{\underset{\sim}{B}}(x)\right\} = \mu_{\underset{\sim}{A}}(x) \cap \mu_{\underset{\sim}{B}}(x)$*;* (3-23)

Union: $\underset{\sim}{A} \cup \underset{\sim}{B}$*;* $\mu_{\underset{\sim}{A}\cup\underset{\sim}{B}}(x) = Max\left\{\mu_{\underset{\sim}{A}}(x), \mu_{\underset{\sim}{B}}(x)\right\} = \mu_{\underset{\sim}{A}}(x) \cup \mu_{\underset{\sim}{B}}(x)$*;* (3-24)

Binary fuzzy relations are fuzzy subsets of $X \times Y$ that are mappings for $X \Rightarrow Y$ (Zimmermann, 1985). (1) Let $X, Y \subseteq \underset{\sim}{R}$ be the universal sets, and then:

$$\underset{\sim}{R} = \left\langle \left((x,y), \mu_{\underset{\sim}{R}}(x,y) \right) \middle| (x,y) \subseteq X \times Y \right\rangle \tag{3-25}$$

is called a fuzzy relation on $X \times Y$, and (2) Let $\underset{\sim}{X} = \left\langle x_{ij} \middle| i = 1,2,...,m;\ j = 1,2,...,n \right\rangle$ and $\underset{\sim}{Y} = \left\langle y_{ij} \middle| i = 1,2,...,m;\ j = 1,2,...,n \right\rangle$ be two $m \times n$ fuzzy relation matrices. Then a $m \times n$ fuzzy matrix $\underset{\sim}{B}$ can be obtained as follows:

$$\underset{\sim}{B} = \underset{\sim}{X} \bullet \underset{\sim}{Y} = \left\langle b_{ij} \middle| i = 1,2,...,m;\ j = 1,2,...,n \right\rangle \tag{3-26}$$

According to the principle of fuzzy set operation, $\underset{\sim}{B}$ can be determined by a MAX-MIN composition (Zadeh, 1971) as:

$$b_j = \sum_{i=1}^{m}\left(x_{ij} \cap y_{ij}\right) = max\left\{min\left(x_{1j}, y_{1j}\right), min\left(x_{2j}, y_{2j}\right), ..., min\left(x_{mj}, y_{mj}\right)\right\} \quad (3\text{-}27)$$
$$j = 1,2,...,n$$

3.2.3.2 Application of fuzzy theory for qualitative analysis

Redesigning the deterministic noise abatement criteria (NAC) is the first step for the qualitative analysis of traffic noise impact. It has been mentioned previously that some factors will affect the accuracy of the assessment, such as variations in the hearing of individuals. Additionally the noise criteria during the day are different to that during night. Using fuzzy sets to modify noise limits is an innovative method for noise impact assessment. Considering the regulations for community noise (shown in Table 3-2), the new criteria can be classified into four categories: quiet, normal, annoyance, and severe-annoyance. Correspondingly, a fuzzy set of this fuzzy criterion (Figure 3-2) is defined as follows:

$$\mu_{Ci}(x) = \begin{Bmatrix} \mu_{C1}(x) / Quiet \\ \mu_{C2}(x) / Normal \\ \mu_{C3}(x) / Annoyance \\ \mu_{C4}(x) / Severe - annoyance \end{Bmatrix} \quad (3\text{-}28)$$

The membership functions are defined as follows:

$$\mu_{C1} = \begin{cases} 1 & x \le 49 \\ (55 - x)/6 & 49 < x < 55 \\ 0 & x \ge 55 \end{cases} \tag{3-29}$$

$$\mu_{C2} = \begin{cases} 1 & x = 57 \\ (x - 52)/5 & 52 < x < 57 \\ (65 - x)/8 & 57 < x < 65 \\ 0 & x \le 52 \text{ or } x \ge 65 \end{cases} \tag{3-30}$$

$$\mu_{C3} = \begin{cases} 1 & x = 67 \\ (x - 59)/8 & 59 < x < 67 \\ (72 - x)/5 & 67 < x < 72 \\ 0 & x \le 59 \text{ or } x \ge 72 \end{cases} \tag{3-31}$$

$$\mu_{C4} = \begin{cases} 1 & x \ge 75 \\ (x - 69)/6 & 69 < x < 75 \\ 0 & x \le 69 \end{cases} \tag{3-32}$$

The NAC is represented in fuzzy form with a membership function value from 0 to 1, but the simulation result generated by the Monte Carlo approach is a distribution that cannot be directly compared with fuzzy values. Therefore, the output undergoes a conversion to make it compatible with the NAC. In order to perform fuzzy operation, we convert a distribution function into a fuzzy set, allowing the probability of mean value to be 1. The corresponding membership function can be defined as:

Table 3-2 Example of the use of noise zones (day/night)

Zone	Planning	Alternative	Alarm
Recuperation	50/40	55/45	65/60
Residential	55/45	60/50	70/65
Mixed	60/50	65/55	70/65
Industrial	65/55	70/60	75/70

Source: Dieter Gottlob, Noise/News International Dec. 1995

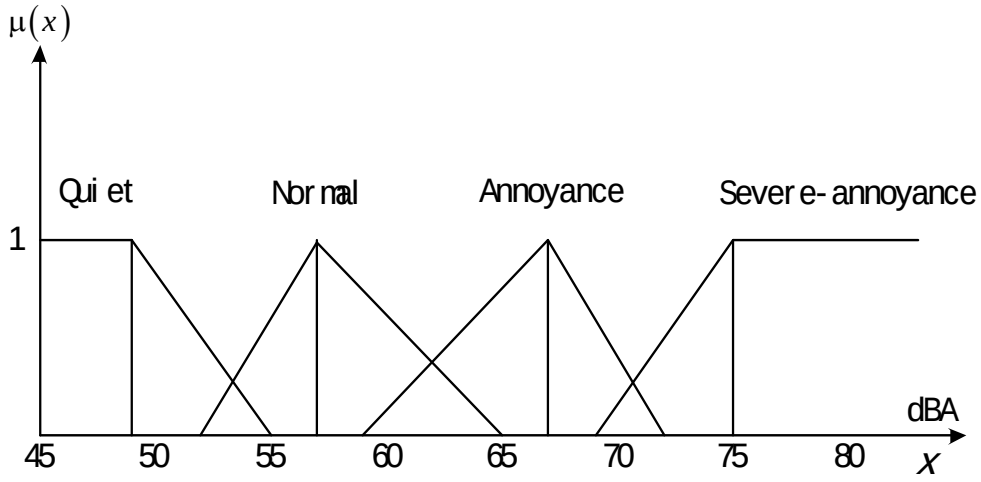

Figure 3-2 The fuzzy noise abatement criteria

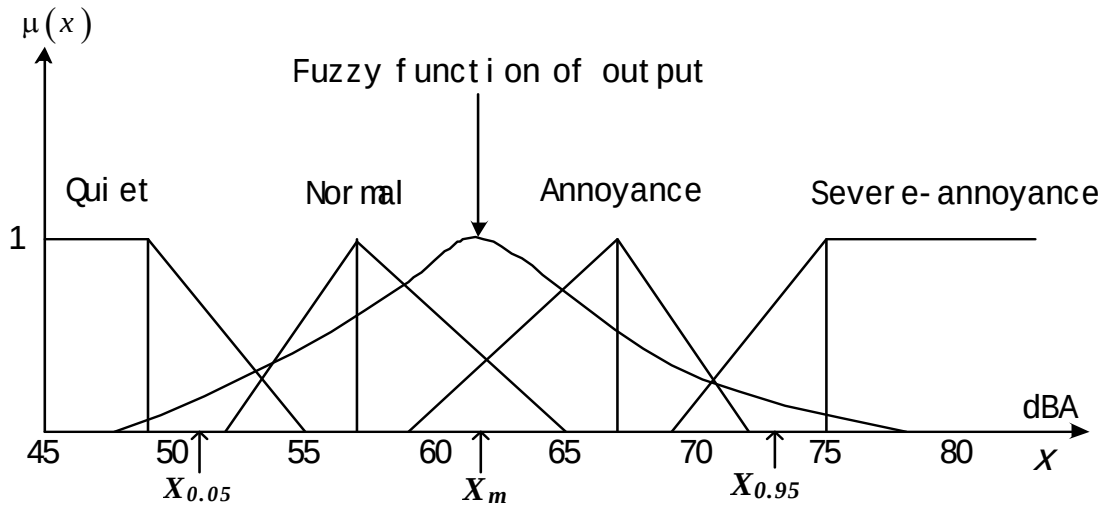

Figure 3-3 The comparison of the probability distribution and fuzzy noise abatement criteria

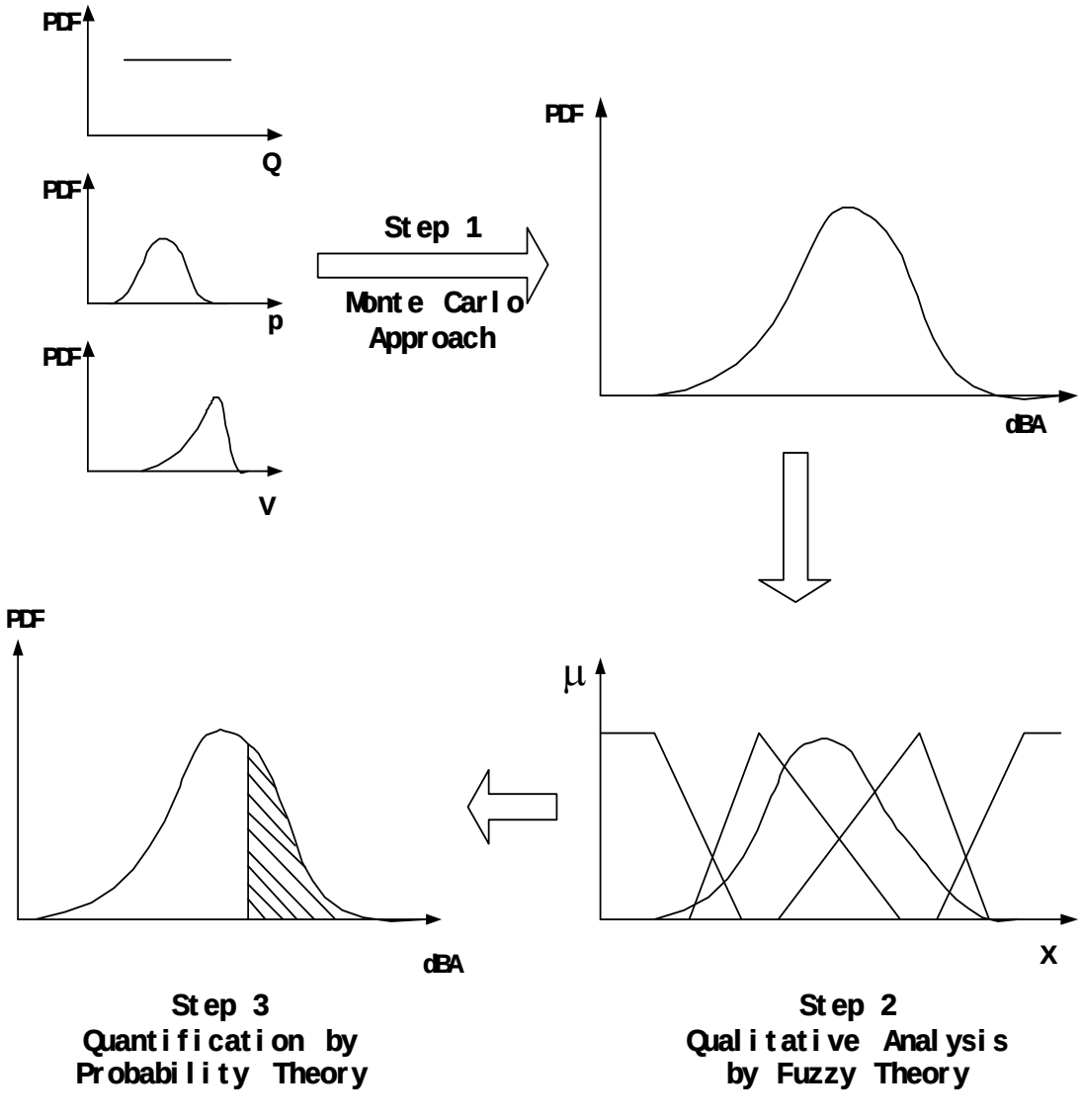

Figure 3-4 The noise impact assessment procedure

$$\mu_R(x) = \tilde{f}(x) \qquad \mu_R(x) \in [0,1] \tag{3- 33}$$

Using MAX-MIN composition, the following result is obtained:

$$\begin{aligned} b &= \sum_{i=1}^{4} (\mu_{Ci} \cap \mu_R) \\ &= max\{min(\mu_{C1}, \mu_R), min(\mu_{C2}, \mu_R), min(\mu_{C3}, \mu_R), min(\mu_{C4}, \mu_R)\} \end{aligned} \tag{3-34}$$

If the simulation result is a normal distribution, *f (x),* the membership function of related fuzzy set of the output could be defined as follows:

$$\mu_R = \sqrt{2\pi\sigma^2}\, f(x) = e^{-\frac{(x-\mu)^2}{2\sigma^2}} \tag{3-35}$$

For example, it assumes that a calculated noise level is a normal distribution defined as N (62.5, 5.612^2), which is of x_m = 62.5 dBA, $x_{0.95}$ = 51.5 dBA and $x_{0.05}$ = 73.5 dBA. $x_{0.95}$ is defined as the value that is exceeded by 95% of the output; $x_{0.05}$ is defined as the value that is only exceeded by 5% of the output; x_m is the mean value (shown in Figure 3-3). According to Equation 3-34, the maximum value of intersections between fuzzy output and four fuzzy criteria is 0.845. This value belongs to the membership grade of $(\mu_R \cap \mu_{C3})$, which identifies the predicted noise that exceeds the fuzzy criterion of annoyance.

3.2.4. Quantification of noise impact

More specifically, the assessment of noise impact level could be expressed using the probability of a predicted noise level exceeding a prescribed limited level, for example, $P_F = P(L \geq C)$. Thus, the noise impact can be quantified as follows:

$$P_F = P(L \geq C) = \int_0^{\infty} \left\{ \int_0^{L} f_{LC}(L,C)\, dC \right\} dL \tag{3-36}$$

where P_F = the impact level quantified as the probability of exceeding the noise emissions, f_{LC} = the probability density function of Monte Carlo output, L = random number of the predicted noise, and C = random number of the noise limit.

If random number C could be defined by local noise abatement guidelines ($C = C_o$), then the noise impact could be quantified as follows:

$$P_F = P(L \geq C_o) = \int_{C_o}^{\infty} f_L(L) dL \tag{3-37}$$

The scheme of noise impact assessment is illustrated in Figure 3-4. It was observed that the predicted noise level exceeds the limit of the annoyance (C_o = 67 dBA). According to Equation 3-37, this noise level is quantified as P_F = 0.22, which means that about 22% of output samples exceed the annoyance criterion.

3.3. Case study

Many factors influence the generation of traffic noise, such as traffic speed, traffic flow, traffic components, road surface conditions, road gradient and distance. To further illustrate the approach of assessing traffic noise impact level under uncertainty, the modified FHWA model is applied while considering the variables of noise, speed, traffic flow and components.

The study site is a Canadian highway in Saskatchewan, Canada. This site has detailed traffic records including hourly, daily and weekly traffic information from the beginning of 1999 to the end of 2000, collected by Saskatchewan Highways and Transportation. This site is the representative of a typical Canadian highway and has typical Canadian highway traffic information and road conditions. On this site, the road surface is covered by smooth asphalt without any 5 mm deep random grooving, gradients, or noise barriers.

The data of traffic speed and components at this site from January 1999 to December 2000 can be fitted into the following possibility distributions:

$$p_L \sim N\left(\mu,\sigma^2\right) = N\left(0.545,0.109^2\right) \tag{3-38}$$

$$p_M \sim N\left(\mu,\sigma^2\right) = N\left(0.008,0.003^2\right) \tag{3-39}$$

$$p_H \sim N\left(\mu,\sigma^2\right) = N\left(0.447,0.108^2\right) \tag{3-40}$$

$$V \sim Beta(\alpha,\beta) = B(0.915,0.684)\times 24.31 + 89.33 \tag{3-41}$$

Table 3-3 Traffic record on the study site (May 17, 2004)

Time	L_{eq} dBA	Flow& Heavy vehicle (hourly)	Average Speed (km/h)
7:00~9:00	67.9	1812/280	110
9:00~11:00	69.1	2128/312	112
11:00~13:00	71.0	2028/300	108
13:00~15:00	72.9	2428/336	105
15:00~17:00	70.3	2320/356	111
17:00~19:00	71.2	1916/286	108
19:00~21:00	69.5	1404/216	108
21:00~23:00	67.8	1184/152	95
23:00~1:00	64.5	984/164	100
1:00~3:00	63.7	996/128	98
3:00~5:00	63.0	804/136	110
5:00~7:00	66.9	1008/264	110

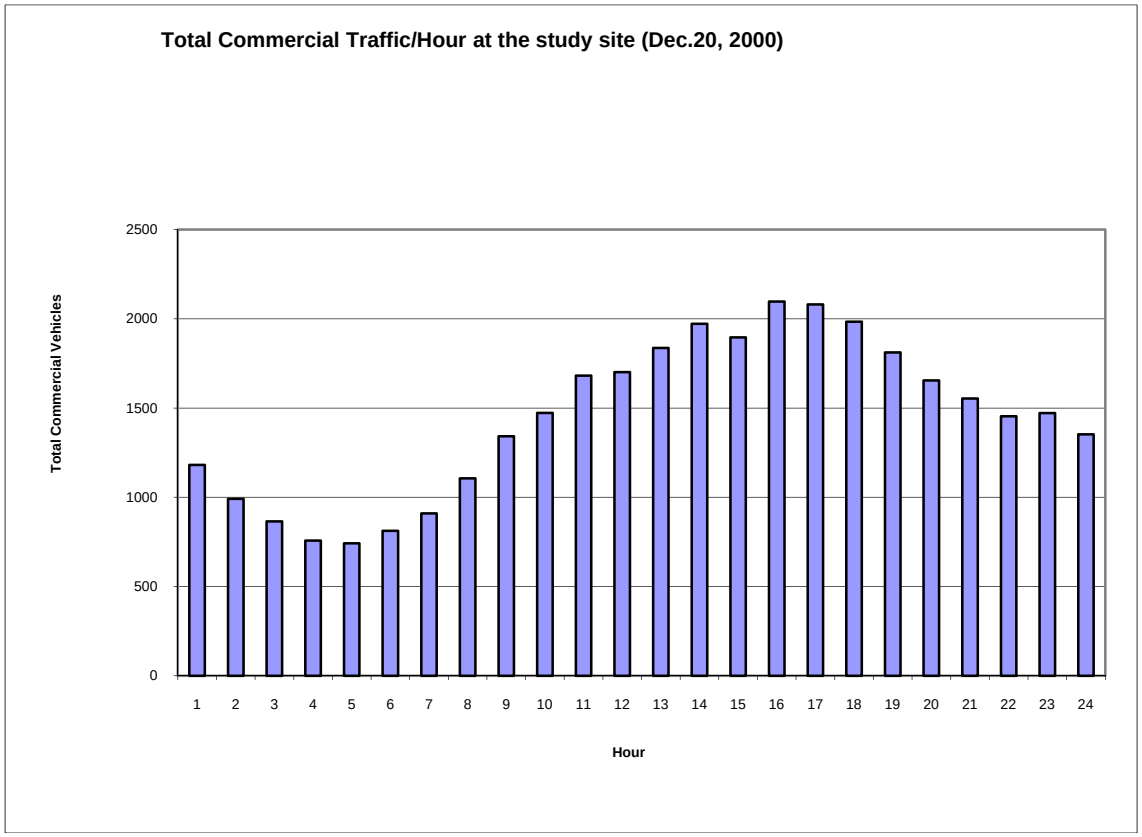

Figure 3-5 The cumulated hourly traffic flow

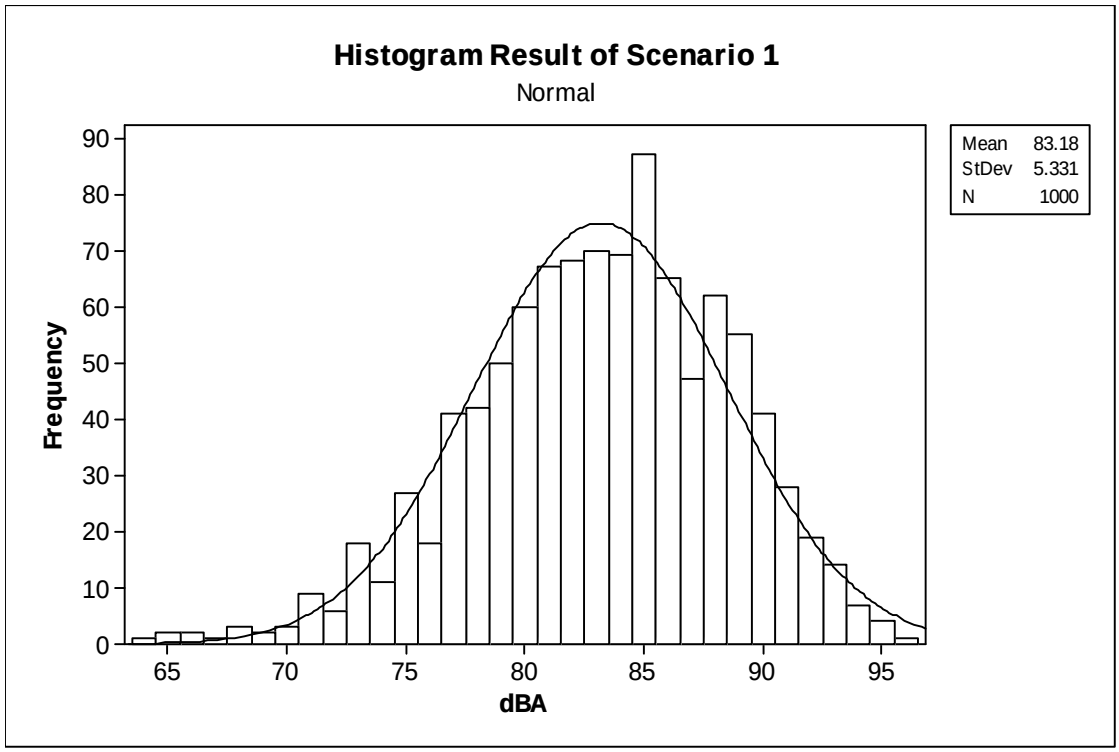

Figure 3-6 The histogram result of scenario 1

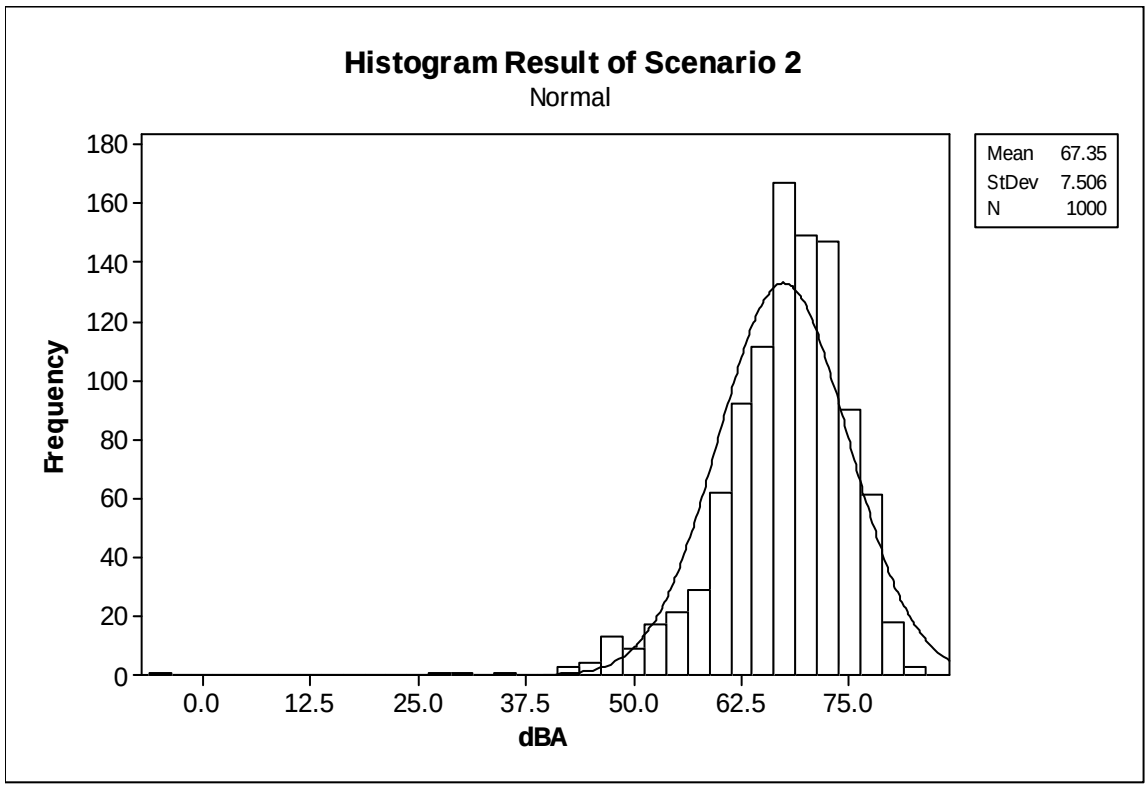

Figure 3-7 The histogram result of scenario 2

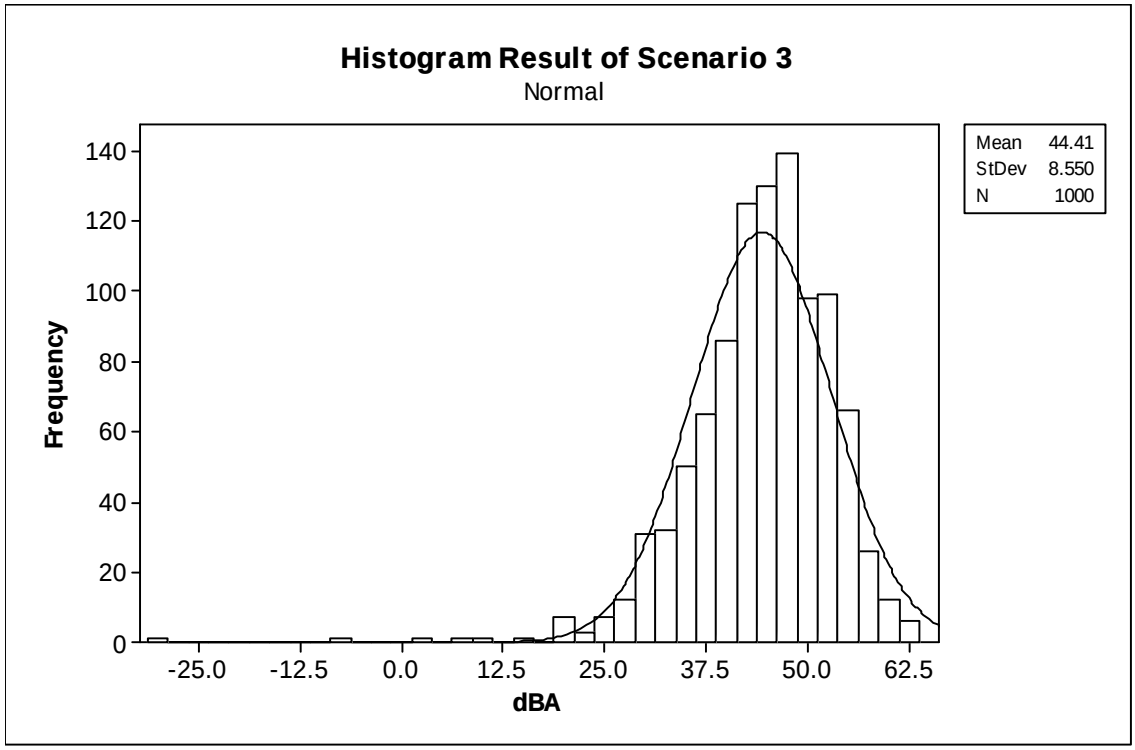

Figure 3-8 The histogram result of scenario 3

The traffic flow at the study site did not show any well-defined probability distribution function (Figure 3-5 illustrates the cumulated hourly traffic flow on December 20, 2000). Therefore, the traffic flow on this site was assumed to follow a uniform distribution

$$Q \sim U\,(891,\ 1936) \tag{3-42}$$

Since the surveillance of Saskatchewan Highways and Transportation did not include traffic noise, another measurement had to be carried out. The noise meter that was used was a Type 2260 Modular Precision Sound Analyzer made by Brüel & Kjær. It was located at a distance of 15 m from the centerline of the closest traffic lane as well as a height of 1.2 m above the local ground level. This noise measurement lasted three days, from May 16 to May 18 in 2004 (a daily record is listed in Table 3-3). In this record, the vehicle components were recorded manually in terms of 13 typical vehicle types of FHWA (US Department of Transportation, 1995). Those vehicle types were eventually classified into three classes: light, medium and heavy. It was found that the rate of medium vehicles was less than 1%.

In terms of the reference mean emission energy level provided by FHWA (shown in Figure 3-1), the basic traffic noise level at a reference distance of 15 m is:

$$\begin{aligned}\Delta L_o &= aLogQ_A + bLogV + c \\ &\quad + aLog\left[\, p_L\left(8.13\times10^{-5}V^{1.34}\right) + p_M\left(6.17\times10^{-3}V^{0.93}\right) + p_H \,\right]\end{aligned} \tag{3-43}$$

The observed traffic data including traffic noise level, traffic speed, traffic flow and traffic components, were then used to calibrate the above equation using the linear regression method using MATLAB. The basic noise prediction model is generated as:

$$\begin{aligned}\Delta L_o &= 38.32 Log Q_A + 8.01 Log V - 25.94 \\ &\quad + 38.32 Log\left[p_L \left(8.13\times 10^{-5} V^{1.34}\right) + p_M \left(6.17\times 10^{-3} V^{0.93}\right) + p_H \right]\end{aligned} \tag{3-44}$$

$$R^2 = 0.886$$

Three different traffic scenarios were designed for predicting the future noise emission on the study site

1) Traffic flow $Q^H \sim U$ (*1100, 2100*), traffic speed $V^H \sim B(0.915,0.684)\times 24.31 + 89.33$, and heavy vehicle component $p_H^H \sim N(0.447,0.108^2)$.
2) Traffic flow $Q^M \sim U$ (*800, 1800*), traffic speed $V^M \sim B(0.915,0.684)\times 24.31 + 89.33$, and heavy vehicle component $p_H^M \sim N(0.220,0.082^2)$.
3) Traffic flow $Q^L \sim U$ (*500, 1300*), traffic speed $V^L \sim B(0.915,0.684)\times 24.31 + 89.33$, and heavy vehicle component $p_H^L \sim N(0.112,0.051^2)$.

These three traffic scenarios use the same traffic speed due to the same speed limitation on the highway. The random variables were automatically generated by using statistical software based on the designed distributions. Each group of random data (Q_A, V and p) will result in one predicted noise emission sample by applying the Monte Carlo

approach. The procedure of the noise impact assessment is illustrated in Figure 3-4. The simulated results of the three scenarios are shown in Figures 3-6 to 3-8. It was found that the outputs of traffic noise in three scenarios are all subject to normal distributions. The following results have been obtained:

1) The result of scenario 1 is subject to a normal distribution of $N\ (83.18, 5.331^2)$, and this predicted noise exceeds the fuzzy criterion of severe-annoyance by 97.3% (See Figure 3-6).
2) The result of scenario 2 is subject to a normal distribution of $N\ (67.35, 7.506^2)$, and this predicted noise exceeds the fuzzy criterion of annoyance by 58.5% (See Figure 3-7).
3) The result of scenario 3 is subject to a normal distribution of $N\ (44.41, 8.550^2)$, and this predicted noise satisfies the fuzzy criterion of quiet (Figure 3-8).

3.4. Summary

In this study, a hybrid stochastic-fuzzy approach for noise impact level assessment is proposed. This method can reflect uncertainties associated with the simulation results and environmental guidelines. This research includes: (1) the effect of traffic noise emission under uncertainty, (2) the relationship between noise emission and related factors such as traffic flow, traffic speed, and vehicle components, (3) the fuzzy qualitative analysis for noise impact level using fuzzy noise abatement criteria, and (4) the probability analysis for the quantification of noise impact. The advantages of this

approach over previous studies are that it not only addresses the uncertainty of noise emission using the Monte Carlo technique but also includes the uncertainty of noise abatement criteria using fuzzy theory. Meanwhile, both qualitative analysis and quantification are applied for the assessment of noise impact levels. This methodology is applied to a highway for predicting noise emission levels and impact levels in three different design scenarios. The results indicate the reasonable solutions have been generated. It is useful for clarifying the effects of noise and supplying important information for city planning.

In next Chapter 4, two innovative approaches are developed to deal with uncertainty in water distribution systems. One is used to assess hydraulic reliability, and the other is used to design a reliability-based optimal schedule of rehabilitation & upgrade.

CHAPTER 4

Hydraulic Reliability Assessment and Optimal Schedule of Rehabilitation and Upgrade in Water Distribution Systems under Uncertainty

4.1. Statement of problems

Water distribution systems (WDSs) require huge investments in their construction and maintenance (Peng and Mayorga, 2010e). For this reason, it is necessary to improve their efficiency by minimizing their costs and maximizing their benefits. In recent decades, a significant number of optimization methods have been developed using linear programming, dynamic programming, enumeration techniques, heuristic methods, and evolutionary techniques (Prasad and Park, 2004). However, water distribution systems are so complex that most of the research only addressed partial issues. For example, the previous optimal maintenance schedule studies, rather than focusing on both hydraulic capacity and mechanical failure, concentrated on only one of them. This study conducts a comprehensive research on WDS, which includes a hydraulic reliability assessment and a rehabilitation & upgrade schedule (RUS) optimization.

Hydraulic reliability assessment is used to study the deterioration of the structural integrity and hydraulic capacity of WDSs; in other words, it is used to study mechanical failure and hydraulic failure. However, there are no universally accepted definitions for hydraulic reliability (Mays 1996). In this chapter, hydraulic reliability is defined as "the ability of a distribution system to meet the demands that are placed on it,

where demands are specified in terms of: (i) the flow to be supplied, and (ii) the range of pressure at which these flow rates must be provided" (Goulter, 1995). Hydraulic failures occur when the demand nodes do not receive sufficient flow and/or adequate pressure due to old pipes with low roughness that arising from corrosion and deposition, increases of demand and pressure head requirements, inadequate pipe sizes, insufficient pumping or/and storage capabilities. In addition, due to the fact that the demand is spatially and temporally distributed, hydraulic failures at critical locations in the distribution system might be more important than the average system reliability (Cullinane, 1989). Mechanical failures involve pipe breakages, pump failures, power outages, and control valve failures. Mechanical failure of the infrastructure components is also integrally linked with hydraulic failure. For instance, pipe breakage is a mechanical failure, and the occurrence of a pipe break will eventually result in an insufficient flow rate and/or inadequate pressure head on the demand nodes.

In the previous studies, two methodologies were developed to compute hydraulic reliability. One is Monte-Carlo simulation (MCS) technique, which can bring more accurate reliability estimation (Bao and Mays, 1990) but requires a large number of trials to ensure accuracy, thereby resulting in a computationally inefficient problem. Another is a linear probabilistic hydraulic model, called the "first-order reliability method" (Madsen et al., 1986; Xu and Goulter, 1998), which can overcome the computationally inefficient problem in MCS but has a lower accuracy. Due to the rapid development of computer technology, MCS has demonstrated its superiority in hydraulic reliability computation. In this chapter, MCS is chosen to calculate the probabilistic problem of hydraulic reliability. Free simulation software, EPANET, is incorporated with MCS to evaluate the nodal and

system reliability of a water distribution system. It is worth noting that the hydraulic reliability assessment here only refers to the hydraulic failure measurement and not to the mechanical failure measurement.

The RUS optimization model in this study is based on the hydraulic reliability assessment. It is subdivided into two stages. The first stage is to design a pipe upgrade/parallel plan due to hydraulic failure potential. This stage is a total failure stage because hydraulic failure direct results in insufficient flow and/or inadequate pressure. The second stage is to schedule a pipe repair/replacement plan due to mechanical failure potential. Mechanical failure only indirectly influences water supply on the demand nodes. For example, an occurrence of pipe break in a parallel pipe system might only slightly affect the water flow rate and/or water pressure, but water supply might still be sufficient.

The previous studies used various methodologies to study the optimal maintenance schedule in pipe networks focusing on either the hydraulic capacity or mechanical failure. In the hydraulic failure based studies, the earlier studies used the linear programming (Quindry et al., 1981) while the later studies utilized nonlinear programming (Lansy and Mays, 1989; Xu and Goulter, 1999). Much of the recent literature includes genetic algorithms for the determination of the lowest repair or replacement costs (Tolson et al., 2004; Prasad and Park, 2004). Their research has shown several advantages over more traditional optimization methods (Savic and Walters, 1997). In the mechanical failure based studies, Shamir and Howard (1979) applied regression analysis to obtain a relationship for the breakage rate of a pipe as a function of time. Ascher and Feingold (1984) gave a threshold break rate function used a statistical

reliability model. Deb et al. (1998) suggested a probabilistic failure model to estimate miles of pipes to be replaced on an annual basis.

Here, two innovative approaches in a WDS are presented. One is to assess hydraulic reliability that accounting for the deterioration of both structural integrity and hydraulic capacity of each pipe; another is to design a reliability-based optimal RUS considering both hydraulic failure potential and mechanical failure potential. The proposed approaches are written into two universal codes: the hydraulic reliability code and the optimal RUS code. They are based on MATLAB and linked to EPANET (free hydraulic software developed by USEPA). The applicability of the approaches (via the two codes) has been verified by an example in a benchmark water distribution system.

4.2. Methodology

4.2.1. Hydraulic reliability assessment

Hydraulic failure occurs when a demand node does not receive sufficient flow and/or adequate pressure. The reasons include high roughness of old pipes arising from corrosion and deposition, increases of demand and pressure head requirements, inadequate pipe sizes, insufficient pumping or/and storage capabilities. Mechanical failures involve pipe breakages, pump failures, power outages, and control valve failures. The mechanical failure of infrastructure components is integrally linked with hydraulic failure. For instance, pipe breakage is a mechanical failure, and the occurrence of a pipe break eventually results in an insufficient flow rate and/or inadequate pressure head on

the demand nodes.

4.2.1.1. Nodal hydraulic failure probability

Hydraulic failure can occur at a given node when the supplied flow or pressure is less than the required minimum flow or required minimum pressure at that node. The hydraulic simulator in EPANET always satisfies water demand but pressure head because it applies the nodal mass balance equation. Similarly, this approach assumes that water demand is satisfied. The nodal mass balance equation can be expressed as:

$$D_i + \sum_{j \in \Omega} f_{ij}(H_i - H_j) = 0 \qquad i = 1, 2, ..., N \qquad (4 - 1)$$

where D_i is demand at node i, H_i is head at node i, H_j is head at node j, N is total number of the demand nodes with unknown heads, Ω is set of nodes connected directly to node i, and $f_{ij}(*)$ is an nonlinear function relating the hydraulic loss and flow rate in the pipe connecting node i to node j. In this study, the nonlinear function, $f_{ij}(*)$, is the Hazen-Williams or the Colebrook-White equation.

In the above equation, the nodal pressure head is an unknown decision variable, and water demands are state variables. This equation can be expressed in a more compact form:

$$F_i(H_i, X_i) = 0 \qquad i = 1, 2, ... N \qquad (4 - 2)$$

where $F_i(*)$ is a vector of functions representing the mass balance at each node, H_i is a vector of supplied pressure heads at each node, $X_i = (x_1, x_2 \ldots x_k)_i^T$ is a vector of state variables, and k is the total number of variables.

In the study of hydraulic failure, water demands, D_i, pipe coefficients, C_i, and tank/storage levels, L_i, are defined as known state variables. Thus, the vector of state variables in this study can be expressed as $X_i = (D_i, C_i, L_i)^T$ (T represents the matrix transposition operation). Moreover, due to uncertainty, those known state variables are treated as random values. Each random variable is expressed as a probability distribution, and then a random number generator is used to generate the values of D_i for each node, the values of C_i for each pipe, and the values of L_i for each tank/storage unit. When incorporated with EPANET, the Monte Carlo simulation (MCS) technique can be applied to produce the random pressure head values.

EPANET is free public hydraulic software developed by USEPA. It performs extended period simulations of hydraulic behavior within pressurized pipe networks. A network consists of pipes, nodes, pumps, valves and storage tanks or reservoirs. EPANET tracks the flow water in each pipe, the pressure at each node, and the level of water in each tank during a simulation period. Running under Windows, EPANET provides an integrated environment for editing network input data, running hydraulic and water quality simulations, and viewing the results in a variety of formats. In this study, water demands, pipe coefficients, and tank/storage levels constitute the input data during the simulation; pressure heads are outputs. It is assumed that pumps and valves are in good operating condition. The failure of pumps and valves is considered mechanical failure.

Monte Carlo Simulation involves the repeated generation of pseudovalues for

the modeling inputs, drawn from known probability distributions within the ranges of possible values. In this study, this process will be completed by a computer, in which three random variables (water demand, D_i, pipe coefficients, C_i, and tank/storage level, L_i) are produced synchronously at each time. The generated pseudovalues are then used as inputs for the EPANET model to produce the supplied pressure head values of H_i. The Monte Carlo simulation implementation in a node, i includes the following steps: (1) the development of the representative probability distribution functions for selected model input parameters, (2) the generation of pseudovalues for each of the selected input parameters from the distribution developed in the previous step, (3) the implementation of EPANET model with the pseudovalues to generate a pressure head value of H_i, (4) a comparison of the calculated value of H_i with the minimum allowable head H_i^L, (5) the repeated application of the previous two steps, and (6) a presentation and analysis of the results for decision making.

In Step (4) of the above MCS procedure, H_i^L is defined as the minimum allowable head at a demand node. Thus, the probability of hydraulic performance failure at a demand node can be expressed as:

$$P_i^H = P(H_i < H_i^L \left| D_i^S = D_i^D \right.) = \int_0^{H_i^L} f\,(H_i) dH_i \qquad (4-3)$$

where $f(H_i)$ is the probability density function of the supplied pressure head, D_i^S is the supplied flow rate at the node i, and D_i^D is the water demand at the node i.

4.2.1.2. Mechanical failure probability

Mechanical failure involves pipe breakages and electric component failures (such as pump failures, power outages, and control valve failures). There are many factors that could cause pipe breaks, for instance, aging, physical bending stress, and chemical and biological corrosion. Among these factors, aging, material type, dimension, and bedding quality are important factors in predicting pipe breakage. Shamir and Howard's (1979) exponential break rate model is such prediction model that describes an exponential relationship between aging and breakage. It is shown as:

$$P(t)_j^p = P(t_0)_j^p e^{A_j (t-t_0)_j} \qquad j = 1, 2, ..., M \qquad (4-4)$$

where A_j is the growth rate coefficient of the pipe j, $P(t)_j^p$ is the number of breaks per 1000 ft. length of pipe j in year t, t is time in years, t_0 is base year for the analysis (pipe installation year, or the first year for which data are available), and M is total number of pipes.

A primary cause of unreliability is the removal of water lines or pumps from service due to breaks or power outages. The probability of an electromechanical component P_k^E ($k = 1, 2, \ldots, U$; *where* U is total number of electric components), such as a pump or a valve, being out of service can be included as another random variable that is supported by historical data.

4.2.1.3. System hydraulic reliability assessment

Different water demand has different important rank. For example, a hospital water demand has the highest important rank, and the water demand of a park area might have a lower important rank. Failure probabilities are weighted to reflect their different important rank. Then, the system failure probability P_S can be defined as the maximum individual failure probability in the system

$$P_S = Max(W_i P_i^H, W_j P_j^P, W_k P_k^E, W^F P^F) \quad (4-5)$$

where W_i, W_j, W_k, W^F are the weighting coefficients, P_i^H is the probability of hydraulic performance failure at the node *i*, P_j^P is the failure probability of pipe *j*, P_k^E is the failure probability of electromechanical component *k*, and P^F is the fire flow failure probability.

The system hydraulic reliability, R_S , is given by:

$$R_S = 1 - P_S \quad (4-6)$$

4.2.2. Optimal rehabilitation & upgrade schedule

A long term maintenance plan of WDSs is an important issue for municipal agents. These agents have paid special attention to improve the efficiency of their planning by minimizing costs and maximizing benefits. However, water distribution systems are so complex that most of the research only addressed partial issues. For

example, the previous optimal maintenance schedule studies only focused on either hydraulic failure or mechanical failure, and not both of them. This study develops an innovative model that includes the deterioration of both the structural integrity and hydraulic capacity of every pipe, and optimizing the RUS for a WDS.

The water network maintenance includes the rehabilitation and upgrade. So, the maintenance schedule is subdivided into two stages. The first stage is to design a pipe upgrade/parallel plan due to hydraulic failure potential. This stage is a total failure stage because hydraulic failure direct results in insufficient flow and/or inadequate pressure. The second stage is to schedule a pipe repair/replacement plan due to mechanical failure potential. Mechanical failure only indirectly influences water supply on the demand nodes. For example, an occurrence of pipe break in a parallel pipe system might only slightly affect the water flow rate and/or water pressure, but water supply might still be sufficient.

It's worth noting that "potential" is used to describe hydraulic failures and mechanical failures. Both prediction models of hydraulic failure and mechanical failure are based on the hydraulic reliability assessment. The hydraulic failure probability is assessed using Monte Carlo simulation, and the pipe breakage probability is computed using Shamir and Howard's exponential break rate model (shown in Equation 4-4). Because mechanical failure probability is obtained in terms of historical data, the optimal upgrading results will not affect the pipe breakage probabilities except for the pipes that had been upgraded in the first stage. A flowchart of the two-stage method is described in Figure 4-3.

4.2.2.1. Rehabilitation optimization model

Although the pipe repair cost is much lower than the replacement fee, frequent breaks will result in a cumulative repair expense that exceeds the replacement cost. Therefore, a methodology is needed that helps find the critical (or threshold) break rate to determine the timing of repair or replacement (Ascher and Feingold, 1984).

Assuming that the pipe be replaced at the time of the nth break, the present worth of the total cost of the pipe is written as:

$$T_n = \sum_{i=1}^{n} \frac{C_t}{(1+\beta)^{t_i}} + \frac{F_n}{(1+\beta)^{t_n}} \qquad (4-7)$$

where β is the discount rate, t_i is the time of the *i*th break measured from the installation year, C_i is the repair cost of the *i*th break, F_n is the replacement cost at time t_n, and T_n is the present worth. Equation 4-7 implies that the previous (n-1) breaks was repaired rather than be replaced.

In order to minimize the total cost, T_n, at time, t_n, the following condition must obtain:

$$T_{n-1} > T_n < T_{n+1} \qquad (4-8)$$

However, the critical check is to determine the first instance when the condition $T_{n+1} > T_n$ holds true. In order to check that, the following solution for $(t_{n+1} - t_n)$ is used:

$$t_{n+1} - t_n < \frac{In(\frac{C_{n+1}}{F_n} + \frac{F_{n+1}}{F_n})}{In(1+\beta)} \qquad (4-9)$$

Recognizing that $t_{n+1} - t_n$ is the time between the nth and *(n+1)*th breaks or time interval for the occurrence of one break, the threshold break rate of Brk_{th} is obtained as the inverse of Δt_n (where $\Delta t_n = t_{n+1} - t_n$). The threshold break rate is defined as the break rate between subsequent breaks:

$$Brk_{th} = \frac{1}{\Delta t_n} = \frac{1}{t_{n+1} - t_n} > \frac{In(1+\beta)}{In(\frac{C_{n+1}}{F_n} + \frac{F_{n+1}}{F_n})} \qquad (4-10)$$

Based on the observed data, a current break rate can be derived to each given pipe. Whenever the current break rate is equal to or more than Brk_{th}, the pipe should be replaced. It is worth noting that the optimal rehabilitation schedule information will be transferred to the next upgrade optimization model (shown in Figure 4-4).

4.2.2.2. Upgrade optimization model

Hydraulic reliability indicates the hydraulic performance information for each demand node. If the hydraulic failure probability on a node is higher than the allowable probability, the water provider should replace the inlet pipe with a larger diameter pipe or build a parallel pipe. Then, the next few questions for the decision maker are: 1) should the existing pipeline be replaced by a bigger diameter pipeline or should a parallel

pipeline be built? 2) what size of pipe should be applied in this replacement or paralleling? 3) what is the duration of the new inlet pipe that can transfer sufficient water?

The study of water distribution systems is often viewed as a least-cost optimization problem in the previous literature. Pipe diameters were considered to be decision variables. Obviously, other parameters, such as reliability, redundancy and water quality, should be considered to be objectives in the optimization process, (Alperovits and Shamir, 1977). However, the difficulty of quantifying these multiple objectives in an optimization model causes researchers concentrating on a single, least-cost objective. Therefore, the overall objective in the upgrade optimization in this chapter is to minimize the total cost. The following formulation describes this objective:

$$Minimize\ f = \sum_{j}^{m} C_j(R_j, L_j) \tag{4-11}$$

where $C_j(R_j, L_j)$ is the cost of pipe j with diameter R_j and length L_j, and m is the number of pipes that must be upgraded. The objective is subject to the following constraints:

$$G(H, D) = 0 \tag{4-12}$$

$$H^L \le H \le H^U \tag{4-13}$$

$$D^L \le D \le D^U \tag{4-14}$$

$$W^L(H, D) \le W(H, D) \le W^U(H, D) \tag{4-15}$$

where Equation 4-12 refers to the conservation of flow constraints and energy equations

(loop equations), Equation 4-13 is for head boundary constraints, Equation 4-14 is designed for water demand boundary constraints, and Equation 4-15 represents general constraints including financial constraints.

The decision of pipe replacement/parallel is dependent on the costs, the geographical situations, and the existing pipe conditions. Some geographical conditions are not suitable for the laying of parallel pipelines and the only choice is to replace the existing pipelines with larger diameter pipes. However, the geographical condition considerations involved in pipe replacement plan is out of the scope of this study. In addition, the duration of the upgraded pipeline must be considered. If one pipe needed upgrade because of low hydraulic capability and it was also aging pipe that would be replaced in the next few years, it would be better to directly replaced it with a new large diameter pipe rather than to build a parallel pipeline.

The objective formulation is modified as follows:

$$Minimize\ f = \sum_{j=1}^{m}\sum_{k=1}^{l} C_{jk}(R_j, L_j)/(1+\beta)^{k-1} \qquad (4\text{-}16)$$

where l is the length of the planning period, and k ($k = 1, 2, \ldots l$) is the year index of pipeline upgrade. The total cost includes the following components:

$$C_{jk}(R_j, L_j) = f1 + f2 \qquad (4\text{-}17)$$

where *f1* represents the pipeline costs including parallel, replacement and repair costs,

and *f2* is the cost of the construction and machinery.

4.2.2.3. Optimization procedure

Pipe Roughness and Water Demand are two dynamic input parameters. The pipe roughness increases at a rate. The magnitude of this roughness growth rate varies with pipe type, water quality, and operation and maintenance practices. To model the effect of aging on the capacity of pipes, the Sharp and Walsli equation (1988) is used:

$$C(t) = 18.0 - 37.2\log[\frac{e_o + a(age)}{R}] \qquad (4\text{-}18)$$

where *C(t)* is the Hazen-Williams coefficient in year *t*, e_o is the roughness at the time of installation (mm), *a* is the roughness growth rate (mm/year), and *R* is the pipe diameter (mm).

A function used to predict nodal water demand was developed by Dandy et al. (1985). It is shown as:

$$D_i = D_{0i}(1 + \frac{DGR}{100})^t (\frac{P_t}{P_0})^{PREL} \qquad (4\text{-}19)$$

where D_{0j} is the base year water demand for the node *j* and DGR is the annual percentage rate of increase in the base demand, DGR was assumed to follow demographic data patterns closely, and so it was taken as the population growth rate with typical values of about 2 to 5, t is the time in years, P_t and P_0 are the price per unit volume of water for

year t and the base year, respectively, and PREL is the price elasticity of demand. A typical range of PREL values is -0.2 to -0.5. Generally it is advisable to increase the price of water in the last 1 or 2 years of the design period for the best results in order to delay the need to upgrade the network. When there is adequate capacity after upgrading, prices can be reduced in order to utilize the system capacity as fully as possible and to maximize economic efficiency. Other demand management options could be used, and the joint effect of all the demand management techniques deployed should be considered.

Genetic Algorithms (GA) is chosen as the optimization method. GA is a search technique used in computing to find exact or approximate solutions to optimization and search problems. It is based on the mechanics of natural selection and natural genetics that use biological techniques including inheritance, mutation, selection, and crossover (Goldberg 1989GA). GA provides a robust and efficient way to search complex parameter spaces for even better solutions to an optimization problem (Goldberg, 1989). Although there are no guarantees that a GA will actually attain the optimum solution, it generally finds one or more extremely good solutions with relatively little computational effort.

An optimal RUS code is written based on MATLAB and EPANET. The following steps give the details of this optimal RUS code.

Step 1 Use Equation 4-4 to calculate each pipeline's break rate *B(i,j)*, use Equation 4-10 to compute each pipeline's Brk_{th}, and then obtain the corresponding replacement year *Yr(j)*, where *i* represents the time of year, and *j* is the pipe index.

Step 2 Set *i = 0.*

Step 3 $i = i+1$.

Step 4 Run the hydraulic reliability model and calculate nodal hydraulic reliability $R(i, j)$ for all studied nodes in a WDS in the i^{th} year.

Step 5 Compare the predicted hydraulic reliability with the minimum allowable hydraulic reliability, $Rm(i, j)$, at the i^{th} year to find the pipes to be upgraded $P(i, j)$.

Step 6 If the replacement year, $Yr(j)$, of the upgraded pipe is equal to or more than the plan term, N. *Then,* parallel is not considered.

Step 7 Run the optimization code (GA) to find the optimal pipe diameter $P(i, j, m)$(where m is the index of pipe diameter; both replacement and paralleling use this diameter index), with the objective of minimizing total cost, subject to the constraint that the $R(i, j)$ should be greater than the maximum of $Rm(i, j)$ during the whole planning period, N. The computation of $R(i, j)$, of course, needs to run the hydraulic reliability prediction model.

Step 8 If $i < N$, then go to step 3.

Step 9 Calculate the total cost and record the optimal rehabilitation and upgrade schedule.

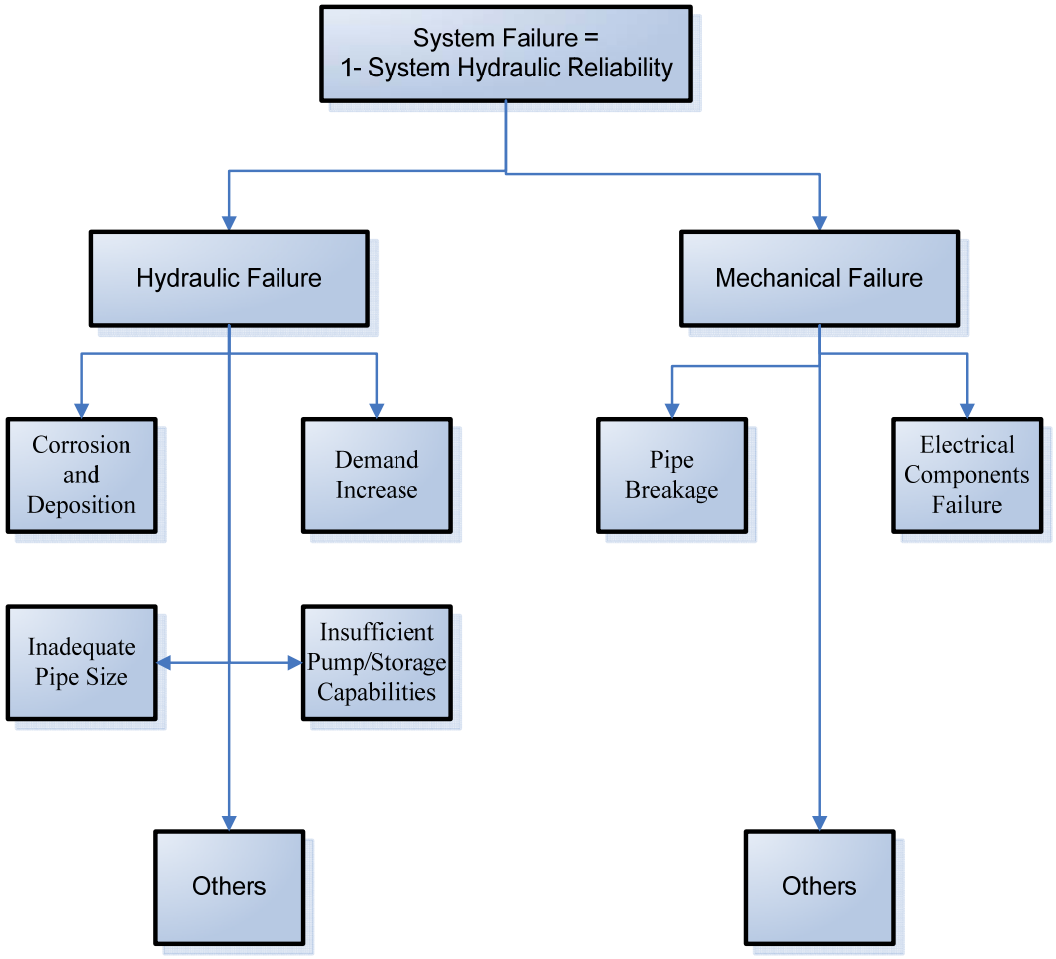

Figure 4-1 Flowchart of system hydraulic reliability

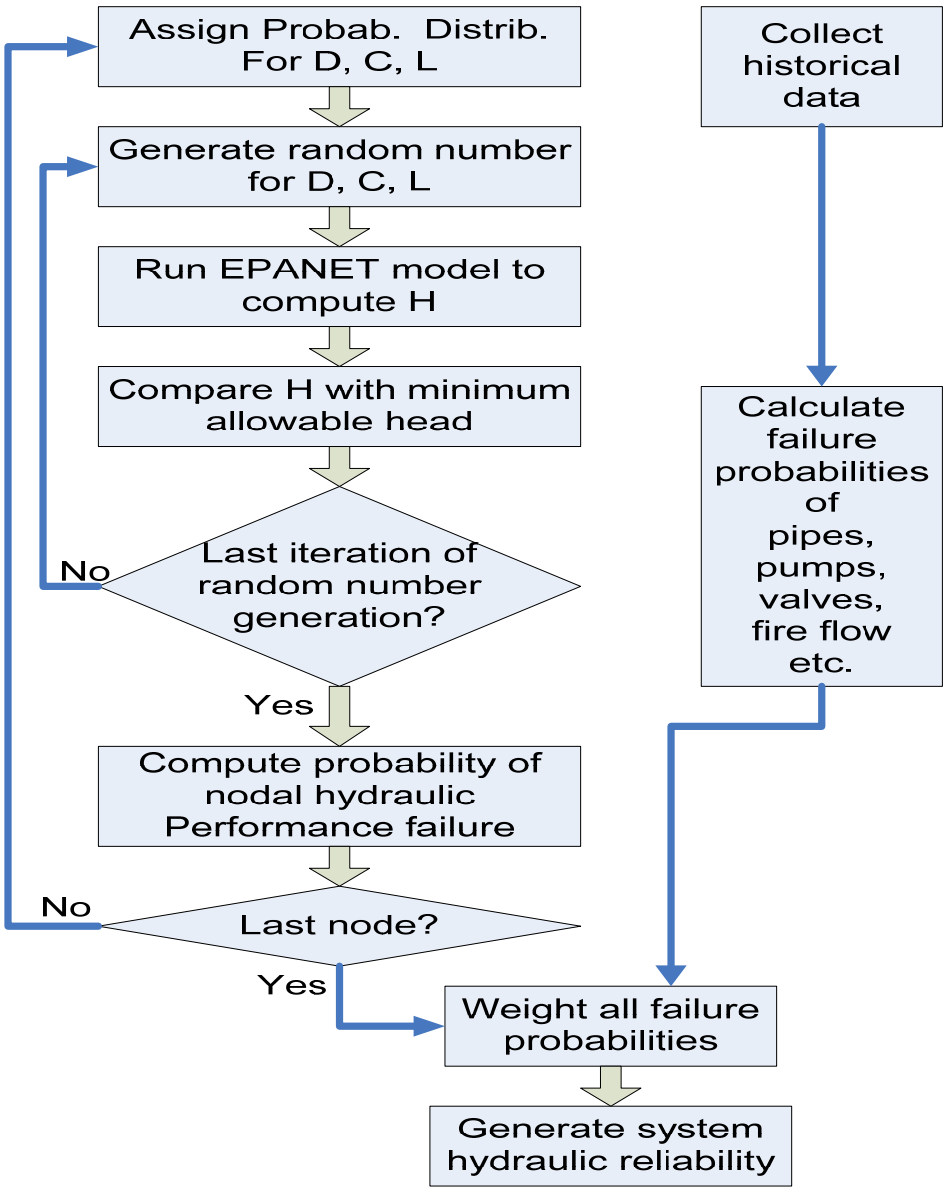

Figure 4-2 The procedure of system hydraulic reliability assessment

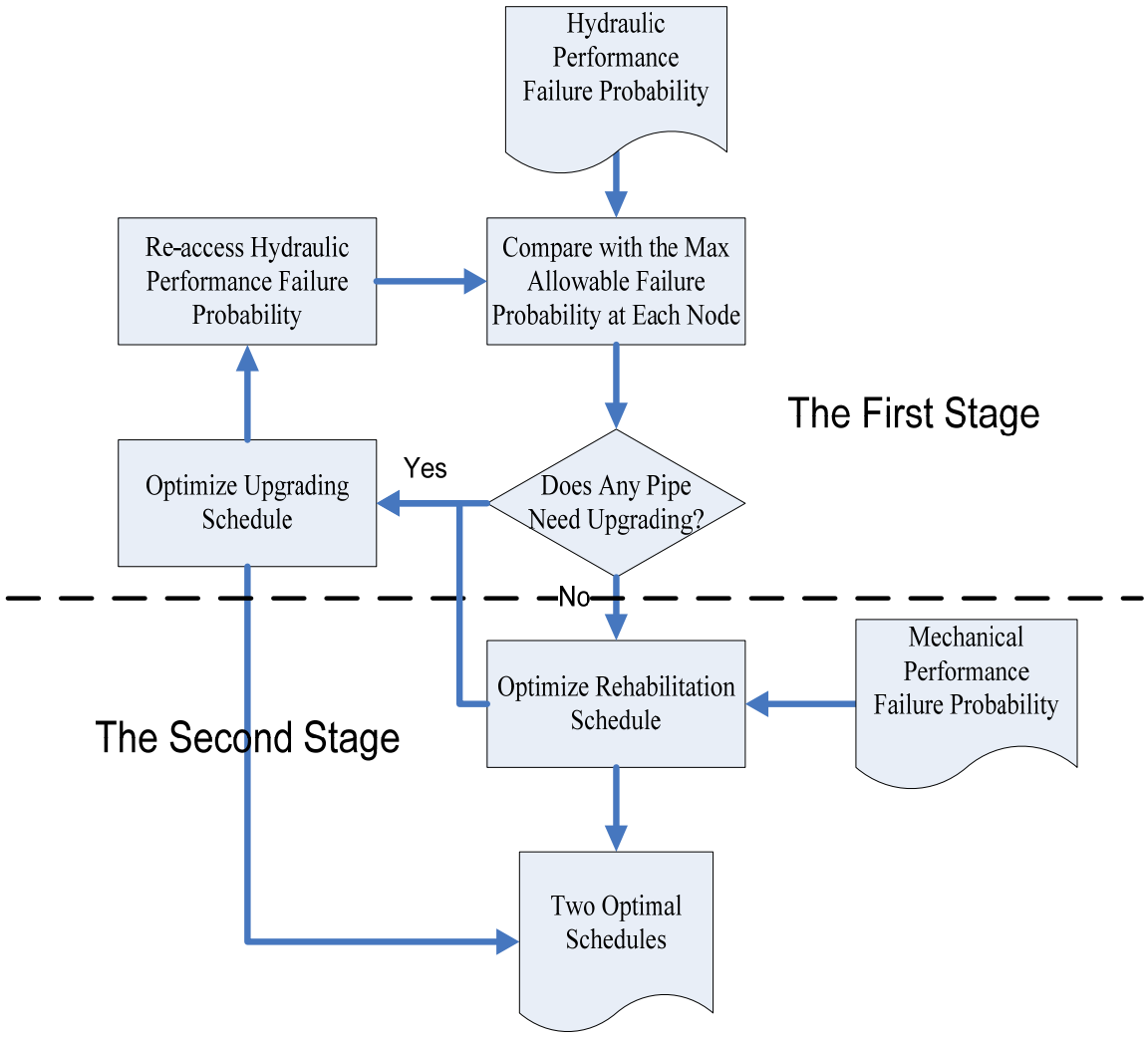

Figure 4-3 The flowchart of two-stage method

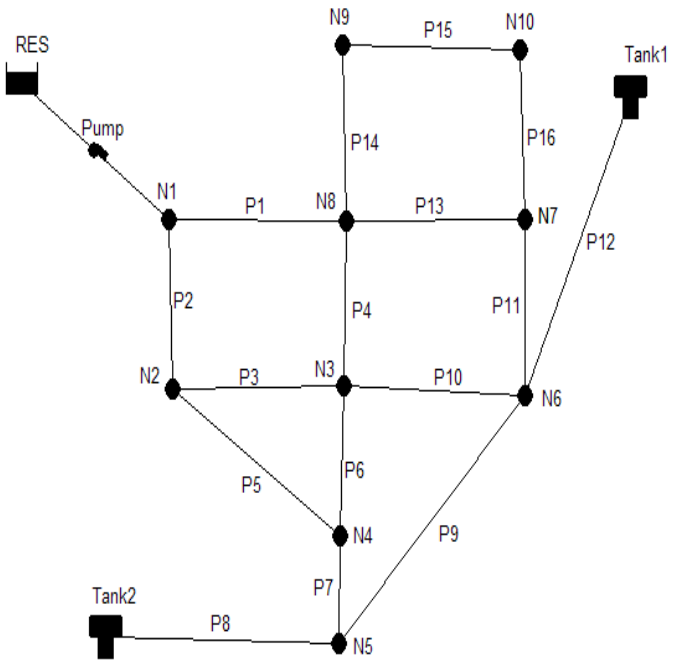

Figure 4-4 Example of the distribution system

4.3. Example

Figure 4-4 shows a benchmark hypothetical water distribution system (Al-Zahrani and Syed 2004) that consists of 16 pipes, 10 demand nodes, two tanks and one reservoir. Tables 4-1 to 4-4 demonstrate the information of system components.

Due to the fact that MCS is used to compute the nodal and system reliability, the iterative process of random number generation of D, C, and L and hydraulic simulation must be repeated a large number of times. According to the previous studies (Bao and Mays, 1990; Xu and Goulter, 1998), the optimal number of iterations is between 500 to 3000 times. Because the difference in results after 2000 iterations is negligible, 2000 iterations are used in this study.

There are several probability distributions that can achieve random number generation of D, C, and L such as the normal, log-normal, uniform, and Pearson and Weibull distributions. According to the literature, the normal distribution is the most popular probability distribution that used in hydraulic studies (Germanopoulos et al., 1986; Lansey et al., 1989; Quimpo and Shamsi, 1991; Mays, 1993; Calvin et al., 1996; Ostfeld, 2001; Shinstine et al., 2002; Kapelan et al., 2005; Giustolisi et al., 2009). Normal distribution is also used for the random number generation of D, C, and L.

Shamir and Howard's exponential break rate model (shown in Equation 4-4 is used to compute the pipe breakage probability. The expected number of failures per year per unit length of pipe A_j is uniformly assumed to be 0.122. The mean values of the normal distribution of D, C, and L are obtained from Tables 4-1 and 4-3. The coefficients of variation for D and L are assumed to be 0.2. According to the conclusion of Bao and Mays (1990), system reliability is somewhat insensitive to the type of probability

distribution of pipe roughness when the coefficient of variation C is less than 0.4, and, thus, the coefficient of variation, C , is assumed to be 0.4.

After conducted the hydraulic reliability code, the results of the nodal hydraulic performance failure probability, the pipe breakage probability, and the system hydraulic reliability were generated. They are shown in Table 4-4. From the results, it is found that *i*) the system reliability shows a great improvement when a reasonable weighing factor is used, *ii*) the system reliability is 0.892 that represents the distribution system in unsafe (the safe system reliability should be greater than 0.999), and *iii*) the nodal hydraulic failure probability is almost one order of magnitude difference lower than the pipe breakage probability.

The water distribution system (illustrated in Figure 4-4) is used to demonstrate the optimization method for the repair schedule, and assuming that this is a 15-year water distribution system maintenance plan (price on the first year). The costs of pipe, installation, construction and labor fees are shown in Table 4-6.

The discount rate is designed as 0.06 (shown in Table 4-7). According to Equation 4-10 and the costs in Table 4-6, the threshold break rate of each pipe can be obtained. Used Equation 4-4, the replacement timing can be calculated for each pipe.

After run the optimal RUS code, an optimal repair schedule was obtained and is shown in Table 4-8. The schedule indicates that the number of pipe break grows with time increasing until the pipe replacement is conducted. The first year has 5 pipe breaks, the number of pipe break increases to 8 in the fifth year, and only two pipe breaks happen in the last year of the schedule term due to the pipe upgrading; The first pipe replacement occurs in the ninth year, pipe P9 is replaced by an 8 inch diameter pipe; Only one parallel

pipe is built in the fifteenth year of the schedule term; the total cost of this schedule is $471,933.

4.4. Summary

This chapter presented two approaches to assess the hydraulic reliability and optimize the rehabilitation/upgrade schedule in a water distribution system. The optimal rehabilitation/upgrade schedule is based on the hydraulic reliability assessment. Both approaches considered hydraulic parameters as uncertain values and treated them as random numbers. Two approaches were written into two universal codes: the hydraulic reliability code and the optimal RUS code, which based on MATLAB and linked to EPANET.

The optimal rehabilitation/upgrade schedule was subdivided into two stages: one stage is to design a pipe upgrade/parallel plan due to hydraulic failure potential, and another is to schedule a pipe repair/replacement plan due to mechanical failure potential. The optimizations of the two stages are performed separately with simultaneous exchange of information between each other. The threshold break rate model and the genetic algorithm participated in this optimization process.

The results demonstrated the applicability of two approaches. The applicability of the two codes was verified by an example in a benchmark water distribution network.

In the next chapter, a mixed methodology is developed to settle uncertainty in binary linear programming.

Table 4-1 Node information

Node No.	Elevation (ft)	Mean demand (gpm)	Min Allowable head (ft)
Res	320	N/A	N/A
N1	390	120	50
N2	420	75	50
N3	425	35	50
N4	430	50	50
N5	450	70	50
N6	445	155	50
N7	420	65	50
N8	415	150	50
N9	420	55	50
N10	420	20	50

Table 4-2 Pipe information

Pipe No.	Length (ft)	Diameter (in)	Mean Hazen-Williams Coefficient	A_j
P1	890	10	115	0.122
P2	1250	6	110	0.122
P3	835	6	110	0.122
P4	1330	8	110	0.122
P5	1010	6	110	0.122
P6	550	8	130	0.122
P7	425	8	130	0.122
P8	990	8	125	0.122
P9	2100	8	105	0.122
P10	745	8	110	0.122
P11	1100	10	115	0.122
P12	560	6	110	0.122
P13	825	10	115	0.122
P14	500	6	120	0.122
P15	690	6	120	0.122
P16	450	6	120	0.122

Table 4-3 Tank information

	Tank1	**Tank2**
Base Elevation (ft)	0	0
Min Elevation (ft)	525	535
Initial Elevation (ft)	545	550
Max Elevation (ft)	565	570
Tank Diameter (ft)	35.7	49.3

Table 4-4 Weighting coefficients

Pipe No.	Weighting Coefficient	Node No.	Weighting Coefficient
P1	1	N1	0.9
P2	0.8	N2	0.8
P3	0.5	N3	0.5
P4	0.5	N4	0.6
P5	0.6	N5	0.5
P6	0.6	N6	0.4
P7	0.6	N7	0.7
P8	0.8	N8	1
P9	0.5	N9	0.9
P10	0.5	N10	0.8
P11	0.7		
P12	0.7		
P13	0.7		
P14	0.9		
P15	0.8		
P16	0.8		

Table 4-5 Results of the reliability assessment

Pipe No.	Weighting Coefficient	Pipe Failure Prob.	Weighted Pipe fail. Prob.	Node No.	Weighting Coefficient	Nodal Failure Prob.	Weighted Nodal fail. Prob.
P1	1	0.098	0.098	N1	0.9	0.0448	0.0403
P2	0.8	0.134	**0.107**	N2	0.8	0.0016	0.0013
P3	0.5	0.092	0.046	N3	0.5	0.0634	0.0317
P4	0.5	0.142	0.071	N4	0.6	0.0240	0.0144
P5	0.6	0.110	0.066	N5	0.5	0.0408	0.0204
P6	0.6	0.062	0.037	N6	0.4	0.0170	0.0068
P7	0.6	0.048	0.029	N7	0.7	0.0772	0.0540
P8	0.8	0.108	0.082	N8	1	0.0018	0.0018
P9	0.5	0.215	**0.108**	N9	0.9	0.0810	0.0729
P10	0.5	0.082	0.041	N10	0.8	0.0534	0.0427
P11	0.7	0.119	0.083				
P12	0.7	0.063	0.044				
P13	0.7	0.091	0.063				
P14	0.9	0.056	0.05				
P15	0.8	0.077	0.062				
P16	0.8	0.051	0.041				
System failure probability				0.108			
System reliability				0.892			

Table 4-6 Costs of different pipe diameters

Diameter (in)	Repair Cost ($)	Replacement Cost ($/ft)	Paralleling Cost ($/ft)
6	281	93	84
8	412	97	94
10	589	106	101
12	775	116	118

Table 4-7 Threshold break rate and replacement timing (discount rate =0.06)

Pipe No.	Length (ft)	Diameter (in)	Threshold Brk (time)	Replacement Timing (year)
P1	890	10	1.4	18
P2	1250	6	1.5	25
P3	835	6	1.1	17
P4	1330	8	1.9	20
P5	1010	6	1.4	21
P6	550	8	0.8	12
P7	425	8	0.7	10
P8	990	8	1.3	23
P9	2100	8	3	35
P10	745	8	1.1	14
P11	1100	10	1.7	22
P12	560	6	0.7	9
P13	825	10	1.4	19
P14	500	6	0.6	7
P15	690	6	0.9	11
P16	450	6	0.6	5

Table 4-8 The optimal repair schedule

Year	Repair	Replace	Paralleling
1	P1; P9; P10; P11; P13		
2	P1; P9; P10; P11; P13; P2		
3	P1; P9; P10; P11; P13; P2		
4	P1; P9; P10; P11; P13; P2; P4		
5	P1; P9; P10; P11; P13; P2; P4; P9		
6	P1; P9; P10; P11; P13; P2; P4; P9		
7	P1; P9; P10; P11; P13; P2; P4; P9		
8	P1; P9; P10; P11; P13; P2; P4; P9		
9	P1; P2; P4; P10; P11; P13	P9(8”)	
10	P1; P2; P4; P10; P11; P13		
11	P1; P2; P4; P10; P11; P13		
12	P1; P2; P4; P10; P11	P13(8”)	
13	P1; P2; P4; P10; P11		
14	P1; P2; P3; P4; P11	P10(10”)	
15	P3; P11	P2(6”) P4(8”)	P1(6”)
Total Cost $(Price on the first year)		471,933	

CHAPTER 5

A Mixed Approach to Settle Uncertainties in Binary Linear Programming

5.1. Statement of problems

Binary linear programming (BLP), also called Boolean linear programming or 0-1 integer linear programming, plays a significant role in many fields such as location and candidate selection in management studies, assignment and assembly line balance in operation research, and representation and reasoning in artificial intelligence (Yu and Li, 2001). The common difficulty in solving a BLP problem is that uncertainties might exist in parameters and model structure. Employing fuzzy set theory is one of the most successful ways to solve this difficulty (Herrera and Verdegay, 1991; Herrera et al., 1993; Yu and Li, 2001; Zimmermann and Pollatschek, 1984).

Fuzzy mathematical programming (FMP) methods are approaches that are derived through the incorporation of fuzzy set theory within ordinary mathematical programming frameworks (Peng and Mayorga, 2010c, d). The FMP methods contain two major categories: fuzzy possiblilistic programming (FPP) and fuzzy flexible programming (FFP) (Inuiguchi and Sakawa, 1990). In the FPP methods, fuzzy parameters are introduced into ordinary mathematical programming frameworks, in which various intermediate models could be formulated based on the problem interpretation (Zadeh, 1978). In the FFP methods, the flexibility in the constraints and fuzziness in the system objective, which are represented by fuzzy sets and denoted as "fuzzy constraints" and "fuzzy goal", are introduced into ordinary mathematical

programming models (Zimmermann, 1991). There are only two algorithms that have been built for solving the FFP: one is called the "min-operator technique," which looks for a solution according to the concept of a maximizing decision, and considers both the fuzzy constraints and a fuzzy goal (Herrera et al., 1993; Zimmermann and Pollatschek, 1984); another is called the "alpha-cut technique," which seeks an answer based on the representation theorem for fuzzy sets (Herrera and Verdegay, 1991; Negoita and Ralescu, 1975).

Many FPP models have been developed for dealing with uncertainties in BLP problems (Yu and Li, 2001; Lin and Wang, 2004; Chang, 2007). For example, Yu and Li (2001) have proposed an algorithm that can simultaneously solve the BLP problems with fuzzy coefficients in the objective function, in the constraint matrix, and in the right-hand side of constraints (Yu and Li, 2001). However, only a few FFP models have been developed for BLP problems (Herrera and Verdegay, 1991; Herrera et al., 1993, Zimmermann and Pollatschek, 1984). This is because the application of the min-operator technique in BLP might result in a nonlinear programming problem (see Zimmermann, 1987 pp.100-108 and 254, and Herrera et al., 1993). Therefore, the alpha-cut technique became a common algorithm for solving the FFP in BLP problems. For instance, Herrera et al. (1993) have developed an alpha-cut-based approach to solve Boolean programming problems with fuzzy constraints (Herrera et al., 1993).

Obviously, a model integrating FPP and FFP could efficiently address uncertainties for both coefficients and model structure. In the mixed-integer linear programming area, some studies have included such an effort. For example, Liu and Sahinidis (1997) presented an approach for the process planning in a fuzzy environment

(Liu and Sahinidis, 1997). Huang et al. (2001) presented an interval-coefficient fuzzy linear programming for the municipal solid waste system optimization (Huang et al., 2001). Both studies used interval values to reflect the parameter uncertainties, and both applied the min-operator technique to solve the model structure uncertainties. In the BLP area, however, there is no record of relative research.

In this chapter, the intent is to fill this gap using an interval-coefficient fuzzy binary linear programming (IFBLP) and the solution for BLP problems. In the IFBLP model, the parameter uncertainties are represented by the interval coefficients, and the model structure uncertainties are reflected by the fuzzy constraints and a fuzzy goal. The essential idea of solution is to convert the original model into one or more crisp-coefficient BLP models. Therefore, the solution of IFBLP should include two major processes: a defuzzification process that converts a crisp-coefficient FBLP into a crisp-coefficient BLP and a crisping process that converts the interval-coefficient BLP into one or more crisp-coefficient BLPs. The alpha-cut technique is applied to the defuzzification process. An interval linear programming algorithm (Chinneck and Ramadan, 2000) is used for the crisping process.

Using the alpha-cut technique, a crisp-coefficient FBLP model can find a range of alpha values. Herrera et al. (1993) developed a method that can determine a single optimal alpha value in a crisp-coefficient FBLP. However, an IFBLP theoretically has infinite optimal alpha values, which entails an unknown distribution function and boundary values. In interval analysis, the basic information for an inexact value is the upper and lower bounds. Without alpha boundary information, the crisping process would not be continued. This chapter provides a Monte Carlo technique based approach that

can determine the boundary values for optimal alpha, so that the linearity of model can be maintained during the solution process. Finally, the IFBLP is converted into two extreme crisp-coefficient BLP models: a best optimum model and a worst optimum model. Due to the fact that the best optimum model has the largest possible feasible domain and the most favorable version of the objective function, and the worst optimum model has the smallest possible feasible domain and the least favorable version of the objective function (Chinneck and Ramadan, 2000), the results of these two extreme models can bound all outcomes of the IFBLP. The IFBLP and its solution were applied to a long-term traffic noise control plan to demonstrate its applicability and advantages.

5.2. Methodology

Considering a general IFBLP model with the fuzzy constraints and the interval coefficients as follows:

$$\begin{aligned} &\min\ f = \sum_{j\in N}[c_j^-, c_j^+]x_j \\ &s.t.\quad \sum_{j\in N}[a_{ij}^-, a_{ij}^+]x_j \lesssim [b_i^-, b_i^+] \quad i \in M, \\ &\qquad x_j \in \{0,1\}. \end{aligned} \tag{5-1}$$

where x_j are the binary variables, $[a_{ij}^-, a_{ij}^+] \in I(\Re)$ represents the *j-th* set of interval numbers in $\Re$ at the *i-th* constraint, a_{ij}^+ and a_{ij}^- represent the upper and lower bound coefficients, respectively, $[b_i^-, b_i^+] \in I(\Re)$ represents the set of interval numbers in $\Re$ on

the *i-th* constraint, b_i^+ and b_i^- are the upper and lower bounds, respectively. $[c_j^-, c_j^+] \in I(\Re)$ represents the *j-th* set of interval numbers in $\Re$ for the objective function, c_j^+ and c_j^- are the upper and lower bound coefficients, respectively, and the symbols "$\tilde{\leq}$" represents fuzzy inequality that the decision-maker permits some violations of the constraints.

Two transferring processes need to be preformed to convert the IFBLP, such as Model 5-1, into one (or more) auxiliary parametric BLP(s). One process is the defuzzification for defuzzifying the fuzzy constraints; another is called the "crisping process," which crisps the interval-coefficient BLP into one or more fixed coefficient BLPs (Peng and Mayorga, 2010c, d).

5.2.1. Defuzzification process

Start by assuming a general crisp-coefficient BLP model with fuzzy constraints as follows:

$$\begin{aligned} \min\ & f = \sum_{j \in N} c_j x_j \\ s.t.\ & \sum_{j \in N} a_{ij} x_j \ \tilde{\leq}\ b_i \quad i \in M, \\ & x_j \in \{0,1\}. \end{aligned} \tag{5-2}$$

There are two approaches can solve Model 5-2. The first algorithm seeks an answer based on the representation theorem for fuzzy sets that applies the α-cut technique

(Negoita and Ralescu, 1975; Herrera and Verdegay, 1991); the second one looks for a solution according to the concept of maximizing decisions (Bellman and Zadeh, 1970; Zimmermann and Pollatschek, 1984) and uses the min-operator technique to connect the objective fuzzy sets and the constraint fuzzy sets.

5.2.1.1. α -cut technique approach

If the membership functions of its *ith* constraint are defined by

$$\mu_i(x)=\begin{cases}1 & \text{if } \sum_{j\in N} a_{ij}x \le b_i,\\ \dfrac{b_i+\Delta b_i-\sum_{j\in N} a_{ij}x}{\Delta b_i} & \text{if } b_i \le \sum_{j\in N} a_{ij}x \le b_i+\Delta b_i,\quad i\in M,\\ 0 & \text{if } \sum_{j\in N} a_{ij}x \ge b_i+\Delta b_i.\end{cases} \tag{5-3}$$

and $\forall \alpha \in (0,1]$, let any α -cut of the constraint set become a classical set: $X(\alpha)=\{x\in\Re \,|\, \mu_X(x)\ge\alpha, x\in\{0,1\}\}$ where $\mu_X(x)=\inf\{\mu_i(x), i\in M\}$. Then Model 5-2 can be written as the following crisp-coefficient BLP problem:

$$\begin{aligned}&\min\ f=\sum_{j\in N} c_j x_j\\ &s.t.\quad \sum_{j\in N} a_{ij}x \le b_i+\Delta b_i(1-\alpha),\quad i\in M,\\ &\qquad x_j\in\{0,1\},\ \alpha\in(0,1].\end{aligned} \tag{5-4}$$

where Δb_i is the tolerance of the right-hand side and $\Delta b_i \ge 0$, and α is used here as an

intermediate variable. The major advantage of the α -cut technique is that it ensures the fuzzy sets $\{\mu_X(x) \geq \alpha\}$ in convexity and bounded. The problem is that α is an interval value in Model 5-4, it is necessary to find a single optimal α value.

5.2.1.2. Min-operator approach

The second approach considers the goal to be fuzzy. A decision-maker can establish an aspiration level " f' " for the objective function value they desire to achieve. Then, Model 5-2 can be converted to:

$$\begin{aligned} &\textit{Find} \quad x \in \{0,1\} \\ &\textit{such that} \quad \sum_{j \in N} c_j x_j \mathrel{\tilde{<}} f' \\ &\qquad\qquad \sum_{j \in N} a_{ij} x_j \mathrel{\tilde{<}} b_i \quad i \in M. \end{aligned} \tag{5-5}$$

where there is no distinction between a fuzzy objective and fuzzy constraints. According to Bellman and Zadeh's (1970) concept of maximizing decisions, the solution of Model 5-5 will be x^*, and the membership function (satisfaction degree) of the optimal decision is:

$$\mu_D(x^*) = \max_x \mu_D(x) = \max_x \min_i [\mu_G(x), \mu_C(x)] \tag{5-6}$$

where $\mu_G(x)$ and $\mu_C(x)$ are the membership functions of the goal and the constraints, and $\mu_D(x)$ may be called "the satisfaction degree of a decision." In order to obtain x^*, let

$\lambda = \mu_D(x) = \min_i[\mu_G(x), \mu_C(x)]$, and the following model is obtained:

$$\begin{aligned} &\max \lambda \\ &s.t. \quad \lambda \le \frac{d_i + \Delta d_i - E_i x}{\Delta d_i}, \quad i \in M+1, \\ &\qquad x \in \{0,1\}, \quad 0 \le \lambda \le 1. \end{aligned} \tag{5-7}$$

where E_i is the *i-th* row of E and $E = [c, a_1, ..., a_i]^T \in \{\Re\}^{(m+1)\times n}$, d_i is the *i-th* row of d and $d = \begin{bmatrix} f' \\ b \end{bmatrix} \in \{\Re\}^{(m+1)}$, and Δd_i is the tolerance of the right-hand side and $\Delta d_i \ge 0$.

The major advantage of the min-operator technique is that it considers the goal to be fuzzy that leading to directly find a single optimal solution. However, Zimmermann pointed out that Model 5-7 might become a nonlinear programming problem due to nonlinear membership functions or the min-operator. (see Zimmermann, 1987, pp.100-108 and 254; and Herrera et al., 1993).

5.2.1.3. The link of two methods

Herrera et al. (1993) developed an approach that link the above two methods for Model 5-4 to find a single optimal alpha value. The approach considers both the fuzzy constraint set, and the fuzzy goal. It uses the t-norm operator to avoid the nonlinear problem during the process of "satisfy constraints and attain goal". In order to solve this approach in the fuzzy solution domain $S(\alpha)$, $S(\alpha) = \{x \in \Re \mid f(x) = \min f(y), y \in X(\alpha)\}$

in Model 5-4, the following propositions had been developed. The proofs related to these propositions were provided by Herrera et al. (1993).

Proposition 1 *Let* $\{\lambda(x) = \sup \alpha, \quad x \in S(\alpha)\}$, *and define* $P(\alpha)$ *as a fuzzy solution of Model 5-4 for each fixed* $\alpha \in (0,1]$. *If* $\alpha' \in (0,1]$ *is a specific fixed value, and* $x(\alpha')$ *is the optimal 0-1 solution of the corresponding problem* $P(\alpha)$, *then*

$\lambda(x\ (\alpha')) = \min\{\mu_i(x(\alpha')), i \in M\}$.

Proposition 2 *Let* $\theta = \lambda(x(\theta)) \in (0,1]$ *and* $\alpha' = \theta + \Delta\theta$ *(where* $\Delta\theta = \Omega / \max\{\Delta b_i\}$, *and*

$$\Omega = \begin{cases} 1 & \text{if } \max\limits_{i \in M}\{b_i + \Delta b_i(1-\alpha)\} = 0 \\ \min\limits_{i \in M}\{b_i + \Delta b_i(1-\alpha)\} & \text{elsewhere} \end{cases}$$

), *if* $\alpha'' = \lambda(x(\alpha'))$, *then*

$\forall \alpha \in (\theta, \alpha'']$, $x(\alpha')$ *is an optimal solution of* $P(\alpha)$.

Proposition 3 *Let* $T(\cdot)$ *be an Archimedean t-norms operator, which is from the Hamacher formulation:*

$$H_\gamma(\mu_A, \mu_B) = \frac{\mu_A \mu_B}{\gamma + (1+\gamma)(\mu_A + \mu_B - \mu_A \mu_B)}, \quad \gamma > 0 \qquad (5\text{-}8)$$

where γ *is an arbitrary parameter. If* γ *=1, then* $H_\gamma(\mu_A, \mu_B) = \mu_A \cdot \mu_B$. *Therefore, the following relation holds:*

$\sup\limits_{\alpha} T(\alpha, \max\limits_{X(\alpha)} \mu_G(x)) = \max\limits_{x \in X} T(\mu_G(x), \mu_C(x))$.

Proposition 4 *Let* α^* *be the value obtained from the Hamacher formulation (Zimmermann, 1978), and suppose* $x(\alpha)$ *is the optimal solution of Model 5-4. If* $\{x_k(\alpha_k)\}$ *denotes the set of points of the solution* $x(\alpha)$, *the optimal value of* α *for Model 5-4 is* $\alpha^* = \max_{\{x_k(\alpha_k)\}} T(\mu_G(x_k(\alpha_k)), \lambda(x_k(\alpha_k)))$.

Algorithm 1 Let α_1, α', and θ be three intermediate values for α. The iteration process to determine optimal solution α^* is described in the following steps:

Step 0*: let* $\alpha = \alpha_1 = \alpha^* = 0$.

Step 1*: Solve* $P(\alpha)$. *Let* $x(\alpha)$ *be an optimal solution of* $P(\alpha)$.

Step 2*: Let* $\theta = \lambda(x(\alpha)) = \min\{\mu_i(x(\alpha)), i \in M\}$.

If $\alpha_1 = 0$, *then* $x(\alpha)$ *is an optimal solution of* $P(\alpha)$, $\forall \alpha \in [\alpha_1, \theta]$,

Else $x(\alpha)$ *is an optimal solution of* $P(\alpha)$, $\forall \alpha \in [\alpha, \theta]$.

Step 3*: Let* $\alpha' = T(\sup \mu_G(x(\alpha), \theta)$.

If $\alpha' > \alpha^*$, *then* $\alpha^* = \alpha'$.

Step 4*: If* $\theta < 1$, *then* $\alpha_1 = \theta$, $\alpha = \theta + \Delta\theta$; *go to Step 1.*

Step 5*: Stop.*

5.2.2. Crisping process

Model 5-4 is a crisp-coefficient BLP that derived from the crisp-coefficient FBLP Model 5-2 through the defuzzification process. It is found that the coefficients of the variables in these two models do not change during the model conversion. If an interval-coefficient BLP is obtained from Model 5-4 by replacing the crisp-coefficients with the interval-coefficients, it can be considered as being derived from an IFBLP after the defuzzification process. We then study such interval-coefficient BLP model as follows:

$$\begin{aligned} \min\ & f = \sum_{j\in N}[c_j^-, c_j^+]x_j \\ s.t.\ & \sum_{j\in N}[a_{ij}^-, a_{ij}^+]x_j \le b_i^- + \Delta b_i(1-U(\alpha^*)), \quad i \in M, \\ & x_j \in \{0,1\}, \alpha^* \in (0,1]. \end{aligned} \tag{5-9}$$

where $\Delta b_i = b_i^+ - b_i^-$; $U(\alpha^*)$ stands for the set of α^* and each α^* in $U(\alpha^*)$ corresponds to a fixed coefficient BLP model.

After applied Algorithm 1, the crisp-coefficient BLP like Model 5-4 has only one α^* *value*. However, the interval-coefficient BLP model like Model 5-9 theoretically has infinite α^* values, $U(\alpha^*)$, which entails an unknown distribution function and boundary values. In interval analysis, the basic information for an inexact value is the upper and lower bounds. Without the boundary information of $U(\alpha^*)$, the crisping process would not be continued.

5.2.2.1. Value range of α^*

According to Proposition 4**,** the optimal value of α^* in a crisp-coefficient BLP is given by:

$$\alpha^* = \max_{\{x_k(\alpha_k)\}} T(\mu_G(x_k(\alpha_k)), \lambda(x_k(\alpha_k))). \tag{5-10}$$

where $\{x_k(\alpha_k)\}$ denotes the set of points of the solution $x(\alpha)$.

Theorem 1 Suppose $x(\alpha)$ is the solution of a crisp-coefficient BLP like Model 5-4. Then $\lambda(x(\alpha))$ has a negative linear correlation relationship with the variable coefficients in the constraints.

Proof *According to Equation 5-3, it obtains that* $\mu_i^0(x) = (b_i + \Delta b_i - \sum_{j \in N} a_{ij}^0 x_j)/\Delta b_i$ *for Model 5-4. Let* $\alpha^0 \in (0,1]$ *be a specific fixed value, and* $x(\alpha^0)$ *be the optimal 0-1 solution of the corresponding problem* $P(\alpha^0)$*. If* $\forall a_{ij}^1 \geq a_{ij}^0$*, then a new membership function:* $\mu_i^1(x) = (b_i + \Delta b_i - \sum_{j \in N} a_{ij}^1 x_j)/\Delta b_i$*. Similarly, let* $\alpha^1 \in (0,1]$ *be a specific fixed value, and* $x(\alpha^1)$ *be the optimal 0-1 solution of the corresponding problem* $P(\alpha^1)$*. According to proposition 1,* $\lambda(x(\alpha^0)) = \min\{\mu_i^0(x(\alpha^0)), i \in M\}$ *and* $\lambda(x(\alpha^1)) = \min\{\mu_i^1(x(\alpha^1)), i \in M\}$*. Due to* $x_j \geq 0$*,* $\mu_i^1(x) \leq \mu_i^0(x)$*, then* $\lambda(x(\alpha^1)) \leq \lambda(x(\alpha^0))$*. Therefore,* $\lambda(x(\alpha))$ *has a negative linear correlation relationship with the variable coefficients in the constraints.*

Theorem 2 Suppose $x(\alpha\ )$ is the solution of a crisp-coefficient BLP like Model 5-4. Then $\mu_G(x\ (\alpha))$ has a positive linear correlation relationship with the variable coefficients in the constraints.

Proof *There are two scenarios: Min crisp-coefficient BLP and Max crisp-coefficient BLP.*

i) For the Min crisp-coefficient BLP like Model 5-4:

Define $X(\alpha^0)=\left\{x\in\Re\middle|\mu_X^0(x)\geq\alpha^0, x\in\{0,1\}\right\}$ *and* $X(\alpha^1)=\left\{x\in\Re\middle|\mu_X^1(x)\geq\alpha^1, x\in\{0,1\}\right\}$, *where,* $\mu_X^0(x)=\inf\left\{\mu_i^0(x), i\in M\right\}$ *and* $\mu_X^1(x)=\inf\left\{\mu_i^1(x), i\in M\right\}$. *Due to* $\forall a_{ij}^1\geq a_{ij}^0$, *according to Theorem 1,* $\lambda(x(\alpha^1))\leq\lambda(x\ (\alpha^0))$, *then* ($\min\{\mu_i^1(x(\alpha^1)), i\in M\}\ \leq\ \min\{\mu_i^0(x(\alpha^0)), i\in M\}$). *Therefore,* $\lambda(x(\alpha^1))\leq\lambda(x(\alpha^0))$ *satisfies* $X(\alpha^0)\subseteq X(\alpha^1)$.

As $c\cdot x(\alpha^0)=\min\{c\cdot x\middle|x\in X(\alpha^0)\}$ *and* $x(\alpha^0)\in X(\alpha^0)\subseteq X(\alpha^1)$, *it follows that* $c\cdot x(\alpha^0)=\min\{c\cdot x\middle|x\in X(\alpha^1)\}$ *; on the other hand,* $c\cdot x(\alpha^1)=\min\{c\cdot x\middle|x\in X(\alpha^1)\}$ *and* $x(\alpha^1)\in X(\alpha^1)$, *but* $\forall x(\alpha^1)\notin X(\alpha^0)$. *Therefore,* $c\cdot x(\alpha^1)\leq c\cdot x(\alpha^0)$.

Using the following membership function equation:

$$\mu_G(x)=\begin{cases}1 & \text{if } cx\leq f^-,\\ \dfrac{f^+-cx}{(f^+-f^-)} & \text{if } f^-\leq cx\leq f^+,\\ 0 & \text{if } cx\geq f^+.\end{cases} \tag{5-11}$$

due to $\mu_G(x(\alpha^0))\leq\mu_G(x(\alpha^1))$, $\mu_G(x\ (\alpha))$ *has a positive linear correlation relationship with the variable coefficients in the constraints.*

ii) For the Max crisp-coefficient BLP, using an objective coefficient substitution:

Let $c' = -c$, and then convert the Max problem to a Min problem. The proof is then identical to the above proof.

According to Theorem 1, Theorem 2, and Equation 5-10, the following consequence logically follows:

- *The value of α^* has a nonlinear relationship with the variable coefficient in the constraints.*

Definition 1 For Model 5-9, if a value of α^* is the maximum (or minimum) in $U(\alpha^*)$, it is then denoted as α^{*+} (or α^{*-}).

Therefore, Model 5-9 can be transferred into the following model:

$$\begin{aligned} \min\ & f = \sum_{j \in N} [c_j^-, c_j^+] x_j \\ s.t.\ & \sum_{j \in N} [a_{ij}^-, a_{ij}^+] x_j \le b_i^- + \Delta b_i (1 - [\alpha^{*-}, \alpha^{*+}]), \quad i \in M, \\ & x_j \in \{0,1\}, \alpha^* \in (0,1]. \end{aligned} \tag{5-12}$$

However, either the distribution type of $U(\alpha^*)$ or the values of α^{*-} & α^{*+} is unknown.

5.2.2.2. Solution for interval-coefficient BLP

Solving a LP requires that specific values be fixed for the coefficients in the

model. An interval-coefficient constraint contains an infinite number of specific constraints, and any value change in those coefficients will affect the result. Chinneck and Rammadan (2000) proposed an approach for the interval-coefficient LP. They declared that the best optimum and the worst optimum values can be obtained by fixing the interval coefficients on their bounds. Their generalizations of the basic idea are used for the interval-coefficient BLP in this chapter.

A specific constraint whose coefficients are fixed at the lower bounds or the upper bounds is an *extreme constraint.* If a model contains *p* interval coefficients in the constraints, then it clearly has 2^{p+1} different *extreme constraint* combinations. Let S_k stand for the set of solutions to the *k-th extreme constraint* and let $S^+ = \bigcup_{k=1}^{2^{p+1}} S_k$, and $S^- = \bigcap_{k=1}^{2^{p+1}} S_k$.

Definition 2 If there is one extreme constraint combination whose solution set is the same as S^+ (or S^-), then it is called the maximum (or minimum) value range constraint combination.

Theorem 3 For Model 5-12, suppose the following interval constraints: $\sum_{j\in N}[a_{ij}^-, a_{ij}^+]x_j \le \left[(b_j^- + \Delta b_j(1-\alpha^{*+})), (b_j^- + \Delta b_j(1-\alpha^{*-}))\right]$, where $i \in M$, and $x_j \in \{0,1\} \ge 0$. Then, $\sum_{j\in N} a_{ij}^- x_j \le (b_j^- + \Delta b_j(1-\alpha^{*-}))$ and $\sum_{j\in N} a_{ij}^+ x_j \le (b_j^- + \Delta b_j(1-\alpha^{*+}))$ are the maximum value range constraint combination and the minimum value range constraint combination, respectively.

Proof *Let* $\sum_{j\in N} a_{ij}x_j \le (b_j^- + \Delta b_j(1-\alpha^*))$ *be any legal version of the interval constraint combination, but not necessarily an extreme one. Then for any particular solution* $x_j \ge 0$, $\sum_{j\in N} a_{ij}x_j \le \sum_{j\in N} a_{ij}^+ x_j$. *Therefore, if* $\sum_{j\in N} a_{ij}^+ x_j \le (b_j^- + \Delta b_j(1-\alpha^{*+}))$ *at* x^* , *then* $\sum_{j\in N} a_{ij}^+ x_j \le (b_j^- + \Delta b_j(1-\alpha^{*+})) \le (b_j^- + \Delta b_j(1-\alpha^{*-}))$, *such that point* x^* *must satisfy all possible versions of the interval constraint combination simultaneously. Therefore* $\sum_{j\in N} a_{ij}^+ x_j \le (b_j^- + \Delta b_j(1-\alpha^{*+}))$ *is the minimum value range constraint combination; similarly, for any particular solution* $x_j \ge 0$, $\sum_{j\in N} a_{ij}^- x_j \le (b_j^- + \Delta b_j(1-\alpha^{*-}))$ *is the maximum value range constraint combination.*

Theorem 4 Suppose an objective function such that $Min\ z = \sum_{j\in N}[c_j^-, c_j^+]x_j$, where $x_j \in \{0,1\} \ge 0$. Then $\sum_{j\in N} c_j^- x_j \le \sum_{j\in N} c_j^+ x_j$ for any given solution x^*.

Proof *Since* $x_j \ge 0$, *the proof is evident.*

Therefore, Theorem 4 shows that it is not necessary to know the distribution type of $[\alpha^{*-}, \alpha^{*+}]$; only the boundary values of α^{*-} and α^{*+} need to be calculated.

5.2.2.3. Monte Carlo simulation for boundary values of α^*

The values of α^{*-} and α^{*+} can be found using a statistical simulation technology: Monte Carlo simulation. Monte Carlo simulation involves the repeated generation of

pseudovalues for the modeling inputs, drawn from known probability distributions within the ranges of possible values.

Algorithm 2 In this study, the Monte Carlo simulation includes the following steps:

Step 1*: generation of the pseudovalues for* $[a_{ij}^{-}, a_{ij}^{+}]$ *and* $[c_j^{-}, c_j^{+}]$*, which both follow the uniform distribution.*

Step 2*: implementation of Model 5-4 and Algorithm 1 with the pseudovalues to find a solution* α^*.

Step 3*: repeat steps 1 and 2.*

Step 4*: compare the values of* α^* *in the solution set to find* α^{*-} *and* α^{*+}.

5.2.2.4. A mathematical approach for boundary values of α^*

Equation 5-11 could be read as: we are fully satisfied ($\mu_G(x)$=1) with the *x*'s for which *f(x)* attains a value lower than the aspiration level f^-; we are less satisfied (0< $\mu_G(x)$<1) with the *x*'s for which *f(x)* is between the highest level f^+ and the lowest level f^-; finally, we are fully dissatisfied ($\mu_G(x)$= 0) with the *x*'s for which *f(x)* is larger than f^+.

The above interpretation is based on the assumption that the decision-maker knows the exact highest and the lowest aspiration levels, f^+ and f^-, respectively, for the objective function. For example, he or she should know the exact maximum cost permit and minimum cost permit for a construction plan. However, human decision-makers,

especially financial decision-makers, might only have empirically knowledge of one aspiration level, $f^{'}$. It is researchers and engineers rather than decision-makers who are good at making use of imprecise information. A good decision maker should give accurate information to the executive layer. Using the same example to express the idea of one aspiration goal: the decision maker is fully satisfied ($\mu_G(x)$ =1) with one construction plan (*x*'s) for which the cost (*f(x)*) attains a value lower than his or her aspiration level, $f^{'}$, and he/she is fully dissatisfied with another construction plan (*x*'s) for which the cost (*f(x)*) is larger than $f^{'}$.

Therefore, it has the following membership function equation:

$$\mu_G(x)=\begin{cases}1 & if\ cx\le f^{'},\\ 0 & if\ cx\ge f^{'}.\end{cases}$$

In the LP area, this single aspiration level for the objective function may be interpreted as an objective function constraint.

Theorem 5 Suppose $x(\alpha)$ is the solution of a crisp Min BLP like Model 5-4. Then, $\lambda(x(\alpha))$ has a negative linear correlation relationship with the coefficients in the objective.

Proof *let* $\{c^{'}=c+\Delta c\,|\,\Delta c\ge 0\}$ *, and suppose* $x(\alpha^0)$ *and* $x(\alpha^1)$ *are the solutions corresponding with c and* $c^{'}$*, respectively. Since* $c\cdot x(\alpha^0)=\min\{c\cdot x\,|\,x\in X(\alpha^0)\}\ \le\ c^{'}\cdot x(\alpha^1)=\min\{c^{'}\cdot x\,|\,x\in X(\alpha^1)\}$*,* $X(\alpha^1)\supseteq X(\alpha^0)$*. Then,* $\{x\in\Re\,|\,\mu_X^{'}(x)\ge\alpha^1, x\in\{0,1\}\}\supseteq$

$\left\{x \in \Re \middle| \mu_X(x) \geq \alpha^0, x \in \{0,1\}\right\}$ *where,* $\lambda(x(\alpha^0)) \geq \lambda(x\ (\alpha^1))$**.** *Therefore,* $\lambda(x\ (\alpha))$ *has a negative linear correlation relationship with the coefficients in the objective.*

Corollary 1 Suppose $x(\alpha\ )$ is the solution of a crisp Max BLP. Then, $\lambda(x\ (\alpha))$ has a positive linear correlation relationship with the coefficients in the objective.

Proof *The proof is similar to Theorem 5.*

Theorem 6 Suppose $x(\alpha\ )$ is the solution of a crisp-coefficient BLP (regardless of the Min model or Max model). Then, $\lambda(x\ (\alpha))$ has a negative linear correlation relationship with the variable coefficients in the constraints.

Proof *According to Equation 5-3, it obtains that* $\mu_i^0(x) = (b_i + \Delta b_i - \sum_{j \in N} a_{ij}^0 x_j) / \Delta b_i$ *for a crisp-coefficient BLP like Model 5-4. Let* $\alpha^0 \in (0,1]$ *be a specific fixed value and* $x(\alpha^0)$ *be the optimal 0-1 solution of the corresponding problem* $P(\alpha^0)$**.** *If* $\forall a_{ij}^1 \geq a_{ij}^0$**,** *then a new membership function arises:* $\mu_i^1(x) = (b_i + \Delta b_i - \sum_{j \in N} a_{ij}^1 x_j) / \Delta b_i$**.** *Similarly, let* $\alpha^1 \in (0,1]$ *be a specific fixed value and* $x(\alpha^1)$ *be the optimal 0-1 solution of the corresponding problem* $P(\alpha^1)$ **.** *According to proposition 1,* $\lambda(x\ (\alpha^0)) = \min\{\mu_i^0(x(\alpha^0)), i \in M\}$ *and* $\lambda(x\ (\alpha^1)) = \min\{\mu_i^1(x(\alpha^1)), i \in M\}$ **.** *Due to* $x_j \geq 0$ **,** $\mu_i^1(x) \leq \mu_i^0(x)$ **,** *then* $\lambda(x(\alpha^1)) \leq \lambda(x\ (\alpha^0))$**.** *Therefore,* $\lambda(x\ (\alpha))$ *has a negative linear correlation relationship with the variable coefficients in the constraints.*

According to Theorem 5 and Theorem 6, the values of α^{*-} and α^{*+} can be obtained from the extreme constraint combination models as follows.

1) The upper bound of $U(\alpha^*)$ of a Min interval-coefficient BLP:

$$\begin{aligned}
&\min\ f = \sum_{j\in N} c_j^- x_j \\
&s.t.\quad \sum_{j\in N} a_{ij}^- x_j \le b_j + \Delta b_j(1-\alpha\ ) \quad i \in M, \\
&\qquad x_j \in \{0,1\}, \quad \alpha\ \in (0,1].
\end{aligned}$$

2) The lower bound of $U(\alpha^*)$ of a Min interval-coefficient BLP:

$$\begin{aligned}
&\min\ f = \sum_{j\in N} c_j^+ x_j \\
&s.t.\quad \sum_{j\in N} a_{ij}^+ x_j \le b_j + \Delta b_j(1-\alpha\ ) \quad i \in M, \\
&\qquad x_j \in \{0,1\}, \quad \alpha\ \in (0,1].
\end{aligned}$$

3) The upper bound of $U(\alpha^*)$ of a Max interval-coefficient BLP:

$$\begin{aligned}
&\max\ f = \sum_{j\in N} c_j^+ x_j \\
&s.t.\quad \sum_{j\in N} a_{ij}^- x_j \le b_j + \Delta b_j(1-\alpha\ ) \quad i \in M, \\
&\qquad x_j \in \{0,1\}, \quad \alpha\ \in (0,1].
\end{aligned}$$

4) The lower bound of $U(\alpha^*)$ of a Max interval-coefficient BLP:

$$\max\ f = \sum_{j\in N} c_j^- x_j$$
$$s.t.\quad \sum_{j\in N} a_{ij}^+ x_j \le b_j + \Delta b_j(1-\alpha\ ) \quad i \in M,$$
$$x_j \in \{0,1\}, \quad \alpha\ \in (0,1].$$

5.2.2.5. The best and the worst optimum models

Algorithm 3 For the interval coefficient BLP model 5-12, $x_j \in \{0,1\} \ge 0$, the best optimum can be found by solving the following BLP:

$$\min z = \sum_{j\in N} c_j^- x_j$$
$$s.t.\quad \sum_{j\in N} a_{ij}^- x_j \le (b_j^- + \Delta b_j(1-\alpha^{*+})) \quad i \in M, \tag{5-13}$$
$$x_j \in \{0,1\}.$$

Also, the worst optimum can be derived by solving the following BLP:

$$\min z = \sum_{j\in N} c_j^+ x_j$$
$$s.t.\quad \sum_{j\in N} a_{ij}^+ x_j \le (b_j^- + \Delta b_j(1-\alpha^{*-})) \quad i \in M, \tag{5-14}$$
$$x_j \in \{0,1\}.$$

Due to the fact that the best optimum model has the largest possible feasible domain and the most favorable version of the objective function, and the worst optimum model has the smallest possible feasible domain and the least favorable version of the objective function, the results of these two extreme models can bound all outcomes of the IFBLP.

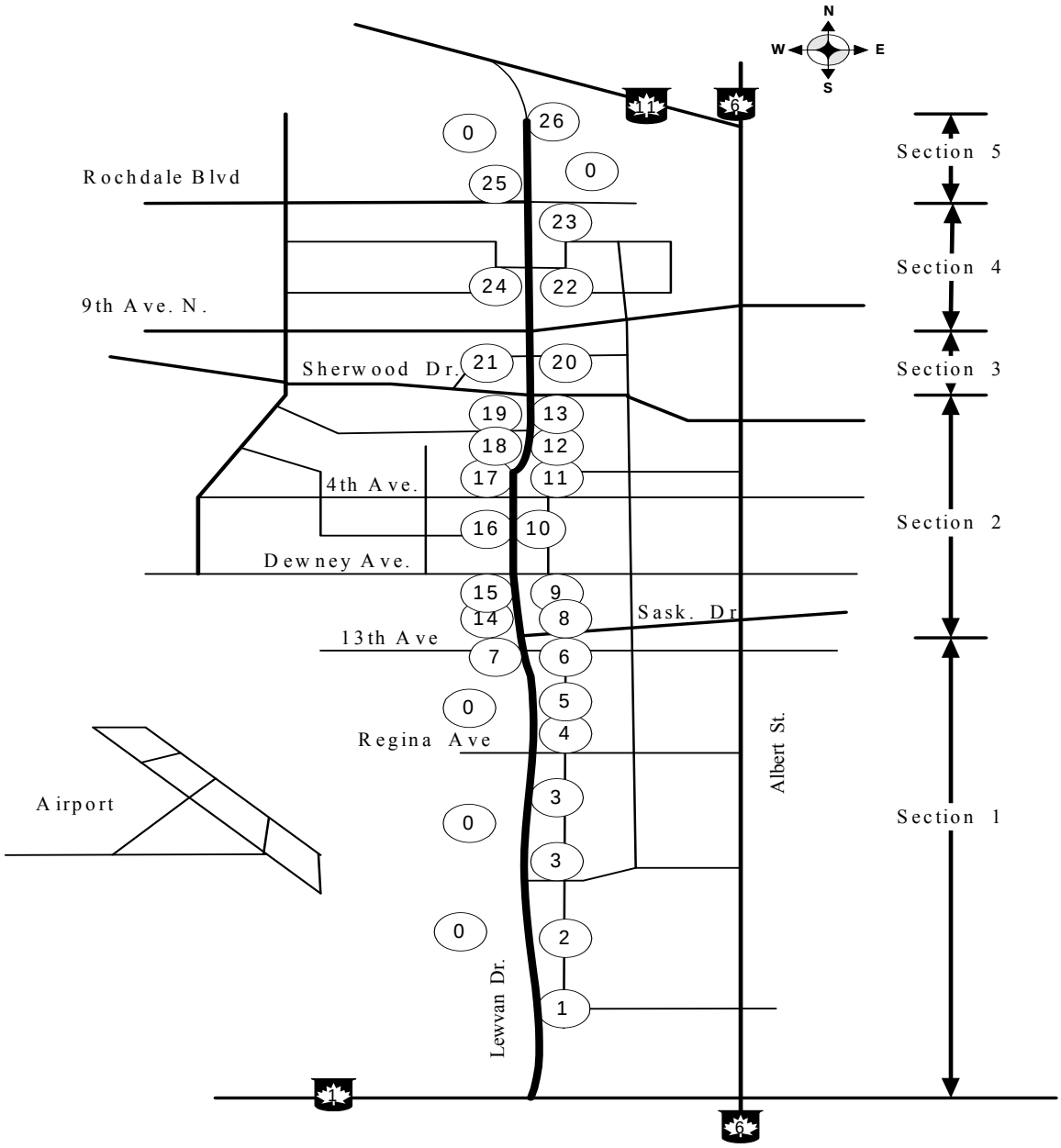

Figure 5-1 The study road sketch

Table 5-1 Noise correction factors of pavements (dBA)

Pavement Type	Noise Correction Factor
16 ~ 20 mm Bitumen Seal	+4 ~ +5
Concrete	+4
5 ~ 14 mm Bitumen Seal	+2 ~ +4
5 mm Bitumen Seal	+1 ~ +2
Dense Graded Asphalt	0
Stone Mastic Asphalt	- 2
Boral Low Noise Asphalt	- 2
Open Graded Asphalt	- 4

Table 5-2 Noise reduction deterioration of OGA

Age of Surface	Noise Reduction (in L_{eq})
0 year	5 – 7 dB(A)
2 years	4 – 5 dB(A)
4 years	1 – 2 dB(A)

Source: Sandberg, 1992

Table 5-3 The interval values of NAC (dBA)

Zone	Day	Night
Quiet	(49, 55)	(39, 48)
Normal	(54, 59)	(44, 53)
Annoyance	(58, 67)	(49, 58)
Severe Annoyance	(66, 72)	(54, 63)
Unlimited	--	--

Table 5-4 26 study zones identification

No	(1)	(2)	(3)	(4)	(5)	(6)	No	(1)	(2)	(3)	(4)	(5)	(6)
0	Undev.	U	--	--	--	--	14	Resid.	N	0.4	50	E	2
1	Resid.	N	0.8	50	E	1	15	Resid.	N	0.35	30	O	2
2	Resid.	N	0.5	80	O	1	16	Resid.	N	0.85	30	O	2
3	Recre.	A	2.1	--	O	1	17	Church	N	0.2	20	O	2
4	Resid.	N	0.5	80	O	1	18	Park	A	0.2	--	O	2
5	Recre.	A	0.4	--	O	1	19	Resid.	N	0.45	30	O	2
6	Resid.	N	0.5	60	O	1	20	Resid.	N	0.9	20	O	3
7	Resid.	N	0.3	40	E	1	21	Resid.	N	0.4	20	O	3
8	Park	A	0.6	--	O	2	22	Resid.	N	0.9	50	O	4
9	Hospi.	Q	0.2	150	O	2	23	Comm.	A	0.35	150	O	4
10	Resid.	N	0.8	15	O	2	24	Resid.	N	0.9	50	O	4
11	School	N	0.2	40	O	2	25	Comm.	A	0.2	150	O	5
12	Park	A	0.5	--	O	2	26	Factory	S	0.5	150	O	5
13	Resid.	N	0.6	20	O	2							

Source: Air photo of Regina city, City of Regina, April 2004.

Note: (1) – Property of the studying zone

(2) – NAC: Quiet (Q); Normal (N); Annoyance (A);
Severe-Annoyance (S); Undeveloped (U)

(3) – The length of the studying zone along the road (km)

(4) – The average distance form receptor in a zone to edge of the road (m)

(5) – Berm: existing (E); none (O)

(6) – Index of section

Table 5-5 Five sections information

Section No.	Vehicle volume (vehicles/day)	Speed (km/hr)	Beginning place	Ending place	Length/width (km/m)
1	19,900 – 12,500	80	HWY #1	Sask. Dr.	5.7/40
2	23,600 – 33800	70	Sask. Dr.	Sherw. Dr.	3.2/35
3	19,100 – 19,800	60	Sherw. Dr.	9th Ave. N.	1.0/25
4	22,200 – 26,100	70	9th Ave. N.	Rochd. Dr.	1.4/35
5	6,200 -	100	Rochd. Dr.	HWY #11	1.1/40

Source: 2003 Traffic Flow Map, City of Regina

Table 5-6 The pavement repaving and maintenance costs (1000 Dollar)

	Time period 1		Time period 2		Time period 3	
	Repaving	Maintenance	Repaving	Maintenance	Repaving	Maintenance
1	1368 – 2508	1026 – 1254	1482 – 2622	1083 – 1311	1596 – 2736	1140 – 1368
2	768 – 1408	576 – 704	832 – 1482	608 – 736	896 – 1536	640 – 768
3	192 – 352	144 – 176	208 – 368	152 – 184	224 – 384	160 – 192
4	336 – 616	252– 308	364 – 644	266 – 322	392 – 672	280 – 336
5	264 – 484	198 – 242	286 – 506	209 - 253	308 – 528	220 – 264

5.3. Application

Traffic noise control planning is a BLP problem. The developed IFBLP and its solution process are applied to a long-term traffic noise control plan to demonstrate its applicability.

5.3.1. Site information

The study road is 12.4 km length and is separated into five sections (shown in Figure 5-1 and Table 5-5). It includes residential zones, public zones, factories, hospitals, churches, schools, and commercial zones. According to these properties and geographic information, a total of 26 study zones are identified along the two sides (shown in Figure 5-1 and Table 5-4). An IFBLP model should be developed for a 15-year noise control plan on this road, and the proposed algorithm should be applied to solve this model.

5.3.2. Traffic noise control techniques

5.3.2.1. Three traffic noise control methods

Source control, propagation control, and receiver control are three basic traffic noise control methods. Source control is the primary choice due to its proactivity and its ability to reduce the need for the latter two methods (Herman, 1997). Propagation control and receiver control could be considered as continual efforts for further mitigating if the noise level is still higher than the guideline at the reception sections, especially for

particular places, such as residences, schools and churches.

For source control, the quality improvement of a road is an effective way of reducing noise. Open-graded asphalt (OGA) is a desirable material for pavement. Vehicles on an OGA surface produced up to 6.5 dB less noise than identical vehicles on a rough surface like Portland cement concrete (Hanson and James, 2004). The installation of building barrier is the most popular noise propagation control method. It is reported that noise level reduction of a barrier with a height of 3.5 m is in the range of 5 to 10 dBA (Canada Government Report, 2004). It is worth noting that some areas, such as commercial areas, might not be suited for the building of a noise barrier. For the receiver control, high-rise buildings in urban areas might use insulated windows to keep noise out.

5.3.2.2. Noise Abatement Criteria (NAC)

The noise criterion is based on the 23CFR772 criteria of NAC (Barry and Reagan, 1978) in which traffic noises are categorized into five noise tolerances classes: quiet, normal, annoyance, severe annoyance, and un-limitation. Considering the "regulations for community noise" (Dieter, 1995), an interval noise abatement criteria has been developed (shown in Table 5-3).

5.3.2.3. Traffic noise prediction

Traffic noise level is derived using a noise prediction model for each year in the plan term and each specific section on the study road (Peng and Mayorga, 2008). The noise level is expressed as an interval value.

Figure 5-2 illustrates the predicted noise levels at zone #11 and indicates that the noise levels in the next 15 years will gradually increase. Figure 5-3 demonstrates the predicted noise levels on the 10th year for all 15-year study zones. It shows that the predicted noise levels will vary in different zones.

5.3.3 Build the IFBLP model

The IFBLP was built for the noise control plan.

Min f =

$$\sum_{u=1}^{U}\sum_{j=1}^{M}[SC_{ju}^{-}, SC_{ju}^{+}]x_{ju} + \sum_{u=1}^{U}\sum_{j=1}^{M}[SM_{ju}^{-}, SM_{ju}^{+}] \tag{5-15a}$$

$$+ \sum_{c=\{0,1\}}\sum_{i=1}^{L}\sum_{k=1}^{N}\left[BC_{cik}^{-}, BC_{cik}^{+}\right]y_{cik} + \sum_{c=\{0,1\}}\sum_{i=1}^{L}\sum_{k=1}^{N}\left[BM_{cik}^{-}, BM_{cik}^{+}\right]y_{cik} + \sum_{i=1}^{L}[BMD_{i}^{-}, BMD_{i}^{+}] \tag{5-15b}$$

$$+ \sum_{i=1}^{L}\sum_{k=1}^{N}\left[WPA_{ik}^{-}, WPA_{ik}^{+}\right]\left[WN_{ik}^{-}, WN_{ik}^{+}\right]z_{ik} + \sum_{i=1}^{L}\sum_{k=1}^{N}\left[WMA_{ik}^{-}, WMA_{ik}^{+}\right]\left[WN_{ik}^{-}, WN_{ik}^{+}\right]z_{ik} + \sum_{i=1}^{L}[WMD_{i}^{-}, WMD_{i}^{+}] \tag{5-15c}$$

$$- \sum_{u=1}^{U}\sum_{j=1}^{M}[SBF_{ju}^{-}, SBF_{ju}^{+}]x_{ju} \tag{5-15d}$$

s.t.

$$-\left[SRL_i^-, SRL_i^+\right]x_{ju} - \left[BRL_k^-, BRL_k^+\right]\sum_{c=\{0,1\}}\sum_{i=1}^{L}\sum_{k=1}^{N} y_{cik}$$
$$-\left[WRL_k^-, WRL_k^+\right]\sum_{i=1}^{L}\sum_{k=1}^{N} y_{cik} \lesssim \left[NAC_{\theta p}^-, NAC_{\theta}^+\right] - \left[NP_{\theta ikpu}^-, NP_{\theta ikpu}^+\right] \quad (5\text{-}15e)$$

$$x, y, z \in \{0, 1\} \quad (5\text{-}15f)$$

$$\sum_{i}^{L} y_{cik} \le 1 \quad (5\text{-}15g)$$

$$\sum_{i}^{L} z_{ik} \le 1 \quad (5\text{-}15h)$$

$$y_{cik} = 0 \text{ when } c = 1 \quad (5\text{-}15i)$$

where (5-15a) = the pavement surface construction and maintenance costs; (5-15b) = the barrier build and maintenance costs; (5-15c) = the insulated windows installation and maintenance costs; (5-15d) = the benefits from a new road surface; (5-15e) = the noise abatement criteria constraints; (5-15f) = the binary constraints; (5-15g) = only one barrier construction in the *k* zone may be applied in the whole study term; (5-15h) = only one insulated window installation in the *k* zone may be applied in the whole study term; and (5-15i) = barrier cannot be built in a commercial area or the zones of an existing barrier. Also *i* = index of the year in a planning term (*i = 1,2,…,L)*; *j* = index of the period in a planning term (*j = 1,2,…M)*; *t* = index of the year in a period *j* (*t = 0,1,…4)*; *u* = index of the road section (*u = 1, 2, …, U)*; *k* = index of the studying zone (*k = 1,2,…,N); p* = index of five classes of noise abatement criteria; θ = binary number index (θ = 1 represents day time, θ = 0 represents in night time); and *c* = binary number index (*c* = 1 represents a commercial area or the zones of existing barrier; *c* = 0 represents the other areas).

Further, $SC_{ju}^{\pm}$ = the pavement surface repaving cost in the period *j*; $SM_{ju}^{\pm}$ = the pavement surface maintenance cost in the period *j*; $BC_{cik}^{\pm}$ = the barrier constructing cost at the k^{th} zone in the i^{th} year; $BM_{cik}^{\pm}$ = the barrier maintenance cost at the k^{th} zone in the i^{th} year; $BMD_i^{\pm}$ = the maintenance cost for all the existing barriers; $WPA_{ik}^{\pm}$ = per insulated window installing cost at the k^{th} zone in the i^{th} year; $WN_{ik}^{\pm}$ = the number of window at the k^{th} zone in the i^{th} year; $WMA_{ik}^{\pm}$ = per insulated window maintenance cost at the k^{th} zone in the i^{th} year; $WMD_i^{\pm}$ = the maintenance cost for all existing insulated windows; $SBF_{ju}^{\pm}$ = the coefficient of benefit from renewing the pavement surface every 5 years; $NP_{\theta ikpu}^{\pm}$ = the predicted noise level (day or night) at the k^{th} zone on the u^{th} road section and belongs to the p^{th} NAC class in the i^{th} year; $BRL_k^{\pm}$ = the reduced noise level by the barrier at the k^{th} zone dBA; $WRL_k^{\pm}$ = the reduced noise level by the insulated window at the k^{th} zone (dBA); $NAC_{\theta p}^{\pm}$ = the noise abatement criteria, and $SRL_t^{\pm}$ represents the reduced noise level (dBA) that benefited from the OGA surface at the t^{th} year in a period.

5.3.4 Solve the IFBLP model

Step 1 Transfer the IFBLP Model 5-15 into an IBLP model with α-cut in terms of Model 5-9.

Min f = (5-15a) + (5-15b) + (5-15c) + (5-15d) (5-16a)

s.t.

$$-\left[SRL_i^-, SRL_i^+\right]x_{ju} - \left[BRL_k^-, BRL_k^+\right]\sum_{c=\{0,1\}}\sum_{i=1}^{L}\sum_{k=1}^{N} y_{cik}$$

$$-\left[WRL_k^-, WRL_k^+\right]\sum_{i=1}^{L}\sum_{k=1}^{N} y_{cik} \tag{5-16b}$$

$$\le (NAC_{\theta p}^- - NP_{\theta ikpu}^+) + (NAC_{\theta p}^+ - NAC_{\theta p}^- + NP_{\theta ikpu}^+ - NP_{\theta ikpu}^-)(1 - U(\alpha^*))$$

(5-15f), (5-15g), (5-15h), (5-15i). (5-16c)

Step 2 Calculate the bound values of $U(\alpha^*)$ in terms of the *Monte Carlo simulation* (Algorithms 2); the values of α^{*-} and α^{*+} can be obtained.

Step 3 Implement Algorithm 3; it has the following two crisp models:

1) The best optimum BLP model

Min f =

$$\sum_{u=1}^{U}\sum_{j=1}^{M} SC_{ju}^- x_{ju} + \sum_{u=1}^{U}\sum_{j=1}^{M} SM_{ju}^- \tag{5-17a}$$

$$+ \sum_{c=\{0,1\}}\sum_{i=1}^{L}\sum_{k=1}^{N} BC_{cik}^- y_{cik} + \sum_{c=\{0,1\}}\sum_{i=1}^{L}\sum_{k=1}^{N} BM_{cik}^- y_{cik} + \sum_{i=1}^{L} BMD_i^- \tag{5-17b}$$

$$+ \sum_{i=1}^{L}\sum_{k=1}^{N} WPA_{ik}^- z_{ik} WN_{ik}^- + \sum_{i=1}^{L}\sum_{k=1}^{N} WMA_{ik}^- z_{ik} WN_{ik}^- + \sum_{i=1}^{L} WMD_i^- \tag{5-17c}$$

$$- \sum_{u=1}^{U}\sum_{j=1}^{M} SBF_{ju}^+ x_{ju} \tag{5-17d}$$

s.t.

$$-SRL_i^+ x_{ju} - BRL_k^+ \sum_{c=\{0,1\}} \sum_{i=1}^{L} \sum_{k=1}^{N} y_{cik} - WRL_k^+ \sum_{i=1}^{L} \sum_{k=1}^{N} y_{cik} \leq (NAC_{\theta p}^- - NP_{\theta ikpu}^+) + (NAC_{\theta p}^+ - NAC_{\theta p}^- + NP_{\theta ikpu}^+ - NP_{\theta ikpu}^-)(1-\alpha^{*-}) \quad (5\text{-}17e)$$

(5-15f), (5-15g), (5-15h), (5-15i). (5-17f)

2) The worst optimum BLP model

Min f =

$$\sum_{u=1}^{U} \sum_{j=1}^{M} SC_{ju}^+ x_{ju} + \sum_{u=1}^{U} \sum_{j=1}^{M} SM_{ju}^+ \quad (5\text{-}18a)$$

$$+ \sum_{c=\{0,1\}} \sum_{i=1}^{L} \sum_{k=1}^{N} BC_{cik}^+ y_{cik} + \sum_{c=\{0,1\}} \sum_{i=1}^{L} \sum_{k=1}^{N} BM_{cik}^+ y_{cik} + \sum_{i=1}^{L} BMD_i^+ \quad (5\text{-}18b)$$

$$+ \sum_{i=1}^{L} \sum_{k=1}^{N} WPA_{ik}^+ z_{ik} WN_{ik}^+ + \sum_{i=1}^{L} \sum_{k=1}^{N} WMA_{ik}^+ z_{ik} WN_{ik}^+ + \sum_{i=1}^{L} WMD_i^+ \quad (5\text{-}18c)$$

$$- \sum_{u=1}^{U} \sum_{j=1}^{M} SBF_{ju}^- x_{ju} \quad (5\text{-}18d)$$

s.t.

$$-SRL_i^- x_{ju} - BRL_k^- \sum_{c=\{0,1\}} \sum_{i=1}^{L} \sum_{k=1}^{N} y_{cik} - WRL_k^- \sum_{i=1}^{L} \sum_{k=1}^{N} y_{cik} \leq (NAC_{\theta p}^- - NP_{\theta ikpu}^+) + (NAC_{\theta p}^+ - NAC_{\theta p}^- + NP_{\theta ikpu}^+ - NP_{\theta ikpu}^-)(1-\alpha^{*+}) \quad (5\text{-}18e)$$

(5-15f), (5-15g), (5-15h), (5-15i). (5-18f)

5.3.5. Results

The above binary linear optimization models are solved using the **bintprog** solver in Matlab. The related inputs are in Tables 5-1 to 5-6. The aspiration goal was designed to be $f^- = \$12{,}000{,}000$ with a tolerance of *$2,000,000* ($f^+ = \$14{,}000{,}000$). The range of α^* was generated using the Monte Carlo simulation method. After computing the model in Matlab, the results were generated and are shown in Table 5-7. It shows that the value of α^* is bounded between the lower bound (0.313) and the upper bound (0.9). The best optimal cost is *$12, 150,000* and the worst optimal cost is *$13,900,000*. The reason for the difference between the aspiration goals and the optimal costs is that the variables in the IFBLP are binary. Moreover, some optimal costs between two extreme optimums might exist (discretely due to binary variables), which can be used as a trade-off by a decision maker.

For the purpose of comparison, an IBLP was built. The only difference between the IBLP from the IFBLP is that the IBLP's structure is not fuzzy. It was solved using Chinneck and Rammadan's method, and the results are illustrated in Table 5-8. The best optimal cost obtained from this IBLP is $11,060,000, which is lower than that of the IFBLP; the worst optimal cost is $14,760,000, which is higher than that of the IFBLP. The comparison explicates that the α-cut based technology can effectively reduce the uncertainty on the right side of the constraints and can provide a more precise result for decision makers.

5.4. Summary

The following conclusions can be drawn:

- An IFBLP is formulated to solve the binary linear problems in an uncertain environment. It uses fuzzy constraints, a fuzzy objective, and interval coefficients to reflect uncertainties.
- The developed solution included two major processes: the defuzzification process and the crisping process. The defuzzification process utilizes the α -cut technique to defuzzify a crisp-coefficient FBLP into a crisp-coefficient BLP. The crisping process uses an interval linear programming algorithm to convert the interval-coefficient BLP into two extreme crisping-coefficient BLPs.
- In order to determine the value range of optimal alpha, a Monte Carlo simulation based approach is developed.
- A mathematical sound approach (based on some mathematical developments) is presented to solve the IFBLP problem. This approach can also determine the boundary values of optimal alpha, so that the linearity of the IFBLP model can be maintained during the crisping process.
- The proposed IFBLP and its solution are applied to a long-term traffic noise control plan. The results demonstrated the applicability of this method. Compared to an IBLP, the IFBLP could effectively reduce uncertainties on the right side of the constraints and could provide a more precise result for decision makers.

In the next chapter, a robust optimization approach is developed for real-time multiple source water blending problem under uncertainty.

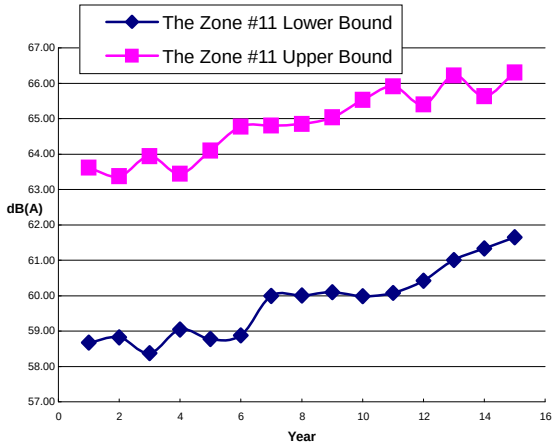

Figure 5-2 The predicted noise level at the zone #11

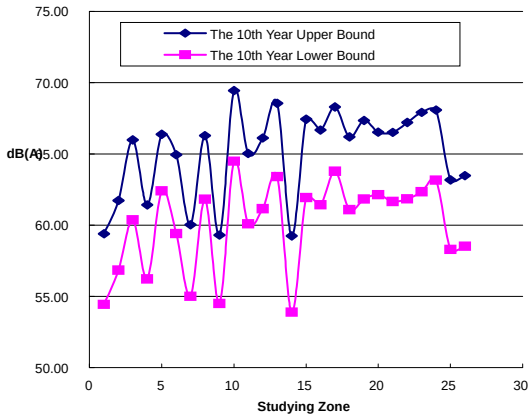

Figure 5-3 The predicted noise level for the future 10th year

Table 5-7 Results of the IFBLP

$f^{\pm}(10^6)$	$\alpha^{\pm}$	$\mathbf{X}_{rc}=1$	$\mathbf{Y}_{i(k)}=1$	$\mathbf{Z}_{i(k)}=1$
12.15	0.313		$Y_{15(9)}$ $Y_{15(11)}$ $Y_{15(13)}$ $Y_{15(15)}$	$Z_{1(2)}$ $Z_{1(4)}$ $Z_{1(6)}$ $Z_{1(10)}$ $Z_{1(13)}$ $Z_{1(15)}$ $Z_{1(16)}$ $Z_{1(19)}$ $Z_{1(20)}$ $Z_{1(21)}$ $Z_{1(22)}$ $Z_{1(23)}$ $Z_{1(24)}$ $Z_{15(17)}$
13.90	0.9	X_{32} X_{34} X_{35}	$Y_{15(6)}$ $Y_{15(9)}$ $Y_{15(10)}$ $Y_{15(11)}$ $Y_{15(13)}$ $Y_{15(15)}$ $Y_{15(16)}$ $Y_{15(17)}$ $Y_{15(19)}$ $Y_{15(20)}$ $Y_{15(21)}$ $Y_{15(22)}$ $Y_{15(24)}$	$Z_{1(1)}$ $Z_{1(7)}$ $Z_{1(11)}$ $Z_{1(13)}$ $Z_{1(14)}$ $Z_{1(15)}$ $Z_{1(16)}$ $Z_{1(19)}$ $Z_{1(20)}$ $Z_{1(22)}$ $Z_{1(23)}$ $Z_{1(24)}$ $Z_{5(2)}$ $Z_{5(4)}$ $Z_{5(6)}$ $Z_{5(10)}$ $Z_{6(21)}$ $Z_{15(17)}$

Note: X=1 *means Road Surface Updating*
Y=1 means Barrier Building
Z=1 means Insulted Window Installing
Period index r = 1, 2, 3.; *Section index* c = 1,…5.
Year index *i = 1,…15.;* Zone index *k = 1,…26.*

Table 5-8 Solution of the IBLP

$f^{\pm}(10^6)$	$\mathbf{X}_{rc}$=1	$\mathbf{Y}_{i(k)}$ = 1	$\mathbf{Z}_{i(k)}$ = 1
11.06		$Y_{15(11)}$	$Z_{1(2)}$ $Z_{1(4)}$ $Z_{1(6)}$ $Z_{1(15)}$ $Z_{1(16)}$ $Z_{1(19)}$ $Z_{1(20)}$ $Z_{1(18)}$ $Z_{1(20)}$ $Z_{1(21)}$ $Z_{15(17)}$
14.76	X_{32}	$Y_{15(6)}$ $Y_{15(7)}$ $Y_{15(8)}$ $Y_{15(9)}$ $Y_{15(10)}$	$Z_{1(1)}$ $Z_{1(6)}$ $Z_{1(7)}$
	X_{33}	$Y_{15(11)}$ $Y_{15(12)}$ $Y_{15(13)}$ $Y_{15(14)}$ $Y_{15(15)}$	$Z_{1(8)}$ $Z_{1(9)}$ $Z_{1(10)}$
	X_{34}	$Y_{15(16)}$ $Y_{15(17)}$ $Y_{15(18)}$ $Y_{15(19)}$ $Y_{15(20)}$	$Z_{1(11)}$ $Z_{1(13)}$ $Z_{1(14)}$ $Z_{1(15)}$ $Z_{1(16)}$
	X_{35}	$Y_{15(18)}$ $Y_{15(19)}$ $Y_{15(21)}$	$Z_{1(18)}$ $Z_{1(19)}$ $Z_{1(20)}$ $Z_{1(19)}$ $Z_{1(20)}$ $Z_{1(21)}$ $Z_{5(2)}$ $Z_{5(3)}$ $Z_{5(4)}$ $Z_{5(5)}$ $Z_{5(12)}$ $Z_{6(18)}$ $Z_{15(17)}$

Note: X=1 *means Road Surface Updating*
Y=1 means Barrier Building
Z=1 means Insulted Window Installing
Period index r = 1, 2, 3.; *Section index* c = 1,…5.
Year index i = 1,…15.; Zone index k = 1,…26.

CHAPTER 6

A Robust Optimization Approach for Real-time Multiple Source Water Blending Problem under Uncertainty

6.1. Statement of problems

Multiple source water blending is a real-time multi-objective nonlinear optimization problem (Peng et al., 2010a, b). The previous approaches with regard to this field are intelligent optimization, model predictive control and optimization, and nonlinear optimization, which contributed to improving product quality, optimizing production rates, reducing production costs, and minimizing pollution. However, intelligent optimization has a high requirement of prior operation knowledge that highly depends on expert experiences which may not be available (Huang et al., 2008). Model predictive control and optimization is capable of dealing with simple nonlinear systems or used in applications with slow dynamics (Wang and Boyd, 2010). Conventional nonlinear optimization methodologies such as gradient-based algorithms and genetic algorithms (Mehrez et al., 1992; Ostfeld et al., 1996; Yang et al., 2000; Tu et al., 2005) cannot to rapidly produce a robust optimum objective. For example, gradient-based algorithms may only find local optimums and genetic algorithms are time-consuming when used to solve a large-scale nonlinear problem.

Imran et al. (2006) presented a method to optimize multiple source water blends with respect to metal corrosion and residual control in the distribution system. They built nonlinear empirical models for copper, lead, and iron, along with a mono-chloramine

decay model. Based on regulation action levels, they determined the maximum metal releases and the minimum mono-chloramine residual. Consequently, the optimal water blending ratio was found in accordance with various scenarios.

However, their optimization method has two main shortcomings. The first is that the solution may be not robust. This might be due to multiple conflicting objectives and the homogeneous variances assumption implicit in the nonlinear empirical equations. Different pipe materials often have conflicting water quality requirements for corrosion abatement. For example, increasing alkalinity would increase the corrosion of copper and lead. Therefore, there would be a benefit in reducing the release of iron. Increasing sulfates would reduce the release of lead but increase iron corrosion (Imran et al., 2006). However, Imran's method did not take into consideration the simultaneous optimization of the conflicting objectives that might result in a non-robust problem. On the other hand, the assumption of a homogeneous variance might not be valid in the real-time water blending operation. This is due to an error between the predicted output of the fitted model and the measured data of the experimental data set. If the error were large enough, the predicted optimum would be non-robust. Secondly, water quality might change with a fluctuation in temperature or other impact factors. Imran's method could not respond rapidly enough to the uncertainty of water quality because the optimization involves high-order nonlinear models that are time-consuming.

A fuzzy multiple response surface methodology (FMRSM) can be used for this type of optimization. Basically, the FMRSM integrates a dual-response surface methodology (RSM) and fuzzy optimization approach (FOA). The RSM is a statistical technique used in empirical study. It approximates the true response surface, estimates the

parameters and works well in solving real response surface problems (Anderson-Cook et al., 2009; Myers et al., 2004). As a consequence, it searches for an optimal set of input variables to optimize the response using a set of designed experiments. The RSM can be solved quickly by any commercial solver because it is based on a quadratic model rather than a high-order nonlinear model. The dual RSM builds two quadratic empirical models, one for the mean and one for the standard deviation, and then optimizes one of the responses subjecting to an appropriate constraint given by the other (Lin and Tu, 1995). Kim and Lin (1998) developed a fuzzy optimization approach to simultaneously optimize the dual response surface model, which can achieve a better balance between bias and variance compared to the other methods. However, due to the characteristics of the recorded experimental data in the water blending problem, two quadratic models are included in this study: one model for the measured experimental data set and the other for its residuals.

The method of dealing with a multi-objective problem is to single out one specific solution from the set of efficient individual solutions which qualifies as an optimal compromise (Zimmerman 1978). In a fuzzy environment, for example, objective functions and constraints can be characterized by their membership functions into a series of fuzzy sets. The min-operator is one fuzzy optimization technique. It can define an optimal solution in terms of the intersection of fuzzy sets with the highest degree of membership. This decision process simultaneously satisfies objective functions and constraints without differences between the former and latter. The min-operator assumes the decision maker knew the aspiration levels for all individual objectives and their related admissible violations.

Therefore, this chapter proposes a FMRSM and uses it to generate a robust solution to respond to the uncertainty of water quality in the real-time multiple source water blending problem. It includes three major steps. First, each original nonlinear empirical model is converted into two quadratic models: one model for the measured experimental data set and the other for its residuals. Second, the FMRSM is developed and integrated with the dual-RSM and FOA. Finally, a decision support system will be produced to guide decision of the water blending in a water distribution system in accordance with six designed scenarios. The FMRSM could be extended to other multi-objective nonlinear optimization problems.

This chapter is structured as follows: Section 6.2 contains an introduction of the dual-RSM and FOA, and the development of a general FMRSM. Section 6.3 shows the model conversions, the specific FMRSM development and scenario designs to a multiple source water blending problem. Section 6.4 presents the results and discussion. Section 6.5 presents the conclusions of the research.

6.2. Methodology

6.2.1. Dual-RSM

Box and Wilson (1951) first used the RSM to study the relationship between a response and a set of input variables. Vining and Myers (1990) first fitted the second-order polynomial models for a mean and standard deviation separately.

$$C_{\mu} = h_o + S^{'}h + S^{'}HS \tag{6-1}$$

$$C_{\sigma} = g_o + S^{'}g + S^{'}GS \tag{6-2}$$

where $g_0 = \alpha_0$, $h_0 = \beta_0$, $g = (\alpha_1, \alpha_2, ...\alpha_k)^{'}$, $h = (\beta_1, \beta_2, ...\beta_k)^{'}$, and

$$H = \frac{1}{2}\begin{bmatrix} 2\beta_{11} & \beta_{12} & \cdots & \beta_{1k} \\ \beta_{12} & 2\beta_{22} & \cdots & \\ \vdots & \vdots & \ddots & \vdots \\ \beta_{1k} & \beta_{2k} & \cdots & \beta_{kk} \end{bmatrix} \tag{6-3}$$

$$G = \frac{1}{2}\begin{bmatrix} 2\alpha_{11} & \alpha_{12} & \cdots & \alpha_{1k} \\ \alpha_{12} & 2\alpha_{22} & \cdots & \\ \vdots & \vdots & \ddots & \vdots \\ \alpha_{1k} & \alpha_{2k} & \cdots & \alpha_{kk} \end{bmatrix} \tag{6-4}$$

where h_0 , *h,* g_0 and *g* are the appropriate vectors for the estimated coefficients, *H* and *G* are the diagonal ($k \times k$) matrices of the estimated coefficients, C_{μ} and C_{σ} are the mean and standard deviation, and *S* and $S^{'}$ are ($k \times 1$) vectors of the input variables and their transverse, respectively.

6.2.2. Min-operator

Using the following model to introduce the min-operator technique:

$$\begin{aligned} &\min\ f = \sum_{j\in N} c_j x_j \\ &s.t.\quad \sum_{j\in N} a_{ij} x_j \mathrel{\tilde{\leq}} b_i \quad i \in M, \\ &\qquad x_j \geq 0. \end{aligned} \tag{6-5}$$

where $a_{ij}, b_i, c_j \in I(\Re)$ x_j are positive variables. The symbol " $\tilde{\leq}$ " represents fuzzy inequality, meaning the decision-maker permits some violations of the constraints.

Considering the goal is fuzzy, a decision-maker can establish an aspiration level " f' " for the desired objective function value. Then, Model 6-5 can be converted to:

$$\begin{aligned} &\textit{Find} \quad x_j \geq 0 \\ &\textit{such that} \quad \sum_{j\in N} c_j x_j \mathrel{\tilde{\leq}} f' \\ &\qquad\qquad \sum_{j\in N} a_{ij} x_j \mathrel{\tilde{\leq}} b_i \quad i \in M. \end{aligned} \tag{6-6}$$

where no distinction is made between fuzzy objectives and fuzzy constraints. According to Bellman and Zadeh (1970), the solution of Model 6-6 will be x^* and the membership function (satisfaction degree) of the optimal decision is:

$$\mu_D(x^*) = \max_x \mu_D(x) = \max_x \min_i [\mu_G(x), \mu_C(x)] \tag{6-7}$$

where $\mu_G(x)$ and $\mu_C(x)$ are the membership functions of the goal and constraints. $\mu_D(x)$ may be called "the satisfaction degree of a decision". In order to obtain x^*, let $\lambda = \mu_D(x) = \min_i [\mu_G(x), \mu_C(x)]$, and implement the following model:

$$\max \lambda$$
$$s.t. \quad \lambda \le \frac{d_i + \Delta d_i - E_i x}{\Delta d_i}, \quad i \in M+1, \tag{6-8}$$
$$x \in \{0,1\}, \quad 0 \le \lambda \le 1.$$

where E_i is the *i-th* row of E, $E = [c, a_1, ..., a_i]^T \in \{\Re\}^{(m+1)\times n}$; d_i is the *i-th* row of d, $d = \begin{bmatrix} f' \\ b \end{bmatrix} \in \{\Re\}^{(m+1)}$, Δd_i is the tolerance of the right-hand side, and $\Delta d_i \ge 0$.

Due to the decision process simultaneously satisfies objective functions and constraints without a difference between the former and latter, a synchronous optimization is achieved.

6.2.3. FMRSM programming

In this study, two types of quadratic models are generated: one model for the measured experimental data set and the other for its residuals. A residual is defined as the difference between the predicted output from the model and measured output from the experimental data set.

Assume there are *n* relationships between the responses and set of input variables to be studied. Each relationship can be fitted into two second-order polynomial models for the measured data sets and residuals. A general optimization programming for the multi-objective response surface problem is shown as follows:

$$Min \quad (C)_n \qquad n \in N \tag{6-9a}$$

$$Min \quad (C_r)_n \qquad n \in N \tag{6-9b}$$

s.t.

$$(C)_n = \left(h_o + S^{'}h + S^{'}HS\right)_n \le (L)_n \tag{6-9c}$$

$$(C_r)_n = \left(g_o + S^{'}g + S^{'}GS\right)_n \le (L_r)_n \tag{6-9d}$$

$$S_k = \sum_{i=1}^{I} x_i U_{ki} \tag{6-9e}$$

$$0 \le x_i \le 1 \tag{6-9f}$$

$$\sum_{i=1}^{I} x_i = 1 \tag{6-9g}$$

where C is the predicted output from the corrosion model, C_r is the predicted residual from the residual model, n is the number of responses, L and L_r are the limitations corresponding to C and C_r, respectively, S_k is the k^{th} input variable, k is an index for the input variables, x_i is the percentage of water source I, i is an index for the water sources, and U_{ki} is the coefficient of the k^{th} input variable for water source i.

The objectives of (6-9a) and (6-9b) are to minimize the responses. Those objectives are also constrained by the constraints of (6-9c) and (6-9d), respectively. The membership function of the fuzzy goal is equal to the membership function of the relative fuzzy constraint.

$$\mu_G(C) = \mu_C(C) = \mu(C) \tag{6-10}$$

$$\mu_G(C_r) = \mu_C(C_r) = \mu(C_r) \tag{6-11}$$

Thus, a general FMRSM programming can be generated as:

$$Max\ \lambda \tag{6-12a}$$

subject to:

$$\mu(C)_n \geq \lambda \qquad n \in N \tag{6-12b}$$

$$\mu(C_r)_n \geq \lambda \qquad n \in N \tag{6-12c}$$

$$(C)_n = \left(h_o + S^{'}h + S^{'}HS\right)_n \tag{6-12d}$$

$$(C_r)_n = \left(g_o + S^{'}g + S^{'}GS\right)_n \tag{6-12e}$$

$$0 \leq \lambda \leq 1 \tag{6-12f}$$

(6-9e), (6-9f), and (6-9g) (6-12g)

6.3. Modeling

Water quality is reflected by various parameters. The water parameters include alkalinity, calcium, silica, sodium, pH, and conductivity. A fixed source has a stable water quality that balances the distribution system. Any change to a fixed historical source will break this balance and cause deterioration of water quality through corrosion, loss of the disinfectant residual and microbiological growth in a distribution system. According to the previous study, the biomass accumulation was further influenced by the nature of the supporting material (such as unlined ductile iron) rather than a change in water quality

(Chang and Jung, 2004). Meanwhile, Imran et al. (2006) confirmed a loss of disinfectant residual is further impacted by the delivery distance and retention time rather than by a change in water quality. Therefore, a change in water quality will directly result in metal corrosion in a distribution system.

Imran et al. (2006) also indicated that various pipe materials often have conflicting water quality requirements for corrosion abatement. For example, increasing alkalinity will increase the corrosion of copper and lead but reduce the release of iron. Increasing sulfates will reduce lead release but increase iron corrosion. The conflicts herein mean utility managers must evaluate tradeoffs between water quality and corrosion response. Therefore, this study will focus on heavy metal corrosion models in water distribution systems.

6.3.1. Quadratic polynomial models

The statistical nonlinear corrosion models for copper, lead and color (iron) have been developed by Imran et al. (2006), Imran et al. (2005b), Taylor et al. (2005) and Xiao (2004). The nonlinear models can be converted into quadratic polynomial models in which the water quality parameters are designed as input variables and the consequences for metal corrosion are designed as responses. Notably, the pH in the nonlinear equations is non-conservative, which is defined as the measure of acidity or alkalinity of a solution. The non-conservative pH must be converted into a conservative alternative in new quadratic equations. The molar concentration of H^+ as substitution for the pH must be chosen so as to retain accuracy to the greatest extent possible. The quadratic corrosion

and quadratic residual models are generated as follows:

Iron-release model

$$(C)_{Fe} = 1.6426$$

$$+(-0.148 \quad -0.0032 \quad 0.0093 \quad 0.009 \quad 0.0014)\begin{pmatrix} T \\ Alk \\ H^+ \\ Cl \\ SO_4^{2-} \end{pmatrix}$$

$$+\begin{pmatrix} T \\ Alk \\ H^+ \\ Cl \\ SO_4^{2-} \end{pmatrix}'\begin{pmatrix} 0.0038 & 0 & -0.0014 & -0.0001 & 0.0001 \\ 0 & 0 & 0.0001 & 0 & 0 \\ -0.0014 & 0.0001 & 0 & 0.0005 & -0.0001 \\ -0.0001 & 0 & 0.0005 & -0.0001 & 0 \\ 0.0001 & 0 & -0.0001 & 0 & 0 \end{pmatrix}\begin{pmatrix} T \\ Alk \\ H^+ \\ Cl \\ SO_4^{2-} \end{pmatrix} \qquad \text{(6-13a)}$$

$R^2 = 0.802$

$$10^8 (C_r)_{Fe} = -17595$$

$$+(2464 \quad 85.8 \quad -2847 \quad -38.1 \quad 9.8)\begin{pmatrix} T \\ Alk \\ H^+ \\ Cl \\ SO_4^{2-} \end{pmatrix}$$

$$+\begin{pmatrix} T \\ Alk \\ H^+ \\ Cl \\ SO_4^{2-} \end{pmatrix}'\begin{pmatrix} -35.2 & -3.4 & 20.7 & -4.6 & -1.6 \\ -3.4 & -0.1 & 7.0 & -0.4 & -0.2 \\ 20.7 & 7.0 & -34.1 & 9.9 & 1.7 \\ -4.6 & -0.4 & 9.9 & 1.1 & 0.5 \\ -1.6 & -0.2 & 1.7 & 0.5 & 0.1 \end{pmatrix}\begin{pmatrix} T \\ Alk \\ H^+ \\ Cl \\ SO_4^{2-} \end{pmatrix} \qquad \text{(6-13b)}$$

$R^2 = 0.99$

where $(C)_{Fe}$ is the iron concentration in *mg/L*, $(C_r)_{Fe}$ is the residual of Model 6-13a,

SO_4^{2-} and *Cl* are the concentrations of sulfate and chloride in *mg/L*, respectively, *Alk* is the concentration of alkalinity in *mg/L* as calcium carbonate ($CaCO_3$), *T* is the temperature in ^oC, R^2 is the correlation coefficient, and H^+ is the activated hydrogen ions equal to (10^{-pH}), the unit of which is in 10^{-9} *mol/L* in order to keep the same order of magnitude as the pH value.

Copper-release model

$$(C)_{Cu} = -0.2523$$
$$+ (0.035 \quad 0.0024 \quad -0.0123 \quad 0.0014 \quad -0.0151) \begin{pmatrix} T \\ Alk \\ H^+ \\ SO_4^{2-} \\ SiO_2 \end{pmatrix}$$
$$+ \begin{pmatrix} T \\ Alk \\ H^+ \\ SO_4^{2-} \\ SiO_2 \end{pmatrix}' \begin{pmatrix} -0.0008 & 0.0001 & 0.0006 & 0 & -0.0003 \\ 0.0001 & 0 & 0 & 0 & -0.0001 \\ 0.0006 & 0 & -0.0007 & 0 & 0.0002 \\ 0 & 0 & 0 & 0 & -0.0001 \\ -0.0003 & -0.0001 & 0.0002 & -0.0001 & 0.0013 \end{pmatrix} \begin{pmatrix} T \\ Alk \\ H^+ \\ SO_4^{2-} \\ SiO_2 \end{pmatrix} \quad \text{(6-14a)}$$

$R^2 = 0.997$

$$10^8 (C_r)_{Cu} = 11159$$

$$+ (-389.1 \quad -156.5 \quad 572.4 \quad 43.3 \quad 494.4) \begin{pmatrix} T \\ Alk \\ H^+ \\ SO_4^{2-} \\ SiO_2 \end{pmatrix}$$

$$+ \begin{pmatrix} T \\ Alk \\ H^+ \\ SO_4^{2-} \\ SiO_2 \end{pmatrix}' \begin{pmatrix} 1.8 & 1.1 & 5.5 & -0.6 & -7.8 \\ 1.1 & 0.5 & -1.9 & 0.2 & -1.3 \\ 5.5 & -1.9 & -51.7 & 0.6 & 37.5 \\ -0.6 & 0.2 & 0.6 & 0.1 & -4.9 \\ -7.8 & -1.3 & 37.5 & -4.9 & -9.7 \end{pmatrix} \begin{pmatrix} T \\ Alk \\ H^+ \\ SO_4^{2-} \\ SiO_2 \end{pmatrix} \qquad \text{(6-14b)}$$

$R^2 = 1$

where $(C)_{Cu}$ is the iron concentration in *mg/L*, $(C_r)_{Cu}$ is the residual of Model 6-14a, T is the temperature in ^oC, Alk is the concentration of alkalinity in *mg/L* as calcium carbonate ($CaCO_3$), SO_4^{2-} and SiO_2 are the concentrations of sulfate and silica in *mg/L*, respectively, R^2 is the correlation coefficient, and H^+ is the activated hydrogen ions equal to (10^{-pH}), the unit of which is in 10^{-9} *mol/L* in order to keep the same order of magnitude as the pH value.

Lead-release model

$$(C)_{Pb} = 6.2387$$

$$+(-0.1587 \quad 0.0486 \quad -1.527 \quad -0.2567 \quad 0.0663)\begin{pmatrix} T \\ Alk \\ H^+ \\ Cl \\ SO_4^{2-} \end{pmatrix}$$

$$+\begin{pmatrix} T \\ Alk \\ H^+ \\ Cl \\ SO_4^{2-} \end{pmatrix}'\begin{pmatrix} -0.0012 & -0.0001 & 0.0177 & 0.0042 & -0.001 \\ -0.0001 & -0.0003 & 0.0019 & 0.0006 & -0.0002 \\ 0.0177 & 0.0019 & -0.0186 & 0.0058 & 0.0009 \\ 0.0042 & 0.0006 & 0.0058 & 0.0022 & -0.0007 \\ -0.001 & -0.0002 & 0.0009 & -0.0007 & 0.0001 \end{pmatrix}\begin{pmatrix} T \\ Alk \\ H^+ \\ Cl \\ SO_4^{2-} \end{pmatrix} \quad \text{(6-15a)}$$

$R^2 = 0.993$

$$10^8 (C_r)_{Pb} = -19375$$

$$+(-1329 \quad 42.1 \quad 5178 \quad 592 \quad -69.3)\begin{pmatrix} T \\ Alk \\ H^+ \\ Cl \\ SO_4^{2-} \end{pmatrix}$$

$$+\begin{pmatrix} T \\ Alk \\ H^+ \\ Cl \\ SO_4^{2-} \end{pmatrix}'\begin{pmatrix} 52.8 & 2.8 & -107 & -1.6 & 2.2 \\ 2.8 & -0.4 & 0.7 & -0.9 & -0.1 \\ -107 & 0.7 & 19.4 & -4.5 & 0.3 \\ -1.6 & -0.9 & -4.5 & -2.7 & -0.4 \\ 2.2 & -0.1 & 0.3 & -0.4 & 0.1 \end{pmatrix}\begin{pmatrix} T \\ Alk \\ H^+ \\ Cl \\ SO_4^{2-} \end{pmatrix} \quad \text{(6-15b)}$$

$R^2 = 1$

where $(C)_{Fe}$ is the iron concentration in *mg/L*, $(C_r)_{Fe}$ is the residual of Model 6-15a, SO_4^{2-} and *Cl* are the concentrations of sulfate and chloride in *mg/L*, respectively, *Alk* is

the concentration of alkalinity in *mg/L* as calcium carbonate ($CaCO_3$), T is the temperature in ^oC, R^2 is the correlation coefficient, and H^+ is the activated hydrogen ions equal to (10^{-pH}), the unit of which is in 10^{-9} *mol/L* in order to keep the same order of magnitude as the pH value.

6.3.2. Membership function design

6.3.2.1. Corrosion models

Assuming the tolerance of the right-hand side in a corrosion model is ΔL, the membership function of the goal and constraints can be defined as:

$$\mu(C) = \begin{cases} 1 & if\ C \le L, \\ \dfrac{L + \Delta L - C}{\Delta L} & if\ L \le C \le L + \Delta L, \\ 0 & if\ C \ge L + \Delta L. \end{cases} \tag{6-16}$$

Figure 6-1 shows the linear membership function of Equation 6-16. It demonstrates the fact that the decision maker does not accept a response over $L + \Delta L$. The degree of satisfaction is equal to 1 when a response is lower than *L*, and the membership function value would decrease monotonically from 1 at $C = L$ to 0 at $C = L + \Delta L$. Thus, the assumption of a linear membership function is sufficient for this study. Any nonlinear membership function assumption would make the computation more complicated.

The Lead and Copper Rule action level for copper stipulates 90% of samples have a copper concentration of less than 1.3 mg/L and a lead concentration of less than 15

μ g/L. The Drinking Water Rule suggests a maximum contaminant level for iron of 0.3 mg/L. These regulations can be used to determine either the limitation of L ($L_{Cu} = 1.3mg/L$; $L_{Pb} = 15\mu g/L$; $L_{Fe} = 0.3mg/L$) or the tolerance of ΔL ($\Delta L_{Cu} = 1.3mg/L$; $\Delta L_{Pb} = 15\mu g/L$; $\Delta L_{Fe} = 0.3mg/L$). If the former regulation is chosen, the values of ΔL still need be decided. However, no reference regarding the fuzzy regulation is found. If the latter is chosen, we then define $L = 0$, and the membership function value can be reasonable and is described as decreasing monotonically from 1 at $C = 0$ to 0 at $C = \Delta L$ (as shown in Figure 6-2). The three membership functions with corrosion levels less than the regulations can be expressed as:

$$\mu(C)_{Fe} = \frac{0.3 - C_{Fe}}{0.3} \tag{6-17}$$

$$\mu(C)_{Cu} = \frac{1.3 - C_{Cu}}{1.3} \tag{6-18}$$

$$\mu(C)_{Pb} = \frac{15 - C_{Pb}}{15} \tag{6-19}$$

6.3.2.2. Residual models

The fitting of the three corrosion models produced the residuals. The residuals follow the normal distributions, as shown in Figure 6-3. If the normal distribution is expressed as *f(x)*, a nonlinear membership function could be standardized as follows:

$$\mu(C_r) = \sqrt{2\pi\sigma^2}\, f(x) = e^{-\frac{(x-\mu)^2}{2\sigma^2}} \tag{6-20}$$

However, the nonlinear membership functions will make optimization a time consuming process. Thus, the nonlinear membership functions are linearized as follows:

$$\mu(C_r)=\begin{cases}\dfrac{L_r-|C_r|}{L_r} & if\ -L_r \le C_r \le L_r, \\ 0 & if\ C_r > L_r\ or\ C_r < -L_r.\end{cases} \tag{6-21}$$

To determine the value of L_r, the corrosion limitations should be taken into consideration ($L_{Cu}=1.3mg/L$; $L_{Pb}=15\mu g/L$; $L_{Fe}=0.3mg/L$). Assuming the predicted residuals do not exceed 20% of the corrosion regulations, the membership functions can be expressed as:

$$\mu(C_r)_{Fe}=\frac{0.06-|(C_r)_{Fe}|}{0.06} \tag{6-22}$$

$$\mu(C_r)_{Cu}=\frac{0.26-|(C_r)_{Cu}|}{0.26} \tag{6-23}$$

$$\mu_G(C_r)_{Pb}=\frac{3-|(C_r)_{Pb}|}{3} \tag{6-24}$$

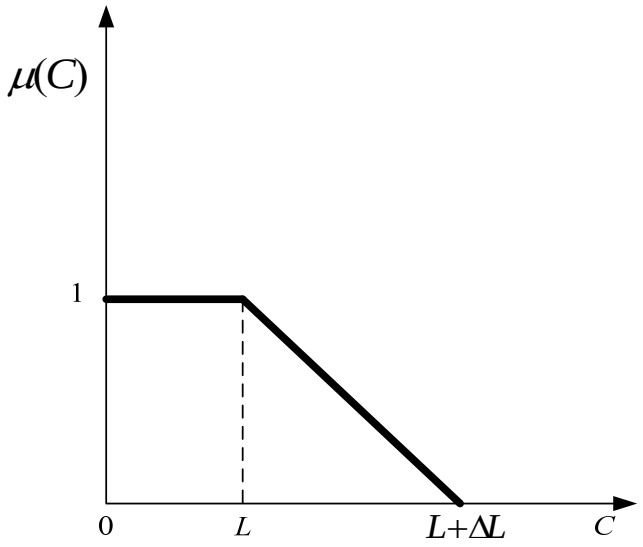

Figure 6-1 The membership function of corrosion model

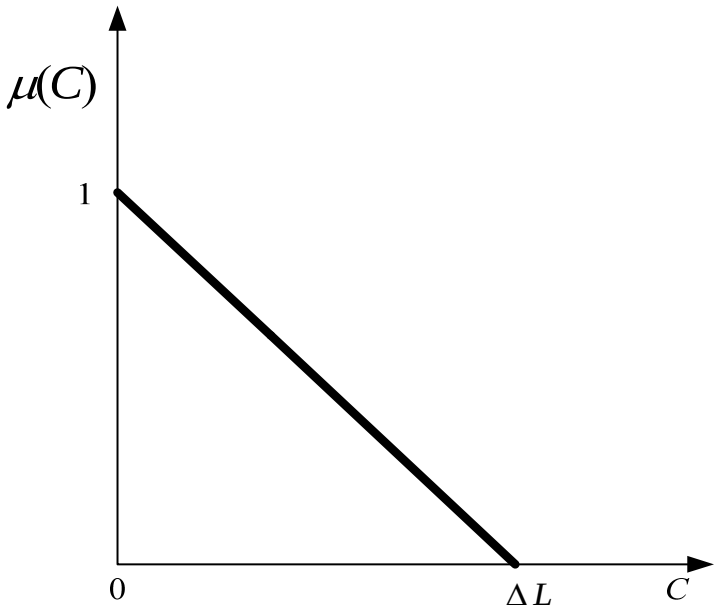

Figure 6-2 The membership function of the corrosion model with L = 0

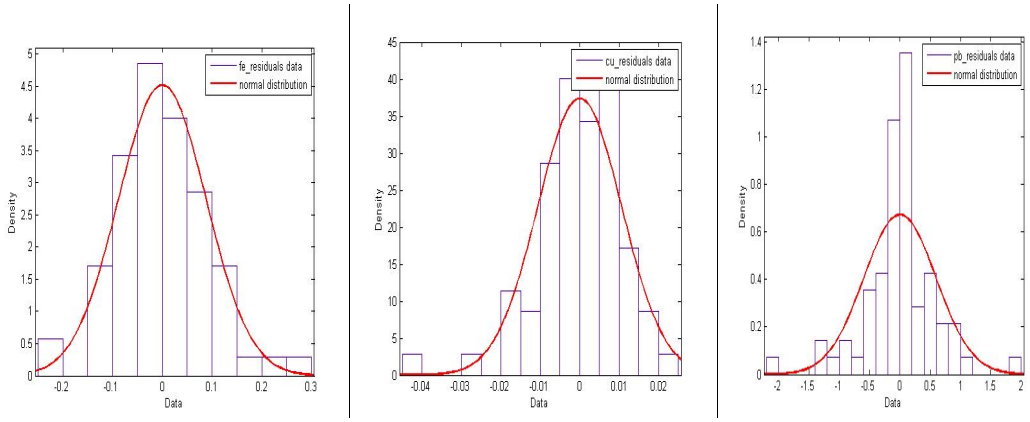

Figure 6-3 The normal distributions for the residuals of iron, copper and lead

where $\mu_{Fe} = 0$, $\sigma_{Fe} = 0.0883$; $\mu_{Cu} = 0$, $\sigma_{Fe} = 0.0107$; $\mu_{Pb} = 0$, $\sigma_{Pb} = 0.5961$

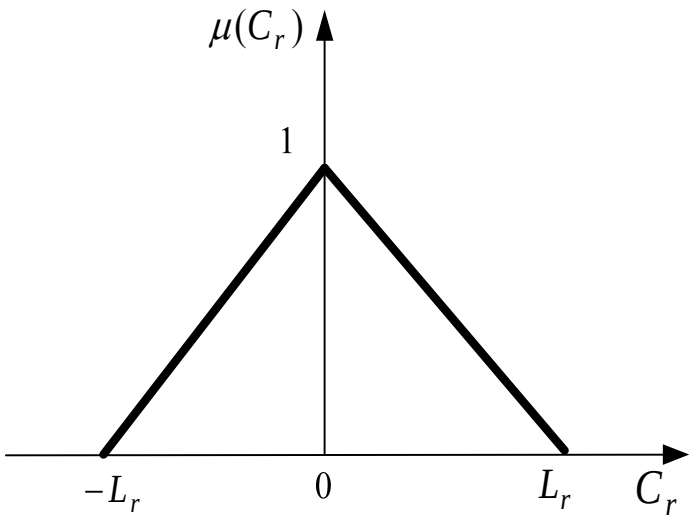

Figure 6-4 The membership function of residual model

Table 6-1 Water quality of the source waters

Parameter	**GW**	**SW**	**DW**
Alkalinity *(mg/L) as* $CaCO_3$	225	50	50
Calcium *(mg/L) as CaCO3*	200	50	50
Dissolved oxygen *(mg/L)*	8	8	8
pH	7.9	8.2	8.3
Silica *(mg/L)*	14	7	1
Sodium *(mg/L)*	10	15	30
Chloride *(mg/L)*	15	10	50
Sulfates *(mg/L)*	10	180	30
Temperature *(*^oC *)*	25	25	25

Notes: Sourced from Imran et al. (2006)
GW is groundwater, SW is surface water
DW is desalination water

Thus, a specific FMRSM programming can be generated for the multiple source water blending problems.

$$Max\ \lambda \tag{6-25a}$$

subject to:

$$\frac{0.3 - C_{Fe}}{0.3} \geq \lambda,\ \frac{1.3 - C_{Cu}}{1.3} \geq \lambda,\ \frac{15 - C_{Pb}}{15} \geq \lambda \tag{6-25b}$$

$$\frac{0.06 - \left|(C_r)_{Fe}\right|}{0.06} \geq \lambda,\ \frac{0.26 - \left|(C_r)_{Cu}\right|}{0.26} \geq \lambda,\ \frac{3 - \left|(C_r)_{Pb}\right|}{3} \geq \lambda \tag{6-25c}$$

(6-13a), (6-14a), (6-15a) (6-25d)

(6-13b), (6-14b), (6-15b) (6-25e)

$$0 \leq \lambda \leq 1 \tag{6-25f}$$

(6-9e), (6-9f), and (6-9g) (6-25g)

6.3.3. Scenario design

Assume three plants produce groundwater (GW), surface-water (SW), and desalinated water (DW) for a distribution system. The proportion of GW in the blend is x_1, the proportion of SW is x_2, and the proportion of DW is x_3. Their water quality information is described in Table 6-1. Several scenarios are defined as follows:

Scenario 1 Assume three plants are fully operational with the following three situations.

1). No limitation.

2). Previous studies showed the delivery capacity may limit water flow. For example, some connections may only receive DW in a range from 0 to 81% and SW in a range from 0 to 90% (Imran et al., 2006). The constraint is modified as:

$$0 \le x_1 \le 1,\ 0 \le x_2 \le 0.9,\ 0 \le x_3 \le 0.5\ . \tag{6-26}$$

3). In many cities, the production capacity of a water plant may not satisfy all water demands. Imran's paper (2006), for example, described how the production capacities of SW and DW plants could only satisfy about 41% and 16% of the total water demands. Moreover, the groundwater withdrawals were reduced to 76% of the original amount. It assumes the production capacity of SW is 30%, changing the constraint to:

$$0 \le x_1 \le 0.76,\ 0 \le x_2 \le 0.30,\ 0 \le x_3 \le 0.16\ . \tag{6-27}$$

Scenario 2: One source is off line.

1). GW is off line. The constraint is modified as

$$x_1 = 0,\quad 0 \le x_2 \le 1,\quad 0 \le x_3 \le 1,\quad x_2 + x_3 = 1\ . \tag{6-28}$$

2). SW is off line.

$$x_2 = 0, \quad 0 \le x_1 \le 1, \quad 0 \le x_3 \le 1, \quad x_1 + x_3 = 1 \ . \tag{6-29}$$

3). DW is off line.

$$x_3 = 0, \quad 0 \le x_2 \le 1, \quad 0 \le x_1 \le 1, \quad x_2 + x_1 = 1 \ . \tag{6-30}$$

Scenario 3: Varying chloride concentration.

Chloride has an important impact factor on the releases of lead and iron. To analyze this influence, two different chloride concentrations are designed for the DW: *100 mg/L* and *300 mg/L.* A large increase in the chloride concentration in the DW may result in the optimal proportion of DW dropping to a very low value (possibly 0) in the blend, this constrains x_3 to a value equal to or greater than 16%.

$$0.16 \le x_3 \le 1 \tag{6-31}$$

Scenario 4: Varying pH value.

The pH value is an important impact factor for the three metal corrosions. The following pH values are considered: *1) pH = 7.2 in DW; 2) pH = 8.5 in GW.*

Scenario 5: Varying alkalinity concentration.

The following alkalinity concentrations are modified as: *1)* C_{Alk} *= 50mg/L in GW; 2)* C_{Alk} *= 400mg/L in GW.*

Scenario 6: Varying sulfates concentration.

Two sulfates concentrations are considered: *1)* $C_{SO_4^{2-}}$ *= 30mg/L in SW; 2)* $C_{SO_4^{2-}}$ *= 360mg/L in SW.*

6.4. Results and Discussion

The water quality values from Table 6-1 are substituted into the specific FMRSM programming (6-25) problem and run through the **fmincon** slover in Matlab 7, based on the above scenarios, to generate the results (as shown in Table 6-2). The run time is several milliseconds, so *the FMRSM can be used for real-time water blending processes to rapidly identify the water quality changes for multiple water sources*.

6.4.1. FMRSM vs. Fuzzy RSOP

In order to describe the results, a fuzzy response surface optimization programming (RSOP) is generated for comparison. This programming has the same structure as the FMRSM with the exception of the residual equation. Based on the same water quality values and scenarios, the results are produced as shown in Table 6-3.

$$Max\ \lambda \tag{6-32a}$$

subject to:

$$\frac{0.3 - C_{Fe}}{0.3} \geq \lambda,\ \frac{1.3 - C_{Cu}}{1.3} \geq \lambda,\ \frac{15 - C_{Pb}}{15} \geq \lambda \tag{6-32b}$$

(6-13a), (6-14a), (6-15a) (6-32d)

$$0 \leq \lambda \leq 1 \tag{6-32f}$$

(6-9e), (6-9f), and (6-9g) (6-32g)

Table 6-2 shows the FMRSM is not feasible for scenarios *2-1, 2-3, 3-1, 3-2,* and *5-1*. On the other hand, the fuzzy RSOP is not feasible for scenarios *2-1* and *3-2* either (shown in Table 6-3). The FMRSM has some residual constraints restricting the feasible regions. Additionally, the scenarios are designed for extreme situations, except for scenario *1*, and the models may not find feasible solutions.

The results in scenarios 1-3 and 6-2 in the two models are different. The values of the satisfaction degree, λ, in Table 6-2 (the FMRSM) are smaller than those of Table 6-3 (the fuzzy RSOP). The locations of the optimum points of the two scenarios are close to the borders of the feasible regions in the fuzzy RSOP. Due to the restraint of the residual constraint in the FMRSM, the feasible region will shrink, and the objective value is reduced.

The Implementation of the min-operator ensures simultaneous optimization of this multi-objective programming (Zimmerman 1978). The global optimum for the given multiple water sources is given by the solution for scenario 1-1. In this situation, the satisfaction degree λ reaches its highest value of 0.54. The optimal blending ratio is 0.33:

0.07: 0.6 (GW: SW: DW). It is worth noting that the λ value is only valid for scenarios 1 and 2, because the water quality parameter values for the three water sources vary with the remaining scenarios. Table 6-2 also lists the finished water quality information for the optimal blending waters.

Therefore, the error between the predicted output of the fitted model and the measured data of the experimental data can be estimated using the residual response surface model in the FMRSM and, hence, *a robust result is generated for the real-time water blending operation in the water distribution system.*

6.4.2. Nonlinear model based optimization

Imran et al. (2006) estimated the metal corrosions for a particular water quality using the following nonlinear models (Imran et al., 2006; Imran et al., 2005b; Taylor et al., 2005; Xiao, 2004).

$$Cu = (T)^{0.72}(Alk)^{0.73}(pH)^{-2.86}(SO_4)^{0.1}(SiO_2)^{-0.22} \quad (6\text{-}32)$$

$$Pb = 1.027^{(T-25)}(Alk)^{0.677}(pH)^{-2.726}(Cl)^{1.462}(SO_4)^{-0.228} \quad (6\text{-}33)$$

$$\Delta C = 10^{-1.321}(T)^{0.813}(Alk)^{-0.912}(Cl)^{0.485}(Na)^{0.561}(SO_4)^{0.118}(DO)^{0.967}(HRT)^{0.836} \quad (6\text{-}34)$$

where *Cu* and *Pb* are the copper and lead concentrations in *mg/L*, ΔC is the increase in apparent color (measured in *cpu*: Co-Pt units), T is the temperature in ^oC, *Alk* is the concentration of alkalinity in *mg/L* as calcium carbonate ($CaCO_3$), SO_4^{2-} and SiO_2 are the

concentrations of sulfate and silica in *mg/L*, respectively, *Cl* is the concentrations of chloride in *mg/L*, *pH* is the dimensionless measure of the acidity or alkalinity of a solution, and (*HRT*) is the hydraulic retention time in days.

The relationship between total iron (*Fe*) concentration (*mg/L*) and apparent color (*cpu*) can be used to calculate the value of ΔC (Imran et al., 2006).

$$Fe = 0.0132 \times Apparent\ Color \tag{6-35}$$

$$R^2 = 0.82$$

Based on the Lead and Copper Rule action level for copper and lead (1.3 mg/L for copper and 15 μg/L for lead), they declaimed the maximum releases of copper and lead were set at 1.0 mg/L and 10 μg/L, respectively. Due to the use of 0.2 mg/L as the Action Level for iron, they set the maximum iron release at 0.15mg/L. They used those maximum metal release settings to optimize the multiple source water blends based on the designed scenarios.

Imran's optimization method generated an approximately maximum metal release setting rather than a global optimal blending ratio. Moreover, the nonlinear model based optimization is a time consuming process that could not rapidly respond to variations in water quality in a real time operation.

6.4.3. Fuzzy RSOP vs. weighted-objective RSOP

A weighted-objective RSOP model was designed as follows:

$$Min\ (50C_{Fe}+11.54C_{Cu}+C_{Pb}) \quad \text{(6-36a)}$$

s.t.

$$C_{cu} \le 1.3,\ C_{pb} \le 15\ ,\ and\ C_{Fe} \le 0.3 \quad \text{(6-36b)}$$

(6-13a), (6-14a), and (6-15a) (6-36c)

(6-9e), (6-9f), and (6-9g) (6-36d)

The result was generated based on six scenarios in Table 6-4. Figure 6-5 illustrates a column chart of optimal ratios of metal corrosions for a weighted-objective RSOP. Obviously, the column heights of three optimal metal corrosions are quite different in each scenario. This entails that the three individual objectives could not be synchronously optimized in the weighted-objective RSOP. On the contrast, Figure 6-6 shows the column chart of the optimal ratios of metal corrosions for the fuzzy RSOP. The column heights of three optimal metal corrosions are quite similar in each scenario. This shows that a synchronous optimization was conducted on the three individual objectives in the fuzzy RSOP.

6.5. Summary

This chapter describes a FMRSM for a real-time multi-source water blending problem in a water distribution system. In the FMRSM, the first quadratic models were fitted by experimental data sets and the second quadratic models were fitted by the residuals. Meanwhile, the multiple objectives were optimized by the fuzzy optimization method (using the min-optimizer). The proposed FMRSM is applied to a real case, based on 6 designed scenarios. The results show that: 1) the quadratic models would reduce the computational time of a FMRSM so it could rapidly respond to changes in water quality, 2) the error between the predicted output and measured data could be automatically evaluated and compensated in the optimization process via the second residual models, so the FMRSM can generate a robust result in each time interval, and 3) the fuzzy optimization method could simultaneously optimize multiple objectives.

In Chapter 7, a Dual-Response-Surface-Based process control is preformed to the operation of an industrial rotary kiln under high uncertainty and complex dynamic.

Table 6-2 Results of the FMRSP in various scenarios

	Scenario 1 *Capacity*			Scenario 2 *Operation*			Scenario 3 *Chloride*		Scenario 4 *pH*		Scenario 5 *Alkalinity*		Scenario 6 *Sulfates*	
	1	2	3	1	2	3	1	2	1	2	1	2	1	2
λ	0.54	0.52	0.41	-	0.46	-	-	-	-	0.54	0.76	0.45	0.74	0.49
x_1	0.33	0.36	0.65	-	0.43	-	-	-	-	0.4	0.71	0.21	0.02	0.31
x_2	0.07	0.14	0.19	-	0	-	-	-	-	0.06	0	0.09	0.98	0.03
x_3	0.60	0.5	0.16	-	0.57	-	-	-	-	0.54	0.29	0.71	0	0.66
C_{Pb}	6.99	5.73	2.85	-	8.03	-	-	-	-	6.96	0.72	8.21	0.52	7.66
C_{Cu}	0.61	0.62	0.76	-	0.66	-	-	-	-	0.6	0.32	0.71	0.33	0.6
C_{Fe}	0.14	0.14	0.15	-	0	-	-	-	-	0.14	0	0.16	0.08	0.15
C_{Alk}	107	113	165	-	126	-	-	-	-	120	50	123	53	114
$C_{SO_4^{2-}}$	34.3	43.9	44.7	-	21.3	-	-	-	-	30.3	15.8	39.5	29.7	32.2
C_{Cl}	35.8	31.8	19.7	-	34.8	-	-	-	-	33.7	25.2	39.1	10.1	38.2
pH	8.12	8.1	7.99	-	8.29	-	-	-	-	8.46	7.98	8.17	8.19	8.13
C_r^{Fe}	0	0.03	0	-	0.01	-	-	-	-	0.1	0	0.16	0.55	0
C_r^{Cu}	0.02	0.01	0.05	-	0.03	-	-	-	-	0.12	0.58	0.02	0.26	0.02
C_r^{Pb}	0.17	0.19	0.37	-	0.23	-	-	-	-	0.23	0.36	0.22	0.67	0.17

Note: 1. x_1 is the blending ratio of groundwater, x_2 is the blending ratio of surface water, and x_3 is the blending ratio of desalination water.

2. C_{Pb} is in $\mu g / L$, others are in *mg/L*.

3. The magnitudes of C_r^{Fe}, C_r^{Cu} and C_r^{Pb} in 10^{-4}.

Table 6-3 Results of the fuzzy RSOP in various scenarios

	Scenario 1 *Capacity*			Scenario 2 *Operation*			Scenario 3 *Chloride*		Scenario 4 *pH*		Scenario 5 *Alkalinity*		Scenario 6 *Sulfates*	
	1	2	3	1	2	3	1	2	1	2	1	2	1	2
x_1	0.33	0.36	0.54	-	0.43	0.48	0.5	-	0.3	0.4	0.71	0.21	0.02	0.34
x_2	0.07	0.14	0.30	-	0	0.52	0.22	-	0.6	0.06	0	0.09	0.98	0.04
x_3	0.60	0.5	0.16	-	0.57	0	0.29	-	0.1	0.54	0.29	0.71	0	0.62
C_{Pb}	6.99	5.73	2.31	-	8.38	0.72	7.91	-	0	6.96	0.72	8.21	0.52	7.18
C_{Cu}	0.61	0.62	0.7	-	0.57	0.66	0.69	-	0.61	0.6	0.32	0.71	0.33	0.62
C_{Fe}	0.14	0.14	0.02	-	0.17	0.15	0.16	-	0.14	0.14	0	0.16	0.08	0.14
C_{Alk}	107	113	145	-	92.2	134	136	-	103	120	*50*	*123*	53	110
$C_{SO_4^{2-}}$	34.3	43.9	64.2	-	25.2	98.2	52.6	-	114	30.3	15.8	39.5	*29.7*	*36.4*
C_{Cl}	35.8	31.8	19.1	-	41.6	12.4	*38.4*	-	15.3	33.7	25.2	39.1	10.1	36.3
pH	8.12	8.1	8.02	-	8.17	8.03	8.04	-	*7.87*	*8.46*	7.98	8.17	8.19	8.11
λ	0.54	0.52	0.46	-	0.46	0.49	0.47	-	0.53	0.54	0.76	0.45	0.74	0.52

Note: 1. x_1 is the blending ratio of groundwater, x_2 is the blending ratio of surface water, and x_3 is the blending ratio of desalination water.

2. C_{Pb} is in $\mu g / L$, others are in *mg/L*.

3. The magnitudes of C_r^{Fe}, C_r^{Cu} and C_r^{Pb} in 10^{-4}.

Table 6-4 Results of the weighted-objective RSOP

	Scenario 1 *Capacity*			Scenario 2 *Operation*			Scenario 3 *Chloride*		Scenario 4 *pH*		Scenario 5 *Alkalinity*		Scenario 6 *Sulfates*	
	1	2	3	1	2	3	1	2	1	2	1	2	1	2
x_1	0.58	0.58	0.55	-	0.43	0.58	0.41	-	0.58	0.75	0.73	0.44	0	0.73
x_2	0.42	0.42	0.30	-	0	0.42	0.43	-	0.42	0.25	0.05	0.41	1	0.24
x_3	0	0	0.15	-	0.57	0	0.16	-	0	0	0.22	0.15	0	0.03
C_{Pb}	0.56	0.56	2.18	-	8.03	0.56	3.29	-	0.56	0.45	0	0	0.45	0
C_{Cu}	0.71	0.71	0.71	-	0.66	0.71	0.63	-	0.71	0.73	0.32	0.95	0.32	0.81
C_{Fe}	0	0	0	-	0	0	0.30	-	0	0	0	0	0.09	0
C_{Alk}	151	151	147	-	126	151	121	-	151	182	50	205	50	178
$C_{SO_4^{2-}}$	81.2	81.2	63.9	-	21.3	81.2	87.1	-	81.2	52	22.6	83.3	30	93.9
C_{Cl}	12.9	12.9	18.6	-	34.8	12.9	26.4	-	12.9	13.8	22.6	18.2	10	14.9
pH	8.0	8.0	8.02	-	8.08	8.0	8.06	-	8.0	8.4	7.98	8.05	8.2	7.96

Note: 1. x_1 is the blending ratio of groundwater, x_2 is the blending ratio of surface water, and x_3 is the blending ratio of desalination water.

2. C_{Pb} is in $\mu g / L$, others are in *mg/L*.

3. The magnitudes of C_r^{Fe} , C_r^{Cu} and C_r^{Pb} in 10^{-4} .

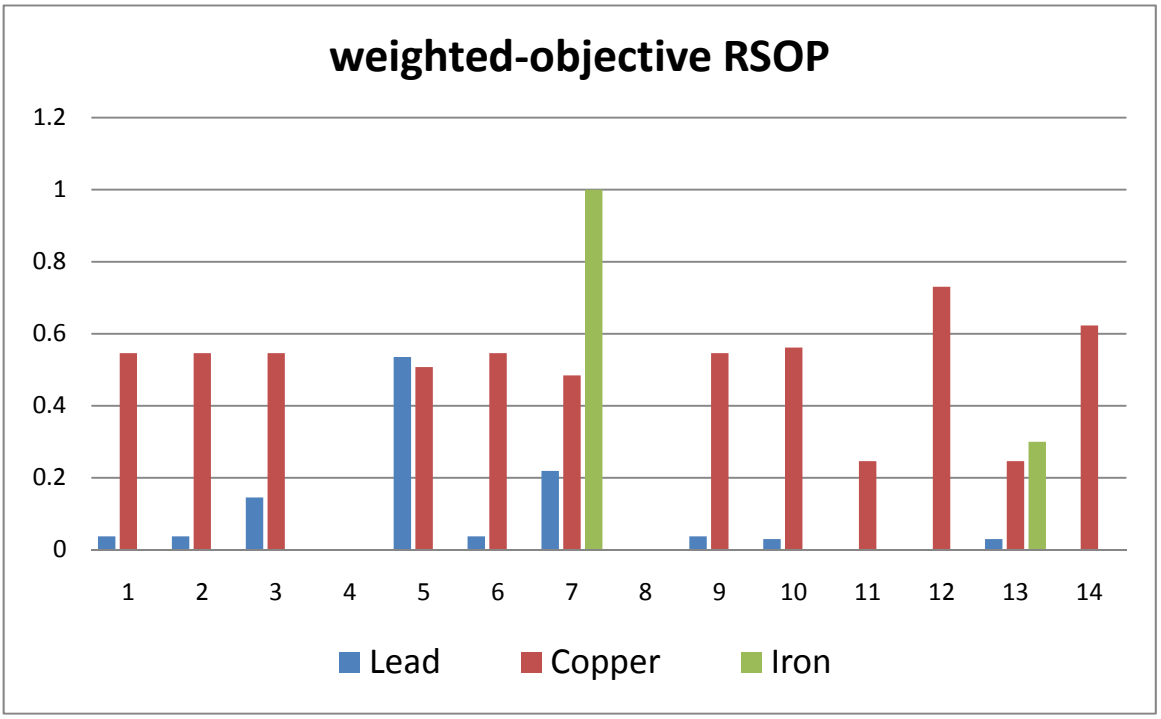

Figure 6-5 The column chart of the ratio of optimal metal corrosion and permitted level--the weighted-objective RSOP

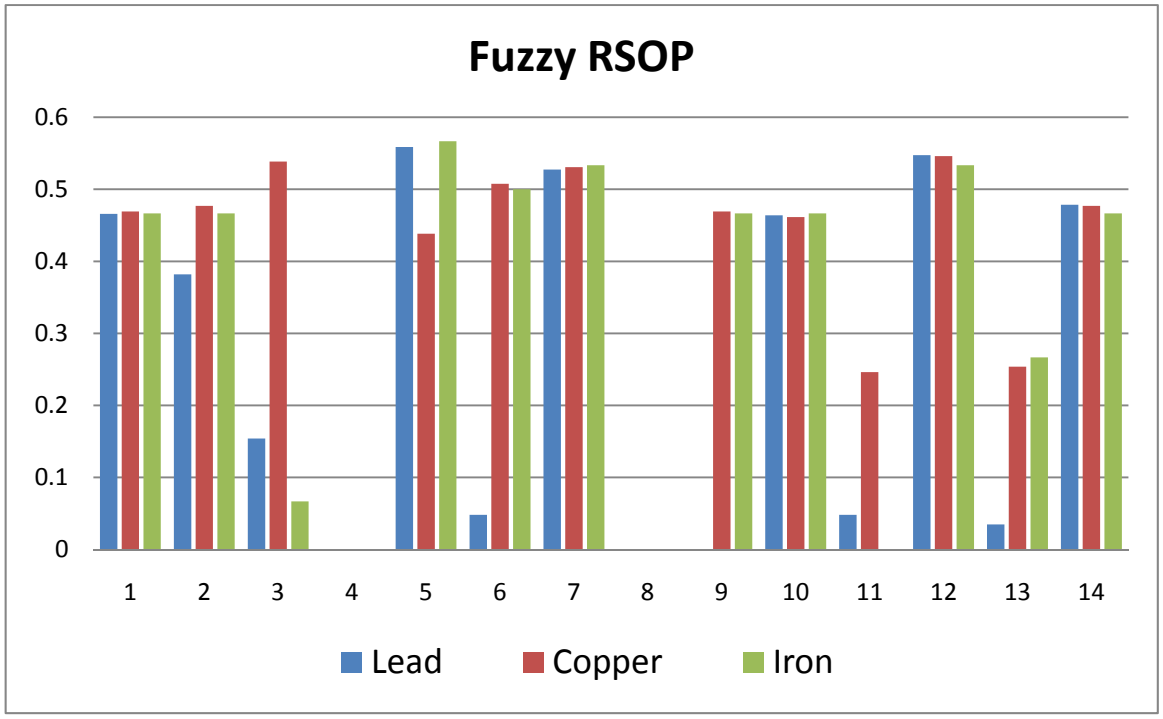

Figure 6-6 The column chart of the ratio of optimal metal corrosion and permitted level--the fuzzy RSOP

CHAPTER 7

Dual-Response-Surface-Based Process Control to an Industrial Rotary Kiln under Uncertainty

7.1. Statement of problems

An industrial rotary kiln is a large scale piece of sintering equipment widely used in chemical, metallurgical, cement and environmental protection industries (Peng et al., 2010f). The high uncertainty and complex dynamics natures of the calcination process, with its nonlinear reaction kinetics, long time delays and variable raw material feed characteristics, make the rotary kiln process inherently difficult to control (Jarvensivu et al., 2001). Moreover, due to the high combustion temperature environment and the uncertainty of operational conditions, it is very hard to measure some key quality parameters in rotary kilns, such as the flame temperature and composition of raw material.

The existing control techniques in this field include proportional integral-derivative (PID), intelligent, model predictive controls, as well as their hybrid approaches, which contribute to improving product quality, maintaining stable operations, reducing production costs and minimizing exhaust pollution (McIlwain, 1992; Wang, 1996; Valiquette and Savoie, 1999; Zanovello and Budman, 1999; Jarvensivu et al., 2001; Chen, 2002; Li and Zhu, 2004). However, in PID control, decoupling is a steady-state process and the constraints are not handled explicitly, leading to a suboptimal result. Intelligent controls have a high demand for prior operational knowledge that depends on expert experience, which may not be available (Huang et al., 2008). Model predictive control is

capable of dealing with simple nonlinear systems or it may be used in applications with slow dynamics (Wang and Boyd, 2010). Therefore, research needs on the process control of rotary kiln are still substantial.

The process control design of a rotary kiln often meets some conflicting requirements. For example, the combustion process is highly nonlinear and complex, and it is better to use a high-order nonlinear model to describe it but the solution process of this high-order nonlinear model is time consuming. During real process control, the two conflicting targets, a high-order nonlinear model for better descriptions and computational efficiency for fast solutions, are required to meet the system's dynamic and complex need. Unfortunately, the current process control techniques are inadequate for satisfying the two conflicting requirements. Hence, a Dual-Response-Surface-Based optimizing control (DRSPC) is considered for the process control of a rotary kiln.

The DRSPC is based on Response Surface Methodology (RSM). RSM is a statistical technique used in empirical study. It approximates the true response surface, estimates the parameters and works well for solving real response surface problems (Anderson-Cook et al., 2009; Myers et al., 2004). As consequence, it searches for an optimal set of input variables to optimize the response by using a set of designed experiments. A RSM programming can be quickly solved by any commercial solver because it contains quadratic models rather than high-order nonlinear models. A dual RSM programming builds two quadratic empirical models, one for the mean and another for the standard deviation, and optimizes one of the responses subjected to an appropriate constraint given by the other (Lin and Tu, 1995). Since the second empirical model considers the standard deviation, a dual RSM programming can produce robust and

optimal outputs for the system.

In this study, the operational data recorded from an industrial rotary kiln are appropriately fitted into the response surface models, which can provide an insight into the uncertainty and dynamics of the kiln system under study. A Dual-Response-Surface-Based process control (DRSPC) programming is used following the implementation of an optimization technique, which can rapidly facilitate robust forecasting under dynamic process conditions to consequently realize the desired real-time process control for the industrial rotary kiln. Finally, the proposed DRSPC is practically implemented during the process control of an industrial aluminum rotary kiln to demonstrate the capability of dealing with uncertainty and dynamic conditions.

In summary, the properties of the proposed approach include:

(1) The ability to rapidly provide optimal outputs to serve the process control of a rotary kiln.

(2) Optimal robust outputs.

(3) A solution for the time delay problem.

(4) A statistical elimination of measurement errors.

(5) A tradeoff between system cost and operational efficiency.

This chapter is structured as follows. Section 7.2 presents the development of the DRSPC programming, and describes how the time delay problem can be solved and how the measurement errors are statistically eliminated by the proposed approach. Section 7.3 demonstrates an application of the DRSPC on an industrial aluminum rotary kiln and performs an analysis of the tradeoff between system cost and operational efficiency. Section 7.4 presents the conclusion.

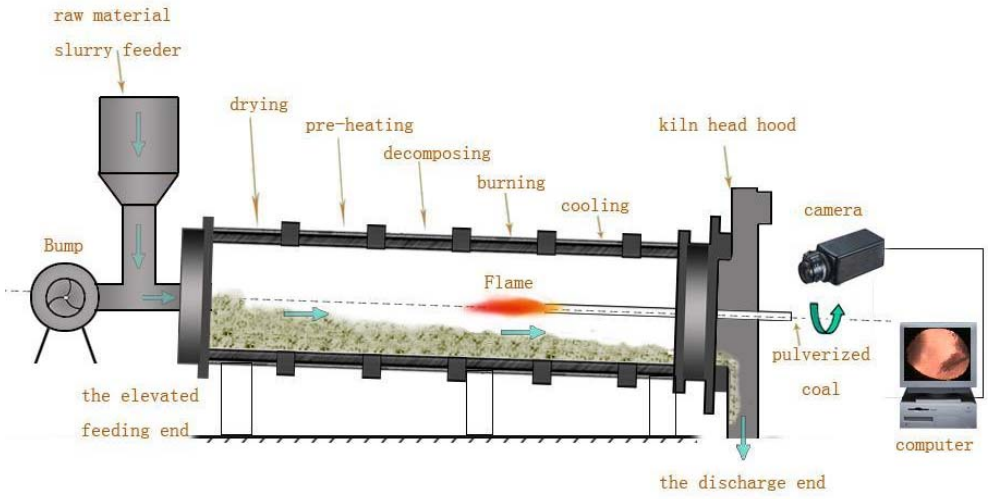

Figure 7-1. Sketch of an industrial rotary kiln.

7.2. Methodology

The development of the proposed DRSPC programming consists of three major steps:

1. Data acquisition, this includes data classification, data range determination, experimental design and a record of operational conditions.
2. Fitting, fits two response surface models based on the prior recorded data.
3. Optimization control, builds a dual response surface optimization model to determine control outputs under dynamic operational conditions.

7.2.1. Data acquisition

Industrial rotary kiln

During data acquisition, the dynamic operational conditions in an industrial rotary kiln are recorded. An industrial rotary kiln is a direct-contract heat exchanger. It is a long refractory cylindrical vessel with a slight incline from horizontal which slowly rotates around its own axis (as shown in Figure 7-1). The process inside a rotary kiln includes drying, preheating, decomposing, burning and cooling. During the process, raw material slurry is fed at the elevated feeding end of the kiln and it flows down to the discharge end of the rotary kiln due to the kiln's inclination and rotation. Meanwhile, pulverized coal is sprayed from a burner-pipe with the primary air in the burning zone. Thus, heat energy supplied by the combustion of pulverized coal is countercurrent transferred to the raw material slurry in the kiln. Finally, the processed material called clinker is cooled and discharged. The clinker quality is customarily classified into three categories: over-

sintered, under-sintered and normal-sintered.

The kiln process involves high uncertainty, complex dynamics, non-linear reaction kinetics, long time delays, variable raw material feed characteristics and is multi-variable in nature. For example, the calcination process is accomplished through heat exchange between the material and hot freeboard gas, flame and rotating kiln wall. If we need useful insights into the kiln process, the sub-models of fluid dynamics, reaction processes, pollutant formation and heat transfer have to be developed. However, the existing phenomenological models are still not accurate enough to describe the rotary kiln process (Tscheng and Watkinson, 1979; Barr et al., 1989; Boateng and Barr, 1996; Mastorakos et al., 1999). Furthermore, due to the high temperature combustion environment and the variability of the operational conditions, it is very difficult to measure key quality parameters in the kiln process, such as the flame temperature and composition of raw material. In practice, the existing control techniques in this field, such as PID, intelligent control, or model prediction control may not work efficiently in the rotary kiln process.

Data classification and data range determination

Major factors affecting clinker quality include the kiln operational temperatures and material retention time. The kiln operational temperatures can be roughly represented by the flame temperature in the burning zone, the gas temperatures on the feed end and air temperature on discharge end. Sufficient operation of the kiln process requires tight control of its temperature profiles. However, the kiln temperatures are complicatedly influenced by all operational factors/parameters, such as the raw material feed rate, kiln rotational speed, fuel flow rate, draft fan speed, air pressure drop at the head hood and even the kiln temperatures. For example, the current flame temperature in the burning

zone will impact its future flame temperature. Conversely, the material retention time can be directly and precisely controlled by the raw material feed rate, although the composition and density of the raw material are difficult to measure.

In fact, the variations in the composition and density of the raw material eventually affect the kiln temperatures. For example, drying high water content material consumes more energy, which leads to a deeper temperature decline in the drying zone. So, we can control the kiln temperatures by responding to variations in the composition and density of the raw material.

In this study, a dual Response Surface Method (dual RSM) is used in the process control of a rotary kiln. The RSM examines the relationships between the response (y) and a number of input variables (x_i), so the optimal setting for the input variables which maximize (or minimize) the response can be identified (Vining and Myers, 1990; Del Castillo and Montgomery, 1993; Lin and Tu, 1995; Vining and Bohn, 1998). A dual RSM programming builds two quadratic empirical models, one for the mean and the other for the standard deviation, and optimizes one of the responses subjected to an appropriate constraint given by the other (Lin and Tu, 1995).

In the kiln process, we design three responses. The first response ($\bar{y}$) is the responding temperature of the flame. The second response ($\sigma_{\bar{y}}$) is the variance of ($\bar{y}$) that is defined as the difference between the predicted flame temperature and measured flame temperature. The above two response surface models form a dual response surface model. The third response ($\sigma_{\Delta y}$) is the standard deviation among the three standardized temperature differences (Δy) of the flame, feed end and discharge end. The standardized temperature difference (Δy) is defined as:

$$\Delta y = \frac{T_D - T_R}{T_D} \times T_S \qquad (7\text{-}1)$$

where T_D is the desired operational temperature, T_R is the responding temperature at the next time interval, (Δt), and T_S is the standard temperature. The time interval is defined as the time difference between two adjacent data samples. The standard temperature is used to standardize the temperature differences and it usually equals to the desired operational temperature of the first response.

The inputs of the dual RSM are designed as important operational factors/parameters in the kiln process. These include the kiln temperatures, raw material feed rate, kiln rotational speed, fuel flow rate, main engine load, draft fan speed, and air pressure drop at the kiln head hood. The outputs are major control factors such as the raw material feed rate, kiln rotational speed, fuel flow rate, and main engine load. It is worth noting the inputs refer to the current time and the outputs and responses refer to the future time.

Determination of the ranges of the responses, inputs and outputs are determined according to the real operational conditions.

Experimental design

Two assumptions are involved in this rotary kiln process control study: (1) the kiln process is continuous, and (2) correlations exist among the input variables.

In order to let the recorded data effectively represent the real kiln process, an experiment is designed as follows: (1) record the operation conditions from a continuous kiln process, (2) the recorded data includes not only the aforementioned control factors

and state parameters but also the clinker quality, (3) the time interval (Δt) between two adjacent date samples is the average time delay of the calcination process, and (4) select a portion of the record that accompanying the stable quality product (normal-sintered clinker).

Two important points need to be mentioned: (1) the time delay problem can be solved using the time interval (Δt), because the proposed DRSPC can predict the responses and outputs of the next time interval (Δt) based on the current inputs; and (2) the purpose of selecting a portion of the record, accompanying the stable quality product, is to find desired operational temperatures in the kiln process. In the proposed DRSPC, these desired operational temperatures are equal to the arithmetic means of their recorded data, so the precise measurement of their actual temperatures is not necessary. Thus, the measurement errors can be statistically eliminated.

Based on the above experiment, data sampling can be conducted on a continuous kiln process, and then a period of adequate samples can be selected. The next step is to use the selected data to fit three response surface models.

7.2.2. Fitting response surface models

Using least squares fitting, three quadratic responses are obtained as follows:

$$\bar{y} = h_o + S^{'}h + S^{'}HS \tag{7-2}$$

$$\sigma_{\bar{y}} = r_o + S^{'}r + S^{'}RS \tag{7-3}$$

$$\sigma_{\Delta y} = g_o + S^{'}g + S^{'}GS \tag{7-4}$$

where $g_0 = \alpha_0$, $r_0 = \gamma_0$, $h_0 = \beta_0$, $g = (\alpha_1, \alpha_2, ...\alpha_k)'$, $r = (\gamma_1, \gamma_2, ...\gamma_k)'$, $h = (\beta_1, \beta_2, ...\beta_k)'$, and

$$H = \frac{1}{2}\begin{bmatrix} 2\beta_{11} & \beta_{12} & \cdots & \beta_{1k} \\ \beta_{12} & 2\beta_{22} & \cdots & \\ \vdots & \vdots & \ddots & \vdots \\ \beta_{1k} & \beta_{2k} & \cdots & \beta_{kk} \end{bmatrix} \tag{7-5}$$

$$R = \frac{1}{2}\begin{bmatrix} 2\gamma_{11} & \gamma_{12} & \cdots & \gamma_{1k} \\ \gamma_{12} & 2\gamma_{22} & \cdots & \\ \vdots & \vdots & \ddots & \vdots \\ \gamma_{1k} & \gamma_{2k} & \cdots & \gamma_{kk} \end{bmatrix} \tag{7-6}$$

$$G = \frac{1}{2}\begin{bmatrix} 2\alpha_{11} & \alpha_{12} & \cdots & \alpha_{1k} \\ \alpha_{12} & 2\alpha_{22} & \cdots & \\ \vdots & \vdots & \ddots & \vdots \\ \alpha_{1k} & \alpha_{2k} & \cdots & \alpha_{kk} \end{bmatrix} \tag{7-7}$$

where h_0, h, r_0, r, g_0 and g are the appropriate vectors for the estimated coefficients, H, R and G are the diagonal ($k \times k$) matrices of the estimated coefficients, $\bar{y}$, $\sigma_{\bar{y}}$ and $\sigma_{\Delta y}$ are the mean and two standard deviations, and S and S' are ($k \times 1$) vectors of the input variables and their transverse, respectively.

The next step is to optimize the three fitted response surface models simultaneously to determine the optimal control actions.

7.2.3. Optimization control

Lin and Tu (1995) proposed an objective function, namely, the Mean Squared Error (*MSE*). The basic idea of the *MSE* is generalized in this chapter.

For the rotary kiln operational system, the objective function of the proposed RSPC model represents a tendency to reach the targets: (1) the minimum difference between the flame temperature and its desired operational temperature, (2) the minimum the variance of first response ($\overline{y}$) and the minimum standard deviation among three standardized temperature differences (Δy) at the flame, feed end, and discharge end, and (3) the minimum system energy consumption.

The first target means the proposed approach can generate optimal control variables to serve the kiln operation, so the responding temperature of the flame attains the desired operational temperature as much as possible. The second target implies the proposed approach achieves robust results, as well as maintains a balance among the three responding temperatures that can simultaneously reach their own desired operational temperatures. The meaning of the third target is straight-forward, in which, the fuel flow rate is the most important factor impacting the operation cost. However, this does not mean the less fuel flow rate the better control. The fuel flow rate is dependent on the temperatures in the kiln and the raw material rate, for example, a high raw material rate needs a high fuel flow rate. In addition, significant fluctuations in the fuel flow rate mean unstable and uneconomical work condition in the kiln, so the optimization process control should minimize the change of the fuel flow rate. Therefore, the above target (3) is represented by a minimum change in the fuel flow rate. It is included in the objective

function of the proposed DRSPC model to reflect the trade-off among the decision variables. This trade-off can be realized through adjusting values of w_1, w_2 and w_3 (shown in Equation 7-8a).

With the constraints related to the variables, an optimization model can be formulated as follows, to identify the optimal control conditions:

$$Min \ \ f = w_1(\bar{y} - T)^2 + w_2(\sigma_{\bar{y}}^2 + \sigma_{\Delta y}^2) \ + w_3(\Delta u)^2 \tag{7-8a}$$

Subject to:

$$\bar{y} = h_o + S'h + S'HS \tag{7-8b}$$

$$\sigma_{\bar{y}} = r_o + S'r + S'RS \tag{7-8c}$$

$$\sigma_{\Delta y} = g_o + S'g + S'GS \tag{7-8d}$$

$$S_L \le S \le S_U \tag{7-8e}$$

where S_L *and* S_U are the lower and upper bounds of S, and w_1, w_2 and w_3 are the weights reflecting different priorities in the calcination process.

Dynamic operational conditions are examined to generate their corresponding optimal and robust control outputs and, consequently, serve the real-time rotary kiln process.

7.3. Proposed approach application

In this section, the developed DRSPC is implemented in the process control of an industrial aluminum rotary kiln to demonstrate its ability to deal with complex and dynamic operational conditions.

7.3.1. Overview of the study rotary kiln

The study kiln is an $\phi 5 \times 110m$ industrial aluminum rotary kiln. It is located at the Aluminum Corporation of China in Henan province. This aluminum rotary kiln process includes the stages of drying, preheating, decomposing, burning and cooling. The main characteristics in the stages are described as follows: **(a)** in the drying stage, most water in the raw material slurry is evaporated by gas heat. The temperature of the gas in the drying zone consequently drops from 700～800□to 180～250□, **(b)** in the preheating stage, the temperature of the material is increased to 600□ and some thermal decomposition reactions are performed to remove crystal water from the raw material, **(c)** in the decomposing stage, the temperature of the material is increased to 1000℃, the crystal water is continually decomposed and the carbonate begins to decompose. Meanwhile, some reactions are occurred to compose new materials such as $Na_2O.Fe_2O_3$, $Na_2O.Al_2O_3$, and $Na_2O.Al_2O_3.2SiO_2$, **(d)** in the burning stage, the temperature of the material is increased to 1200～1300℃, and the actual temperature of the gas reaches up to 1500℃. The sintering procedure is completed in this zone, which can be described by

the following chemical equations:

$$Na_2O.Al_2O_3.2SiO_2 + 4CaO = Na_2O.Al_2O_3 + 2(2CaO.\ SiO_2) \quad (7\text{-}9)$$

$$2CaO + SiO_2 = 2CaO.\ SiO_2 \quad (7\text{-}10)$$

$$CaO + TiO_2 = CaO.\ TiO_2 \quad (7\text{-}11)$$

Stage **(e)** is the cooling, the processed material called clinker is cooled and discharged, and the temperature of the gas is 400～600℃.

7.3.2. Variable design

Data acquisition was continually preformed from January 23, 2008 to April 27, 2008. A total of 28,068 data sets were recorded. The time interval between two adjacent data samples was set at 5.5 minutes. The recorded data include the flame temperature, feed end temperature, discharge end temperature, fuel flow rate, draft fan speed, main drive load, cooling motor load and air pressure drop at the kiln head hood. The product quality of clinker was tracked. In practice, the fuel flow is controlled by a fuel flow pump, so the pump speed was used to represent the fuel flow rate. The flame temperature in the burning zone was measured through an image processing algorithm while the gas temperatures at the discharge and feed ends were measured with two thermocouples.

A portion of the record was selected which accompanying the stable quality product (normal-sintered alumina) after studied the operation conditions. The period of the selected record is from January 23, 2008 to February 20, 2008, which involves 7,237 data

sets. Furthermore, according to the operational experiences (Yi, 2008), 5 inputs were initially chosen for the DRSPC model. They were the flame temperature ($\boldsymbol{T_1}$), feed end temperature ($\boldsymbol{T_3}$), discharge end temperature ($\boldsymbol{T_2}$), main engine load ($\boldsymbol{R}$) and the fuel flow rate ($\boldsymbol{U}$). Table 7-1 lists a portion of the recorded data for the 5 inputs.

In real-time operation, all control factors are fixed (only with very small fluctuations) except the fuel flow rate, to achieve stable operation. In this situation, the control factors actually become state parameters. Major factors affecting the stable operational conditions in the kiln are variations in the composition and density of the raw material slurry and ambient temperature, which are uncontrollable. Due to the aforementioned reasons, the uncontrolled factors eventually influence the kiln temperature. The adjustments (changes) in the fuel flow rate are used to respond to temperature changes in the kiln. These adjustments are required to be small due to significant fluctuations in the fuel flow rate creating unstable and uneconomical operations. The small adjustment in the DRSPC model is realized by minimizing it in the objective function. Thus, we use the adjustment in fuel flow rate (represented by the adjustment of the fuel flow pump speed) as a control variable (output) and describe it by (Δu). It is defined as the fuel flow rate of the next time interval minus the fuel flow rate of the current time interval.

Table 7-2 lists statistical results (includes maximum values, minimum values, averages, and standard deviation) of 6 inputs (including 1 control variable), and 3 responses. The constrain values of the inputs and responses are derived from Table 7-2. $\boldsymbol{T_1}$ and $\bar{y}$ have same value range but are separated by a time difference of Δt.

7.3.3. Response surface models

Using the recorded data of the operational conditions, two response surface models can be fitted. Three models are generated with a confidence level of $\alpha = 0.05$, and correlation coefficients are: $CC(\bar{y})$ = 0.994, $CC(\sigma_{\bar{y}})$ = 0.977 and $CC(\sigma_{\Delta y})$ = 0.972. The detailed relationships between the system coefficients and operating conditions are described as follows:

$$\begin{aligned}\bar{y} = 1132.14 &+ (642.42\,\Delta u - 7837.5\boldsymbol{U} + 9403\boldsymbol{T_1} + 12.88\boldsymbol{T_2} - 22580\boldsymbol{T_3} - 9532.4\boldsymbol{R} \\ &- 0.0094\,\Delta u^2 - 3.18\boldsymbol{U^2} - 2.28\boldsymbol{T_1^2} - 1.76\boldsymbol{T_2^2} - 0.474\boldsymbol{T_3^2} + 2.19\boldsymbol{R^2} \\ &- 1.5\,\Delta u\,\boldsymbol{U} - 0.663\,\Delta u\,\boldsymbol{T_1} + 0.635\,\Delta u\,\boldsymbol{T_2} + 1.03\,\Delta u\,\boldsymbol{T_3} + 3.15\,\Delta u\,\boldsymbol{R} \\ &+ 6.43\boldsymbol{UT_1} + 6.5\boldsymbol{UT_2} + 14.7\boldsymbol{UT_3} + 1.26\boldsymbol{UR} \\ &- 4.55\boldsymbol{T_1T_2} - 0.254\boldsymbol{T_1T_3} + 1\boldsymbol{T_1R} \\ &- 6.28\boldsymbol{T_2T_3} + 1.43\boldsymbol{T_2R} + 11.6\,\boldsymbol{T_3R}) \times 10^{-4}\end{aligned} \tag{7-12}$$

$$\begin{aligned}\sigma_{\bar{y}} = 1046.8 &+ (-239.7\,\Delta u - 12411\boldsymbol{U} + 6945.1\boldsymbol{T_1} - 2756.9\boldsymbol{T_2} - 11564\boldsymbol{T_3} - 14280\boldsymbol{R} \\ &+ 0.075\,\Delta u^2 + 5.893\boldsymbol{U^2} - 2.207\boldsymbol{T_1^2} + 1.83\boldsymbol{T_2^2} + 4.27\boldsymbol{T_3^2} + 5.53\boldsymbol{R^2} \\ &+ 0.435\,\Delta u\,\boldsymbol{U} - 0.354\,\Delta u\,\boldsymbol{T_1} - 0.664\,\Delta u\,\boldsymbol{T_2} + 1.8\,\Delta u\,\boldsymbol{T_3} + 0.092\,\Delta u\,\boldsymbol{R} \\ &- 2.38\boldsymbol{UT_1} + 0.338\boldsymbol{UT_2} - 5.29\boldsymbol{UT_3} + 3.21\boldsymbol{UR} \\ &- 0.952\boldsymbol{T_1T_2} + 5.42\boldsymbol{T_1T_3} + 1.03\boldsymbol{T_1R} \\ &+ 7.45\boldsymbol{T_2T_3} - 0.79\boldsymbol{T_2R} + 7.26\,\boldsymbol{T_3R}) \times 10^{-4}\end{aligned} \tag{7-13}$$

$$\begin{aligned}\sigma_{\Delta y} = 1117.75 &+ (-1788.9\,\Delta u - 6564.2\boldsymbol{U} + 3635.6\boldsymbol{T_1} - 5891.8\boldsymbol{T_2} - 33081\boldsymbol{T_3} - 10163\boldsymbol{R} \\ &+ 0.261\,\Delta u^2 - 0.0188\boldsymbol{U^2} - 0.522\boldsymbol{T_1^2} + 4.93\boldsymbol{T_2^2} + 78.2\boldsymbol{T_3^2} + 7.34\boldsymbol{R^2}\end{aligned}$$

$$+ 0.239\,\Delta u\,\boldsymbol{U} - 0.128\,\Delta u\,\boldsymbol{T_1} - 0.435\,\Delta u\,\boldsymbol{T_2} + 7.85\,\Delta u\,\boldsymbol{T_3} - 0.234\,\Delta u\,\boldsymbol{R}$$

$$+ 0.362\boldsymbol{UT_1} + 5.38\boldsymbol{UT_2} - 16.4\boldsymbol{UT_3} + 11.1\boldsymbol{UR}$$

$$- 4.25\boldsymbol{T_1T_2} + 19.8\boldsymbol{T_1T_3} - 8.57\boldsymbol{T_1R}$$

$$- 7.7\boldsymbol{T_2T_3} + 1.83\boldsymbol{T_2R} - 12.6\,\boldsymbol{T_3R}) \times 10^{-4} \qquad (7\text{-}14)$$

A nonlinear optimization program is developed to optimize the aluminum rotary kiln operational conditions:

$$Min\ \ f = w_1(\bar{y} - 1350)^2 + w_2(\sigma_{\bar{y}}^2 + \sigma_{\Delta y}^2) + w_3(\Delta u)^2 \qquad (7\text{-}15a)$$

Subject to:

$$750 \le \bar{y} \le 1500\,, \quad -120 \le \sigma_{\bar{y}} \le 120\,, \quad 0 \le \sigma_{\Delta y} \le 700 \qquad (7\text{-}15b)$$

$$-150 \le \Delta u \le 150 \qquad (7\text{-}15c)$$

$$750 \le T_1 \le 1500\,, \quad 550 \le T_2 \le 750\,, \quad 260 \le T_3 \le 360 \qquad (7\text{-}15d)$$

$$600 \le R \le 750\,, \qquad 750 \le U_1 \le 1450 \qquad (7\text{-}15e)$$

where coefficients w_1, w_2 and w_3 are used to reflect the trade-off between system cost and efficiency. In order to strengthen the restrictions on Δu, we directly reduce its value range (narrower than that shown in Table 7-2) in the constraint that is given by Equation 7-15c.

It is important to mention that only one control variable (Δu) was designed in the proposed approach. The main engine load (***R***) and fuel flow rate (***U***) are considered state parameters. However, an optimization model may need more control variables under different operational conditions, such as air pressure drop at the kiln head hood which could be designed as a control variable.

7.3.4. Results and discussion

The Fmincon slover in Matlab 7 was used to solve the above quadratic models. The run time is several milliseconds. Based on dynamic operational conditions, the proposed DRSPC programming can rapidly generate corresponding optimal and robust outputs to serve the real-time rotary kiln process during each 5.5 minute period.

A variety of weighted coefficients are analyzed to examine the effects of varied efficiency targets and cost-efficiency tradeoffs. These examinations are based on one real operational condition that extracted from the recorded data, and the results are shown in Table 7-3. Through comparison with the observed data, the predicted results show the proposed approach can generate better control outputs for helping the system achieve an optimum kiln process. Through comparison with variations of the weighted coefficients, the predicted results demonstrate that the system is sensitive to the weights w_1 and w_2 but not w_3.

Six operational condition scenarios are extracted from the recorded data to further test the effects of different efficiency targets and cost-efficiency tradeoffs. Four different sets of weighted coefficients are designed for the deeper tests. When w_1: w_2: w_3 = 1000: 1: 1 (shown in Table 7-4), the predicted values of $\bar{y}$ can rapidly reach the target value of 1350℃, but the control outputs of Δu are much higher than the observed values. When w_1: w_2: w_3 = 100: 1: 1 (shown in Table 7-5), $\bar{y}$ can also quickly reach the target value of 1350℃, and the standard deviation values of $\sigma_{\Delta y}$ begin to decrease. When w_1: w_2: w_3 = 10: 1: 1 (shown in Table 7-6), $\bar{y}$ begins to slow down the speed of approach to the target value. Meanwhile, the Δu values decrease significantly. When w_1: w_2: w_3 = 1: 1: 1

(shown in Table 7-7), the results show the system cost is economical but the system is inefficient.

The aforementioned analysis shows the reasonable range of the weighted coefficients is from (w_1: w_2: w_3 = 10: 1: 1) to (w_1: w_2: w_3 = 100: 1: 1). This value range can ensure a cost-effective decision space for the aluminum rotary kiln system, and provide useful information to decision makers for varied efficiency targets.

7.4. Summary

This chapter has presented a Dual-Response-Surface-Based process control (DRSPC) programming for real-time process control of industrial rotary kilns. Two quadratic models are appropriately fitted by response surface method in terms of the prior recorded data of the operational conditions from an industrial rotary kiln. Following an optimization technique with the Mean Squared Error (MSE), the proposed DRSPC programming is developed. It has the following properties:

- Based on the dynamic operational condition inputs, it can rapidly provide corresponding optimal outputs to serve the real-time rotary kiln process due to quadratic models.
- Its optimal outputs are robust due to the standard deviation of the predicted temperatures under consideration.
- The time delay problem can be solved due to the fact the programming can predict the corresponding outputs and responses for next time interval.

- It can statistically eliminate the measurement errors due to desired operational parameters are calculated by the arithmetic means of their recorded data rather than the actual values.

The developed approach has been applied to a real case study of an aluminum rotary kiln in China. The results provide a solid basis for guiding the real-time process control of industrial rotary kilns. The results are also useful for decision makers to analyze tradeoffs between system cost and operational efficiency.

Table 7-1. A portion of the recorded data

Recorded time	*Flame temp.T_1 (℃)*	*Feed end temp.T_3 (℃)*	*Discharge end temp.T_2 (℃)*	*Main engine load R (KW)*	*Fuel flow pump speed U (RPM)*
08/1/23 2:18	1293.38	272.0626	538.4818	687.7386	1263.274
08/1/23 2:24	1275.115	271.6429	534.7856	686.6686	1256.159
08/1/23 2:29	1295.816	274.4081	539.3751	672.5079	1286.249
08/1/23 2:35	1286.683	276.418	542.3651	672.8234	1259.175
08/1/23 2:40	1288.089	279.2472	545.5787	672.6556	1273.462
08/1/23 2:46	1309.52	277.6271	551.015	672.6859	1279.935
08/1/23 2:51	1277.479	279.5642	550.2545	672.6265	1251.966

Table 7-2. Statistical results of the recorded data

Name	Δu *(RPM)*	$\sigma_{\Delta y}$	T_1& $\bar{y}$ *(℃)*	T_3 *(℃)*	T_2 *(℃)*	*R (KW)*	*U (RPM)*
Max	243.70	678.5	1478.47	355.05	709.68	736.08	1422.69
Min	-334.57	0.161	759.64	32.41	365.00	628.19	767.96
Averag	0.0049	16.31	1352.88	260.37	554.11	669.59	1260.49
StdDev	18.86	17.22	117.9	14.00	35.29	21.55	69.05

Table 7-3. Results for variations of the weighted coefficients

Name	w_1	w_2	w_3	Δu *(rpm)*	$\sigma_{\bar{y}}$	$\sigma_{\Delta y}$	$\bar{y}$ *(℃)*
1	1	1	1	0.343	12.51	4.63	1297.97
2	10	1	1	3.3723	12.66	4.93	1300.00
3	100	1	1	24.176	14.08	8.25	1314.08
4	1000	1	1	63.526	18.53	20.72	1340.45
5	10	10	1	0.347	12.51	4.63	1297.97
6	100	10	1	3.38	12.66	4.93	1300.03
7	1000	10	1	24.19	14.08	8.26	1314.10
8	100	100	1	0.347	12.51	4.63	1297.97
9	1000	100	1	3.38	12.66	4.93	1300.03
10	1000	1000	1	0.347	12.51	4.63	1297.97
Observed value				-7.115	------	8.073	1275.12

Note: the operation conditions are shown in Table 7-1 on 08/1/23 2:18

Table 7-4. Results for a variety of scenarios when w_1=1000, w_2=1, and w_3 =1.

		Δu (rpm)	$\sigma_{\Delta y}$	$\bar{y}$ (℃)	$\sigma_{\bar{y}}$	T_1 (℃)	T_3 (℃)	T_2 (℃)	R (KW)	U (RPM)
1	Observed	125.5	118.9	1156.2	**36.9**	990.0	297.3	540.9	644.7	1025.4
	Predicted	**150.0**	**110.5**	**1147.5**						
2	Observed	67.18	34.43	1133.9	**29.5**	1082.1	269.0	562.0	703.6	1066.4
	Predicted	**150.0**	**69.5**	**1252.5**						
3	Observed	19.87	31.98	1292.9	**26.0**	1255.1	268.4	537.5	703.9	1257.1
	Predicted	**101.7**	**38.95**	**1336.2**						
4	Observed	-4.64	34.58	1395.3	**12.2**	1400.9	270.6	578.0	703.9	1241.1
	Predicted	**-51.32**	**5.10**	**1357.1**						
5	Observed	-14.29	17.10	1458.3	**23.0**	1470.6	258.4	533.3	674.5	1302.3
	Predicted	**-150**	**61.3**	**1401.9**						
6	Observed	-1.87	21.3	1395.5	**14.9**	1411.6	252.6	534.1	660.5	1237.3
	Predicted	**-78.99**	**22.88**	**1364.5**						

Table 7-5. Results for a variety of scenarios when w_1=100, w_2=1, and w_3 =1.

		Δu (rpm)	$\sigma_{\Delta y}$	$\bar{y}$ (℃)	$\sigma_{\bar{y}}$	T_1 (℃)	T_3 (℃)	T_2 (℃)	R (KW)	U (RPM)
1	Observed	125.5	118.9	1156.2	**36.9**	990.0	297.3	540.9	644.7	1025.4
	Predicted	**150.0**	**110.5**	**1147.5**						
2	Observed	67.18	34.43	1133.9	**25.7**	1082.1	269.0	562.0	703.6	1066.4
	Predicted	**133.6**	**56.8**	**1233.6**						
3	Observed	19.87	31.98	1292.9	**16.5**	1255.1	268.4	537.5	703.9	1257.1
	Predicted	**43.1**	**13.3**	**1292.6**						
4	Observed	-4.64	34.58	1395.3	**9.67**	1400.9	270.6	578.0	703.9	1241.1
	Predicted	**-20.8**	**0.51**	**1378.9**						
5	Observed	-14.29	17.10	1458.3	**5.57**	1470.6	258.4	533.3	674.5	1302.3
	Predicted	**-45.3**	**5.08**	**1450.3**						
6	Observed	-1.87	21.3	1395.5	**8.43**	1411.6	252.6	534.1	660.5	1237.3
	Predicted	**-23.7**	**3.76**	**1394.5**						

Table 7-6. Results for a variety of scenarios when w_1=10, w_2=1, and w_3 =1.

		Δu (rpm)	$\sigma_{\Delta y}$	$\bar{y}$ (℃)	$\sigma_{\bar{y}}$	T_1 (℃)	T_3 (℃)	T_2 (℃)	R (KW)	U (RPM)
1	Observed	125.5	118.9	1156.2	**10.8**	990.0	297.3	540.9	644.7	1025.4
	Predicted	**36.71**	**23.92**	**1021.6**						
2	Observed	67.18	34.43	1133.9	**11.1**	1082.1	269.0	562.0	703.6	1066.4
	Predicted	**27.95**	**9.13**	**1111.0**						
3	Observed	19.87	31.98	1292.9	**13.2**	1255.1	268.4	537.5	703.9	1257.1
	Predicted	**6.45**	**6.42**	**1264.9**						
4	Observed	-4.64	34.58	1395.3	**8.86**	1400.9	270.6	578.0	703.9	1241.1
	Predicted	**-2.99**	**0.06**	**1391.7**						
5	Observed	-14.29	17.10	1458.3	**3.68**	1470.6	258.4	533.3	674.5	1302.3
	Predicted	**-19.4**	**0.00**	**1461.9**						
6	Observed	-1.87	21.3	1395.5	**7.17**	1411.6	252.6	534.1	660.5	1237.3
	Predicted	**-2.94**	**0.69**	**1405.4**						

Table 7-7. Results for a variety of scenarios when w_1=1, w_2=1, and w_3 =1.

		Δu (rpm)	$\sigma_{\Delta y}$	$\bar{y}$ (℃)	$\sigma_{\bar{y}}$	T_1 (℃)	T_3 (℃)	T_2 (℃)	R (KW)	U (RPM)
1	Observed	125.5	118.9	1156.2	**6.79**	990.0	297.3	540.9	644.7	1025.4
	Predicted	**4.08**	**11.4**	**984.9**						
2	Observed	67.18	34.43	1133.9	**10.1**	1082.1	269.0	562.0	703.6	1066.4
	Predicted	**3.15**	**6.37**	**1081.9**						
3	Observed	-19.87	31.98	1292.9	**12.8**	1255.1	268.4	537.5	703.9	1257.1
	Predicted	**0.68**	**5.97**	**1260.5**						
4	Observed	-4.64	34.58	1395.3	**8.78**	1400.9	270.6	578.0	703.9	1241.1
	Predicted	**-0.31**	**0.13**	**1393.6**						
5	Observed	-14.29	17.10	1458.3	**3.68**	1470.6	258.4	533.3	674.5	1302.3
	Predicted	**-19.4**	**0.00**	**1461.9**						
6	Observed	-1.87	21.3	1395.5	**7.06**	1411.6	252.6	534.1	660.5	1237.3
	Predicted	**-0.3**	**0.47**	**1406.8**						

CHAPTER 8
Conclusions and Recommendations

8.1. Summary

Here, a set of methodologies has been presented for dealing with uncertainty in engineering and management practices. They include: (a) a hybrid stochastic-fuzzy approach for noise impact level assessment, (b) a hybrid stochastic method for hydraulic reliability assessment, (c) a reliability-based simulation-optimization approach for a long-term rehabilitation and upgrading schedule of a water distribution system, (d) a mixed fuzzy-interval-stochastic approach for binary linear programming, (e) a fuzzy multiple response surface methodology for the real-time multiple source water blending problem, and (f) a Dual-Response-Surface-Based process control for an industrial rotary kiln. They have been applied to a number of real and hypothetical cases.

(1) The hybrid stochastic-fuzzy approach for noise impact level assessment was developed. It can reflect the fate of noise emission from traffic under uncertainty, reveal the relationship between noise emission and related impact factors, conduct a fuzzy qualitative analysis for noise impact level under fuzzy noise abatement criteria, and perform probability analysis for the quantification of noise impact. The advantages of this approach over previous studies are: it not only addresses uncertainty of noise emission using the Monte Carlo

technique but also consider the uncertainty of noise abatement criteria using fuzzy theory. This methodology has been applied to a highway for predicting noise emission levels and impact levels in three different design scenarios. The results indicated that reasonable solutions have been generated. It can be used for clarifying the noise effects and supplying important information in city planning.

(2) The hybrid stochastic method was generated for hydraulic reliability assessment using the Monte Carlo simulation technique and the EPANET simulation software in MATLAB. A universal code of hydraulic reliability assessment was written in Matlab. This model considered both hydraulic failure and mechanical performance failure. The uncertain hydraulic parameters were treated as random numbers. An example of a benchmark water distribution network verified the applicability of this method and its code.

(3) The reliability-based simulation-optimization approach was developed for a long-term rehabilitation and upgrading schedule of a water distribution system. The approach considered the uncertainty of hydraulic parameters and treated them as random numbers following the normal distribution. It subdivided the high complexity water distribution systems' optimization problem into two stages: one stage for hydraulic performance optimization and another for mechanical performance optimization. The two stages are performed separately with simultaneous exchange information between each other.

Meanwhile, the threshold break rate model and the genetic algorithm participated in this optimization process. A computer code of the long-term maintenance schedule based on this approach was written in the MATLAB langrage and was applied to a benchmark water distribution system. The results demonstrated the applicability of this approach.

(4) The mixed fuzzy-interval-stochastic approach (IFBLP) was set up for binary linear problems in an uncertain environment by use of fuzzy constraints, a fuzzy objective, and interval coefficients to reflect uncertainties. The developed solution included two processes: the defuzzification process and the crisping process. The defuzzification process utilized the α-cut-based technique to defuzzify the IFBLP into an interval-coefficient binary linear programming (BLP); the crisping process used the interval linear programming algorithm to convert the interval-coefficient BLP into two extreme crisping-coefficient BLPs. In order to determine the value range of optimal alpha, a Monte Carlo simulation based approach was developed. Meanwhile, an alternative mathematical approach was developed to determine the boundary values of the optimal alpha. The developed IFBLP and its solution were applied to long-term traffic noise control planning. The results demonstrated they were applicable. Compared to an IBLP, the IFBLP could effectively reduce uncertainties on the right side of constraints, and could provide a more precise result for decision makers.

(5) The fuzzy multiple response surfaces methodology (FMRSM) was built for the real-time multiple source water blending problem in water distribution systems. In the FMRSM, the experimental data sets were fitted into the first quadratic models, their residuals were fitted into the second quadratic models, and multiple objectives were optimized by the fuzzy optimization method (using the min-optimizer). The proposed FMRSM was applied into a real case based on 6 designed scenarios. The results show that: (a) the quadratic models would help the optimization to dramatically reduce the running time of the computation, so that FMRSM could consequently rapidly response to changes of water quality, (b) the error between the predicted output and the measured data could be automatically evaluated and compensated in the optimization process though the second residual models so that the FMRSM can subsequently generate a robust result in each time interval, and (c) the fuzzy optimization method could simultaneously optimize multiple objectives.

(6) A Dual-Response-Surface-Based process control (DRSPC) programming was presented for real-time operation of industrial rotary kilns. Two quadratic models were appropriately fitted by response surface method in terms of the prior recorded data of the operational conditions from an industrial rotary kiln. Following an optimization technique with the Mean Squared Error (*MSE*), the novel DRSPC programming was presented. It has the following properties: (a) based

on the dynamic operational condition inputs, it can rapidly provide corresponding optimal outputs to serve the real-time rotary kiln process due to quadratic models, (b) its optimal outputs are robust due to the standard deviation of the predicted temperatures under consideration, (c) the time delay problem can be solved due to the fact the programming can predict the corresponding outputs and responses for next time interval, (d) It can statistically eliminate the measurement errors due to desired operational parameters that are calculated by the arithmetic means of their recorded data rather than the actual values.

The proposed approach has been applied to a real case study of an aluminum rotary kiln in China. The results provide a solid basis for guiding the real-time process control of industrial rotary kilns. The results are also useful for decision makers to analyze tradeoffs between system cost and operational efficiency.

8.2. Research achievements

(1) The proposed hybrid stochastic-fuzzy approach (SFA) improves upon the previous traffic noise impact assessment methods. Through integrating fuzzy and stochastic methods, the SFA could be applied under various traffic conditions, could deal with uncertainties in a more natural way, and generate more accurate results.

(2) The developed hybrid stochastic method improves upon the previous

hydraulic reliability assessment methods. Through considering both hydraulic failure and mechanical performance failure, it has a strong ability of dealing with uncertainty and can provide more precise results of hydraulic reliability.

(3) The reliability-based simulation-optimization approach is a new attempt for optimizing the long-term rehabilitation and upgrading schedule of a water distribution system. Though a universal computer code, the complex and expensive hydraulic maintenance plan can be easily and economically carried out by a computer.

(4) For the first time, the mixed fuzzy-interval-stochastic approach was applied to the BLP problems. It integrated interval programming and fuzzy flexible programming to efficiently deal with the uncertainties of the parameters and the model structure.

(5) The fuzzy multiple response surfaces methodology (FMRSM) is a new attempt for real-time multiple source water blending optimization. The FMRSM could help realize real-time robust operations with characteristics of high complexity and nonlinearity and has relatively low computational requirements.

(6) The Dual-Response-Surface-Based process control (DRSPC) programming is a totally new way to the process control of industrial rotary kiln. The DRSPC could solve many problems, which are caused from the high uncertainty and complex dynamics natures of the calcination process, during the process control such as the time delay

problem and the measurement errors problem.

8.3. Recommendations for future research

(1) As a new method for environmental impact assessment, the hybrid stochastic-fuzzy approach could be extended to other environmental fields that possess complex characteristics such as water / air / soil pollution impact assessment.

(2) In the hydraulic reliability assessment and reliability based optimization, uncertain information has been expressed as probability distributions rather than as simpler inexact numbers such as interval values or fuzzy sets. A more advanced methodology that incorporates interval, fuzzy and stochastic programming may allow for a more flexible reflection of the uncertainties.

(3) Traffic noise control planning is a location and candidate selection problem in management studies. As a new optimization methodology for binary linear programming, it is desirable to extend the mixed fuzzy-interval-stochastic approach to other studies such as assignment and assembly line balance in operation research, and representing and reasoning with propositional knowledge in artificial intelligence.

(4) In the fuzzy multiple response surfaces methodology (FMRSM), only three metal corrosions were considered as impact factors of water blending optimization. In reality, water distribution systems are complicated and many intricate relationships and interactions exist

among a variety of system components. Therefore, improvements in the nonlinear optimization models through considering more factors as well as their interactions would help extend the applicability of the FMRSM.

(5) In the Dual-Response-Surface-Based process control (DRSPC) programming, only several calcination process zones are considered. For example, there are only three temperatures in the rotary kiln that are measured. An improvement of the DRSPC need to be conducted by studying more calcination process zones and research more dynamic operational conditions.

REFERENCES

Ahmed HO, Dennis JH, Badran O, Ismail M, Ballal SG, Ashoor A, and Lerwood D (2000) Occupational noise exposure and hearing loss of workers in two plants in eastern Saudi Arabia. *Ann Occup Hyg,* 45(5): 371-380.

Alleyne BC, Dufresne RM, Kanji N, Reesal MR (1989) Costs of workers' compensation claims for hearing loss. *Journal of Occupational Medicine,* 31(2): 134-8.

Alperovits E, and Shamir U (1977) Design of optimal water distribution systems.*Water Resour. Res.*, 13(6): 885-900.

Al-Zahrani M and Syed J (2004) Hydraulic reliability analysis of water distribution system. *J of The Institution of Engineers,* 1(1): 76-92.

Ambrose RB, Wool TA, Connolly JP and Schanz RW (1988) In: *WASP4, A Hydrodynamic and Water Quality Model — Model Theory, User's Manual, and Programmer's Guide U.S. Environmental Protection Agency, EPA/600/3-87/039*

Anderson-Cook CM, Borror CM, and Montgomery DC (2009) Response surface design evaluation and comparison. *J. of Stat. Plann. and Infer.*, 139:629-641.

Arevalo JM (2003) *Modeling the effect of pipe material, water quality, and time on chlorine dissipation* . Master's thesis, University of Central Florida, Orlando.

Ascher H, and Feingold H (1984) *Repairable systems reliability.* Marcel Dekker, NY.

Barr PV, Brimacombe JK, and Watkinson AP (1989) A heat transfer model for the rotary kiln. *Met Trans B*, 20B(6) : 391-419.

Barry TM. and Reagan JA (1978) *FHWA-RD-77-108*, FHWA highway traffic noise prediction model, U. S. Department of Transportation, Washington DC.

Bass B, Huang GH, Russo J (1997) Incorporating climate change into risk assessmentusing grey mathematical programming. *Journal of Environmental Management,* 49(1): 107-123.

Bao Y and Mays LM (1990) Model for water distribution system reliability. *J. Hydraul. Eng.*, 116(9): 1119-1137.

Beck MB (1985) *Water quality management: a review of the development and application of mathematical models.* Springer Verlag, New York.

Bellman RE and Zadeh LA (1970) Decision making in a fuzzy environment. *Management Science,* 17 : 141-164.

Ben-Israel A and Robers PD (1970) A decomposition method for interval linear programming. *Management Science,* 15: 374-384.

Beck MB (1987) Water quality modeling: a review of the analysis of uncertainty. *Water Resources Research,* 23(8): 1393-1442.

Biscos C, Mulholland M, Le Lann MV, Buckley CA, Brouckaert CJ (2003) Optimal operation of water distribution networks by predictive control using MINLP. *Water SA*, 29(4): 393-404.

Bit AK, Biswal MP, and Alam SS (1993) An additive fuzzy programming model for multiobjective transportation problem. *Fuzzy Sets and Systems*, 57: 313-319.

Bitran GR (1979) Theory and algorithms for linear multiple objective programs with zero–one variables. *Mathematical Programming,* 17: 362–390.

Boateng AA and Barr PV (1996) A thermal model for the rotary kiln including heat transfer within the bed. *Int J Heat Mass Transfer*, 39(10): 2131-2147.

Borkowski A and Grabska E (2001) Graphs in layout optimization. In: Artificial

Intelligence in Construction and Structural Engineering. *Proceedings of the 8th International Workshop of the European Group of Structural Engineering Applications of Artificial Intelligent (EG-SEA-AI).* ISBN 1 897811 24 6 (eds C.J. Anumba, O.O. Ugwu & Z. Ren) Loughborough University, pp. 114–121.

Box GEP, and Wilson KB (1951) On the Experimental Attainment of Optimum Conditions. *J. of the Royal Statistical Soc.,* B(13):1-45.

Brown K and Rastogi L (1983) Mathematical modeling and computer control of lime kilns. *Proceedings of the Tappi pulping conference*, pp: 585-592. Atlanta, USA.

Burmaster SE and von Stackelberg K (1991) Using Monte Carlo simulation in public health risk assessments: Estimating and presenting full distributions of risk. *Journal of Exposure Analysis and Environmental Epidemiology*, 1(4): 491-512.

Calixto A, Diniz FB, Zannin PHT (2003) The statistical modeling of road traffic noise in an urban setting. *Cities*, 20(1): 23-29.

Calvin RS, Yacov YH, Duan L, and James HL (1996) Capacity reliability of water distribution networks and optimum rehabilitation decision making. *Water Resources Research,* 32(7): 2271-2278.

Cammarata G, Fichera A, Graziani S, and Marletta L (1995) Fuzzy-logic for urban traffic noise prediction. *Journal of The Acoustical Society of America,* 98(5): 2607-2612.

Canada Government Report (2004) *Canadian Handbook on Health Impact Assessment*. In: Decision making environmental health impact assessment, volume 2.

Cannas B, CELLi G, Fanni GA, and Pilo F (2001) Automated recurrent neural network design of a neural controller in a custom power device. *Journal of Intelligent and Robotic Systems*, 31: 229–251.

Cano RAR. and Odloak D (2003) Robust model predictive control of integrating processes. *Journal of Process Control*, 13: 101-114.

Castillo E, Granados M, Prat MD, Cortina JL (1999) Characterization and evaluation of levextrel extraction chromatographic resins for trace metal separation schemes inautomatic water quality control systems. *Solvent Extraction and Ion Exchange,*17(6): 1571-1586.

Castro JL, Herrera F and Verdegay JL (1994) Knowledge based systems and fuzzy Boolean programming. *International Journal of Intelligent Systems,* 9:211–225.

Chakraborty M. and Gupta S (2002) Fuzzy mathematical Programming for multiobjective linear fractional programming problem. *Fuzzy Sets and Systems,* 125: 335-342.

Chang CT (2007) Binary behavior of fuzzy programming with piecewise linear membership functions. *IEEE Transactions on Fuzzy Systems,* 15:342-349.

Chang CT (2010) An approximation approach for representing s-shaped membership functions. *IEEE Transactions on Fuzzy Systems,* 18(2): 412-424.

Chang YC and Jung K (2004) Effect of Distribution System Materials and Water Quality on Heterotrophic Plate Counts and Biofilm Proliferation. *J. of microbiology and biotechnology,*14(6):1114-1119.

Chen Z, Huang GH, Chakma A (2003) A hybrid fuzzy-stochastic modeling approach for assessing environmental risks at contaminated groundwater systems. J *of Env Eng (ASCE),* 129(1): 79-88.

Chen WC, Chang NB, and Chen JC (2002) GA-based fuzzy neural controller design for municipal incinerators. *Fuzzy Sets and Systems,* 129: 343-369.

Chien Y, Ton S, Lee M, Chia T, Shu H, Wu Y (2003) Assessment of occupational health hazards in scrap-tire shredding facilities. *The Science of the Total Environment*, 309: 35-46.

Chinneck JW and Ramadan K (2000) Linear programming with interval coefficients. *Journal of the Operational Research Society*, 51:209-220.

Chipperfield AJ, Fleming PJ, Pohleim H, and Fonseca CM (1994) *Genetic Algorithm Toolbox User's Guide*, ACSE Research Report No. 512, University of Sheffield.

Copeland K and Nelson P (1996) Dual response optimization via direct function minimization. *Journal of Quality Technology*, 28: 331-336.

Cox BA (2003) A review of currently available in-stream water-quality models and their applicability for simulating dissolved oxygen in lowland rivers. *The Science of the Total Environment,* Volumes 314-316: 335-377.

Cullinan MJ (1989) *Methodologies for the evaluation of water distribution system reliability/availability*. Thesis presented to the Department of Civil Engineering, University of Texas, at Austin, Tex.

Dahab MF, Lee YW, Bogardi I (1994) A rule-based fuzzy-set approach to risk analysis of nitrate-contaminated groundwater. *Water Science and Technology*, 30 (7): 45-52.

Dandy GC, Mcbean EA, and Hutchinson BG (1985) Pricing and expansion of a water supply system. *J of Water Resources Planning and Management*, 111 (1):24-41.

Das I and Potra FA (2003) Subsequent convergence of iterative methods with applications to real-time model-predictive control. *Journal of Optimization Theory and Applications*, 119(1): 37-47.

Davies POAL, Holland KR (1999) I. C. engine intake and exhaust noise assessment.

Journal of Sound and Vibration, 223(3): 425-444.

Davis L (1991) *Handbook of genetic algorithms*, Van Norstrand Reinhold, New York

Deb AK, Hasit Y, Grablutz F, and Herz R (1988) Quantifying future rehabilitation and replacement needs of water mains. *American Water Works Association Research Foundation*, Denver.

Del Castilo E and Montgomery D (1993) A nonlinear programming solution to the dual response problem. *Journal of Quality Technology*, 25(3): 199-204.

Del Castillo E (1996) Multiresponse process optimization via constrained confidence regions. *Journal of Quality Technology,* 28(1): 61-71.

Dhavlikar MN, Kulkarni MS, and Mariappan V (2003) Combined Taguchi and dual response method for optimization of a centerless grinding operation. *Journal of Materials Processing Technology,* 132: 90-94.

Diehl RJ (1998) Statistical and connectionist approaches to modeling the assessment of noise annoyance inside passenger vehicles. *Applied Acoustic,* 55(4): 275-291.

Dieter G (1995) *Regulations for Community Noise.* In: Noise/news international, December 1995.

Downing DJ, Gardner RH, and Hoffman FO (1985) Response surface methodologies for uncertainty analysis in assessment model. *Technometrics,* 27(2): 151-163.

Dubois D and Prade H (1980) Systems of Linear Fuzzy Constraints. *Fuzzy Sets and Systems*, 3: 37-48.

Elshorbagy WE, Abu-Qdais H, and Elsheamy MK (2000) Simulation of THM species in water distribution systems. *Water Research*, 34(13): 3431-3439.

EPA (1997) *Risk Assessment Forum: Guiding Principles for Monte Carlo Analysis,*

EPA/630/R-97/001(p15). (http://www.epa.gov/NCEA/pdfs/montcarl.pdf).

EPANET (2008) *Hydraulic Simulation software*, download from: http://www.epanet.com/downloads.asp?skid=CEO_NA_HAE_GOOG_EPA&WT.srch=1&gclid=CParhrqm-ZgCFRYiagod8V2ToQ

Eschenroeder AQ and Faeder EJ (1988) A Monte Carlo analysis of health risks from PCB-contaminated mineral oil transformer fires. *Risk Analysis,* 8: 291-197.

Fen CS, Chan CC, and Cheng HC (2009) Assessing a Response Surface-Based Optimization Approach for Soil Vapor Extraction System Design. *Journal of* Water *Resources Planning & Management,* 135(3):198-207.

Ferrer J, Rodrigo MA, Seco A, and Penya-roja JM (1998) Energy saving in the aeration process by fuzzy logic control. *Water Science and Technology*, 38(3): 209-217.

Franssen EAM, Staatsen BAM, Lebret E (2002) Assessing health consequences in an environmental impact assessment: the case of Amsterdam Airport Schiphol. *Environmental Impact Assessment Review*, 22: 633-653.

Gen M, Ida K, Lee J, and Kim J (1997) Fuzzy nonlinear goal programming using genetic algorithm. *Computers & Industrial Engineering*, 33(1-2): 39-42.

Germanopoulos G, Jowitt PW, and Lumbers JP (1986) Assessing the reliability of supply and level of service for water distribution systems. *Proc. Instn. Civ. Engrs.,* Part 1, Water Engineering Group, 413-428.

Giustolisi O, Laucelli D, and Colombo AF (2009) Deterministic versus stochastic design of water distribution networks. *Journal of Water Resources Planning and Management-ASCE,* 135(2): 117-127.

Gokcen H and Erel E (1997) A goal programming approach to mixed-model assembly

line balancing problem. *International Journal of Production Economics*, 48:177–185.

Goldberg D (1989) *Genetic algorithms in search, optimization, and machine learning*, Addison-Wesley, New York.

Goulter I (1995) Analytical and simulation models for reliability analysis in water distribution systems. *In: E. Cabrera and A. Vela (eds), Improving Efficiency and Reliability in Water Distribution Systems, Kluwer Academic Publishers, Dordrecht*, 235-266.

Guh RS (2003) Integrating artificial intelligence into on-line statistical process control. *Quality and Reliability Engineering International*, 19: 1-20.

Guu SM and Wu YK (1999) Two-phase approach for solving the fuzzy linear programming. *Fuzzy Sets and Systems*, 107: 191-195.

Hanson DI and James RS (2004) *Colorado DOT tire/pavement noise study*. Report No. CDOT-DTD-R-2004.

Hardy AEJ (2000) Measurement and assessment of noise within passenger trains. *Journal of Sound and Vibration*, 231(3): 819-829.

Herrera F and Verdegay JL (1991) Approaching fuzzy integer linear programming problems, in: M. Fedrizzi, J. Kacprzyk and M. Roubens, Eds., *Interactive Fuzzy Optimization*, Springer-Verlag, Berlin, p78-91.

Herrera F, Verdegay JL, and Zimmermann HJ (1993) Boolean programming problems with fuzzy constrains. *European Journal of Operation Research*, 55:285-293.

Herrera F and Verdegay JL (1996) Fuzzy Boolean programming problems with fuzzy costs: A general study. *Fuzzy Sets and Systems*, 81:57–76.

Herman LA (1997) Analysis of strategies to control traffic noise at the source. *Transportation Research Record* 1626, paper no. 97-1519: 41-48

Hardy AEJ (2000) Measurement and assessment of noise within passenger trains. *Journal of Sound and Vibration,* 231(3): 819-829.

Holland J (1975) *Adaptation in natural and artificial systems.* University of Michigan Press, Ann Arbor, Mich.

Hoogeweg CG (1999) *Impact of Uncertainty in Model Input Data on Predicted Pesticide Leaching*, Ph.D. dissertation, University of Florida, FL.

Huang GH, Baetz BW, and Patry GG (1993a) Grey integer programming: an application to waste management planning under uncertainty. *European Journal of Operational Research,* 83: 594-620.

Huang GH, Baetz BW, and Patry GG (1993b) A grey fuzzy linear programming approach for municipal solid waste management planning under uncertainty. *Civil Engineering Systems,* 10: 123-146.

Huang GH (1994) *Grey mathematical programming and its application to municipal solid waste management planning*, Ph.D. thesis, Department of Civil Engineering, McMaster University.

Huang GH, Baetz BW, and Patry GG (1994) Grey dynamic programming for waste-management planning under uncertainty. *Journal of Urban Planning and Development*, 120(3): 132-156.

Huang GH, Baetz BW, and Patry GG (1995) Grey fuzzy integer programming: an application to regional waste management planning under uncertainty. *Socio-Economic Planning Sciences,* 29(1): 17-38.

Huang GH, Baetz BW, Patry GG, and Terluk V (1997) Capacity planning for an integrated waste management system under uncertainty: A North American case study. *Waste Management & Research,* 15: 523-546.

Huang GH (1998) A hybrid inexact-stochastic water management model. *European Journal of Operational Research,* 107: 137-158.

Huang GH, Sae-Lim N, Chen Z, and Liu L (2001) Long-term planning of waste management system in the City of Regina – An integrated inexact optimization approach. *Environmental Modeling and Assessment,* 6:285-296.

Huang YC and Wang XZ (1999) Application of fuzzy causal networks to waste water treatment plants. *Chemical Engineering Science*, 54: 2731-2738.

Huang YF, Li JB, Huang GH, Chakma A, and Qin XS (2003) An integrated simulation-optimization approach for real time dynamic modeling and process control of surfactant enhanced remediation at petroleum contaminated site. *Practice Periodical of Hazardous, Toxic, and Radioactive Waste Management (ASCE),* 7(2): 95-105.

Huang YF, Wang GQ, Huang GH, Xiao HN and Chakma A (2008) IPCS: An integrated process control system for enhanced in-situ bioremediation. *Environmental Pollution* 151 (3), 460-469.

Hume K, Gregg M, Thomas C, Terranova D (2003) Complaints caused by aircraft operations: an assessment of annoyance by noise level and time of day. *Journal of air Transport Management,* 9: 153-160.

Imber M and Paschkis V (1962) A new theory for a rotary-kiln heat exchanger. *International Journal of Heat Mass Transfer*, 5: 623-638.

Imran S, Dietz JD, Mutoti G, Taylor JS, Randall AA, Cooper CD (2005b) Red Water Release in Drinking Water Distribution Systems, *J. AWWA,* 97(9):93-100.

Imran S, Dietz J.D, Mutoti G, Xiao W, Taylor JS, Desai V (2006) Optimizing Source Water Blends for Corrosion and Residual Control in Distribution Systems. *J. AWWA,* 98(5):107-115.

Ignizio JP and Daniels SC (1983) Fuzzy Multi-Criteria Integer Programming Via Fuzzy Generalized Networks, Fuzzy Sets and Systems, 10: 261-270

International Association for Impact Assessment (1999) *Principle of Environmental Impact Assessment Best Practice*. (Form: http://www.iaia.org/modx/assets/files/Principles%20of%20IA_web.pdf)

Inuiguchi M and Sakawa M (1990) Robust optimization under softness in a fuzzy linear programming problem. *International Journal of Approximate Reasoning,* 18: 21-34.

Inuiguchi M and Sakawa M (1995) Minimax regret solution to linear programming problems with an interval objective function. *European Journal of Operational Research,* 86: 526-536.

Jackson PS, Hockenbury RW, and Yeater ML (1981) Uncertainty analysis for system reliability and availability assessment. *Nuclear Engineering and Design,* 68: 5-29.

Jamshidi M (2003) Tools for intelligent control: fuzzy controllers, neural networks and genetic algorithms, Philosophical Transactions Mathematical. *Physical & Engineering Science*, 361: 1781-1808.

Jarvensivu M, Saari K, and Jamsa-Jounela SL (2001) Intelligent Control System of an Industrial Lime Kiln Process. *Control Engineering Practice*, 9(6): 589-606.

Jarvensivua M, Esko J, and Olli A (2001) Intelligent Control of a Rotary Kiln Fired with Producer Gas Generated from Biomass. *Engineering Applications of Artificial Intelligence*, 14(5): 629-653.

Jaumard B, Ow PS and Simeone B (1988) A selected artificial intelligence bibliography for operations researchers. *Annals of Operational Research,* 12:1–50.

Kapelan ZS, Savic DA, and Walters GA (2005) Multiobjective design of water distribution systems under uncertainty. *Water Resource Research,* 41(11): W11407-1–W11407-15.

Kaplan S and Garrick BJ (1981) On the quantitative definition of risk. *Risk Analysis,* 1(1): 11-27.

Khalid M (1993) Adaptive fuzzy control of a water bath process with neural networks, *Engg. Applic. Artif. Intel.,* 7(1): 39-52.

Kim, KJ and Lin D (1998) Dual response surface optimization: a fuzzy modeling approach. *J of Quality Technology*, 30(1):1-10.

Kim M, Rao AS, and Yoo C (2009) Dual Optimization Strategy for N and P Removal in a Biological Wastewater Treatment Plant. *Industrial & Engineering Chemistry Research,* 48(13): 6363-6371.

Klir GJ (1997) Fuzzy arithmetic with requisite constraints. *Fuzzy Sets and Systems,* 91:165–175.

Kluijver H, Stoter J (2003) Noise mapping and GIS: optimizing quality and efficiency of noise effect studies. *Computers, Environment and Urban Systems*, 27: 85-102.

Koksoy O (2003) Joint optimization of mean and standard deviation using response surface methods. *Journal of Quality Technology,* 35(3): 239-252.

Kurze UJ (1971) Statistics of road traffic noise. *J. Sound and Vibration,* 18(2): 171-95.

Lam WHK, Tam ML (1998) Reliability analysis of traffic noise estimates in Hong Kong. *Transpn Res,* 3(4): 239-248.

Lansey KE, Duan N and Mays LW (1989) Water distribution system design under uncertainties. *Journal of Water Resources Planning and Management-ASCE,* 115(5): 630-644.

Lee DH, Jeong IJ, Kim KJ (2010) A posterior preference articulation approach to dual-response-surface optimization. *Journal of Quality Technology,* 42(2): 161-171.

Lee ES and Li RJ (1993) Fuzzy multiple objective programming and compromise programming with pareto optimum. *Fuzzy Sets and Systems*, 53: 275-288.

Lee JH., Natarajan S, and Lee KS (2001) A model-based predictive control approach to repetitive control of continuous processes with periodic operations. *Journal of Process Control,* 11: 195-207.

Lee S, Moon JW, and Moon HS (2003) Heavy metals in the bed and suspended sediments of Anyang River, Korea: Implications for water quality. *Environmental Geochemistry and Health*, 25(4): 433-452.

Letha J and Sheeja AR (2003) Computer aided cost effective design of a water distribution network- a case study in kerala. *IE (I) Journal CV,* 84:223-232.

Li B, Tao S, Dawson RW, Cao J, Lam K (2002) AGIS based road traffic noise prediction model. *Applied Acoustics*, 63: 679-691.

Li CX and Zhu J (2004) The Application of Dual Mode Fuzzy Prediction Control in Raw Material System of Cement Rotary Kiln. *Automation Instrumentation*, 25(2): 37-39.

Li JB, Huang GH, Chakma A, Zeng GM, Liu L (2003) Integrated fuzzy-stochastic modeling of petroleum contamination in subsurface. *Energy Sources*, 25: 547-563.

Li YQ, Cui ZS, Ruan XY, and Zhang DJ (2006) CAE-based six sigma robust optimization for deep-drawing process of sheet metal. *International Journal of Advanced Manufacturing Technology,* 30: 631-637.

Li ZZ, Heo KS, and Seol SY (2008) Time-dependent optimal heater control in thermoforming preheating using dual optimization steps. *International Journal of Precision Engineering And Manufacturing,* 9 (4): 51-56.

Liang TF (2009) Fuzzy multi-objective project management decisions using two-phase fuzzy goal programming approach. *Computers & Industrial Engineering*, 57 (4): 1407-1416.

Lin D and Tu W (1995) Dual response surface optimization. *J of Quality Technology,* 27:34-39.

Lin WH and Wang CH (2004) An enhanced 0-1 mixed-integer LP formulation for traffic signal control. *IEEE Transactions on Intelligent Transportation Systems,* 5:238-245.

Liu ML and Sahinidis NV (1997) Process planning in a fuzzy environment, *European Journal of Operation Research,* 100:142-169.

Madsen HO, Krenk S, and Lind NC (1986) Methods of structural safety. Prentice-Hall, Englewood Cliffs, N.J.

Maeda H and Murakami S (1988) A fuzzy decision-making method and its application to a company choice problem. *Information Sciences*, 45: 331–346.

Malakooti B (1994) Assembly line balancing with buffers by multiple criteria

optimization. *International Journal of Production Research,* 32: 2159–2178.

Mastorakos E , Massias A , and Tsakiroglou CD (1999) CFD predictions for cement kilns including flame modeling, heat transfer and clinker chemistry. *Appl. Math Modeling*, 23 (1): 55-76.

Mays LW (1993) Methods for risk and reliability analysis. *Conf. Proc.,* Part of *Risk-based Decision Making in Water Resources VI*, 26-44.

McIlwain JA (1992) Kiln control. *Pulp and Paper Canada*, 93(11), 34-37.

Mecray EL and ten Brink MRB (2000) Contaminant distribution and accumulation in the surface sediments of Long Island Sound. *Journal of Coastal Research*, 16(3): 575-590.

Mehrez C, Percia C and Oron G (1992) Optimal Operation of a Multisource and Multi-quality Regional Water System. *Water Resour. Res.*, 128(5):1199-1206.

Miedema HME, and Oudshoorn, CGM (2001) Annoyance from transportation noise: Relationships with exposure metrics DNL and DENL and their confidence Intervals. *Environmental Health Perspectives,* 109 (4): 409-416.

Miller WT, Sutton RS, and Werbos PJ (1990) *Neural networks for control*, Cambridge MA: MIT Press.

Milford JB, Russell AG, and McRea GJ (1989) Spatial patterns in photochemical pollutant response to NOx and ROG reductions. *Environmental Science and Technology,* 23:1290-1301.

Morgan MG and Henrion M (1990) *A guide to dealing with uncertainty in quantitiative risk and policy analysis*. Cambridge University press.

Munavalli GR, Kumar MSM (2003) Optimal scheduling of multiple chlorine sources in

water distribution systems. *Journal of Water Resources Planning and Management-ASCE*, 129 (6): 493-504.

Munavalli GR, Kumar MSM (2005) Water quality parameter estimation in a distribution system under dynamic state. *Water Research*, 39(18): 4287-4298.

Myers RH (1971) *Response surface methodology*. Allyn & Bacon, Newton, Mass.

Myers RH, Montgomery DC, Vining GG, Borror CM, Kowalski SM (2004) Response surface methodology: a retrospective and literature survey. *J. Quality Tech.*, 36:53-77.

Negoita CV and Ralescu DA (1975) *Applications of Fuzzy Sets to Systems Analysis*, Birkhauser, Stuttgart.

Ohta M, Yamaguchi S, Ikuta A (1980) Statistical estimation of road traffic noise in an arbitrary sound propagation environment by use of Stratonovich's theory for a random point system. *Journal of Sound and Vibration*, 69(2): 275-284.

Ostfeld A and Shamir U (1996) Design of Optimal Reliable Multi-Quality Water Supply Systems. *J. of Water Resources Planning and Management, ASCE,* 122(5):322-333.

Ostfeld A (2001) Reliability analysis of regional water distribution systems. *Urban Water,* 3 253-260.

Prasad TD, and Park NS (2004) Multi-objective genetic algorithms for design of water distribution networks. *J of Water Resource Planning and Management ASCE* 130 (1):73-82.

Peng W, Mayorga RV (2008) Assessing traffic noise impact based on probabilistic and fuzzy approaches under uncertainty. *Stochastic Environmental Research and Risk*

Assessment, 22(4): 541-550.

Peng W, Mayorga RV and Imran S (2010a) A rapid optimization approach to source water blending problems in distribution systems based on fuzzy response surface methodology. Submitted to *Urban Water Journal*.

Peng W, Mayorga RV and Imran S (2010b) A robust optimization approach for real-time multiple source water blending problems. Submitted to *Journal of Water Supply: Research and Technology*.

Peng W and Mayorga RV (2010c) An interval-coefficient fuzzy binary linear programming, the solution, and its application under uncertainties. Submitted to *Journal of Operation Research Society*.

Peng W and Mayorga RV (2010d) A mixed approach to settle uncertainties in binary linear programming. Submitted to *International Journal of Uncertainty, Fuzziness and Knowledge-Based Systems.*

Peng W and Mayorga RV (2010e) Hydraulic reliability assessment and optimal rehabilitation/ upgrading schedule for water distribution systems. Submitted to *Journal of Civil Engineering and Environmental Systems.*

Peng W, He M, Zhang J, and Mayorga RV (2010f) Dual-response-surface-based process control to an industrial Rotary kiln. In process paper, submitted to *Control Engineering Practices*.

Quimpo RG and Shamsi UM (1991) Reliability-based distribution system maintenance. *Journal of Water Resources Planning and Management*-ASCE, 117(3):321-339.

Quiondry QE, Liebman JC, and Brill ED (1981) Optimization of looped water distribution systems. *Proc., J. Environ. Eng. Div.* 107(4):665-679.

Radovanovic H and Koelmans AA (1998) Prediction of in situ trace metal distribution coefficients for suspended solids in natural waters. *Environ. Sci. Technol.,* 32(6):753–759.

Raimbault M, Lavandier C, Berengier M (2003) Ambient sound assessment of urban environments: field studies in two French cities. *Applied Acoustic*, 64: 1241-1256.

Ramakrishnan V and Sai PST (1999) Mathematical modeling of pneumatic char injection in a direct reduction rotary kiln. *Metallurgical and Materials Transactions B,* 30(5):969-977.

Rao C V and Rawlings JB (2000) Linear programming and model predictive control. *Journal of Process Control*, 10: 283-289.

Reckhow KH (1994) Water quality simulation modeling and uncertainty analysis for risk assessment and decision making. *Ecological Modeling,* 72(1): 1-20.

Rogevich EC, Hoang TC, and Rand GM (2008) The effects of water quality and age on the acute toxicity of copper to the Florida apple snail, Pomacea paludosa. *Archives of Environmental Contamination and Toxicology,* 54(4): 690-696.

Ruedi MW (2004) A method to include in LCA road traffic noise and its health effects. International *Journal of Life Cycle Assessment*, 9(2): 76-85.

Sakawa M and Yumine Y (1983) Interactive fuzzy decision-making for multiobjective linear fractional programming problems. *Large Scale Systems*, 5(2): 105-114.

Sakawa M and Yano H (1990) An interactive fuzzy satisfying method for generalized multiobjective linear programming problems with fuzzy parameters. *Fuzzy Sets and Systems,* 35: 125-142.

Sakawa M and Yano H (1991) Feasibility and Pareto optimality for multiobjective

nonlinear programming problems with fuzzy parameters. *Fuzzy Sets and Systems*, 43: 1-15.

Sakawa M and Kato K (1998) Interactive decision-making for multiobjective linear fractional programming problems with block angular structure involving fuzzy numbers. *Fuzzy Sets and Systems,* 97: 19-31.

Sakawa M, Nishizaki I, and Uemura Y (2000) Interactive fuzzy programming for multi-level linear programming problem with fuzzy parameters. *Fuzzy Sets and Systems*, 109: 3-19.

Sanchez LFJ, Gil GMD, Martinez VJL, Aguilera PA, Garrido FA (2004) Assessment of metal contamination in Donana National Park (Spain) using crayfish (Procamburus clarkii). *Environ Monit Assess*, 93(1): 17-29.

Sass A (1967) Simulation of the heat-transfer phenomena in a rotary kiln. *I&EC Process Design and Development,* 6(4):532-535.

Savic DA, and Walters GA (1997) Genetic Algorithms for least-cost design of water distribution systems. *J of Water Resource Planning and Management ASCE,* 123 (2):67-77.

Scherm H (2000) Simulating uncertainty in climate–pest models with fuzzy numbers. *Environmental Pollution*, 108(3):373-379.

Schulte-werning B, Jager K, Strube R, Willenbrink L (2003) Recent development in noise research at Deutsche Bahn: noise assessment, noise source localization and specially monitored track. *Journal of Sound and Vibration*, 267: 689-699.

Shamir U, and Howard CDD (1979) An analytic approach to scheduling pipe replacement. *J. Am. Water Works Assoc.,* 71(5):248-258.

Sharp WW, and Walski TM (1988) Predicting internal roughness in water mains. *J of American Water Works Association*, 80(11):34-40.

Shih C J and Wangsawidjaja RAS (1996) Mixed fuzzy-probabilistic programming approach for multiobjective engineering optimization with random variables. *Computers and Structures,* 59(2): 283-290.

Shinstine DS, Ahmed I, and Lansey KE (2002) Reliability/Availability analysis of municipal water distribution networks: case studies. *ASCE J. Water Resources Planning & Management,* 128(2):140-151.

Skarlatos D and Manatakis E (1989) Noise probability density functions for Poissontype traffic flow. *Applied Acoustics,* 27:47-55.

Skarlatos D (1993) A numerical method for calculation of probability density function of equivalent level in the case of traffic noise. *Applied Acoustics,* 38 (1): 37-50.

Sopasakis A (2004) Stochastic noise approach to traffic flow modeling. *Physica A*, 342 (3-4): 741-754.

Stanciulescu C, Fortemps P, Install M, and Wertz V (2003) Multiobjective fuzzy linear programming problems with fuzzy decision variables. *European Journal of Operational Research,* 149: 654-675.

Sun GY, Li GY, Gong ZH, Cui XY, Yang XJ, and Li Q (2010) Multiobjective robust optimization method for drawbead design in sheet metal forming. *Materials & Design,* 31(4): 1917-1929.

Tan Y (1996) Optimization techniques for the design of a neural predictive controller. *Neurocomputing*, 10: 83-96.

Tang LC and Xu K (2002) A unified approach for dual response surface optimization.

Journal of Quality Technology, 34(4): 437-447.

Taylor JS et al. (2005) Effects of Blend on Distribution System Water Quality. *AwwaRF*, Report No. 91065F, Denver.

Tolson BA, Maier HR, Simpson AR, and Lence BJ (2004) Genetic Algorithms for reliability- based optimization of water distribution systems. *J of Water Resource Planning and Management ASCE,* 130 (1):63-72.

Tong SC (1994) Interval number and fuzzy number linear programming. *Fuzzy Sets and Systems,* 66: 301-306.

Tscheng SH and Watkinson AP (1979) Convective heat transfer in a rotary kiln. *Can J Chem Eng.*, 57(8): 433-441.

Tu MY, Tsai FTC, Yeh WWG (2005) Optimization of Water Distribution and Water Quality by Hybrid Genetic Algorithm. *J. of Water Resources Planning and Management-ASCE,* 131(6):431-440.

US Army Environmental Hygiene Agency (1990) *Environmental natural Resource Study*. February 1990.

US Department of Transportation (1995) *Highway traffic noise analysis and abatement policy and guidance.* Federal highway administration of Environment and planning noise and air quality branch, Washington, D.C.

Valiquette J, Savoie M (1999) Practical Aspects of model predictive control implementation on an industrial lime kiln. *Tappi Journal*, May 1999, pp.130-136.

Van Hop N (2006) A heuristic solution for fuzzy mixed-model line balancing problem. *European Journal of Operational Research,* 168(3): 798-810.

Vaurio JK (1982) *Statistical identification of effective input variables, reactor analysis*

and safety division, ANL-82-57, Argonne National Laboratory, Argonne, III.

Vining GG and Myers RH (1990) Combining taguchi and response surface philosophies: a dual response approach. *J of Quality Technology*, 22(1):38-45.

Vining GG and Bohn LL (1998) Response surfaces for the mean and variance using a nonparameteric approach. Journal of Quality Technology, 30(3), 282-291.

Viswamurthy SR, and Ganguli R (2007) Optimal placement of trailing-edge flaps for helicopter vibration reduction using response surface methods. *Engineering Optimization,* 39(2): 185-202.

Wang HF and Liao YC (2001) Fuzzy nonlinear integer program by parametric programming. *Fuzzy Sets and Systems,* 122: 245-251.

Wang Y (1996) A Hybrid Intelligent Control for Industrial Rotary Kiln Plant. *Control Theory and Application*, 13(6): 770-777.

Wang Y and Boyd S (2010) Fast model predictive control using online optimization. *IEEE Transactions on Control Systems Technology,* 18 (2): 267-278.

Willis MJ (1992) Artificial neural networks in process estimation and control. *Automatica*, 28(60): 1181-1187

Wilson JM (1990) Compact normal forms in prepositional logic and integer programming formulations. *Computers and Operations Research,* 17: 309–314.

Wong WK, Ng SH, and Xu K (2006) A statistical investigation and optimization of an industrial radiography inspection process for aero-engine components. *Quality and Reliability Engineering International,* 22 (3): 321-334.

World Health Organization (2001) *Occupational and Community Noise*. Fact sheet N^{o}258, media centre.

Wu DD, Zhang YD, Wu DX, and Olson DL (2010) Fuzzy multi-objective programming for supplier selection and risk modeling: A possibility approach. *European Journal of Operational Research,* 200(3): 774-787.

Xiao W (2004) *Effect of Source Water Blend on Copper Release in a Pipe Distribution System:Thermodynamic and Empirical Models*, Doctoral dissertation, University of Central Florida, Orlando.

Xu C, and Goulter IC (1998) Probabilistic model for water distribution reliability. *J. Water Resour. Plan. Maneag.,* 124(4):218-228.

Yakimow SE, Krause PE, Hahn GW, and Palumbo RD (1994) Initial kinetic study with a chemical equilibrium analysis of the ZnO+Ti2O3 reaction. *Industrial &Engineering Chemistry Research*, 33:436-439.

Yang SL, Sun YH, and Yeh WWG (2000) Optimization of regional water distribution system with blending requirements. *Journal of Water Resources Planning and Management-ASCE*, 126(4): 229-235.

Yi ZM (2008) Thermal analysis and process control application in aluminum rotary kiln. PhD dissertation, Central South University, Changsha 410083, China.

Yu CS and Li HL (2001) An algorithm for generalized fuzzy binary linear programming problems. *European Journal of Operation Research,* 133:496-511.

Zadeh LA (1965) Fuzzy sets. *Information and Control,* 8 (3): 338–353.

Zadeh LA (1971) Similarity relations and fuzzy orderings. *Inform. Sci.*, 3:177-206.

Zadeh LA (1978) The concept of a linguistic variables and its application to approximate reasoning. *Inform.Sci.*, 8:199-249.

Zahedi F (1987) Quantitative programming for selection decision. *Computers and*

Operations Research, 14(5): 395–407.

Zimmermann HJ (1978) Fuzzy programming and linear programming with several objective functions. *Fuzzy Sets and Systems, 1* : 45-55.

Zimmermann HJ and Pollatschek MA (1984) Fuzzy 0-1 linear programs, in: H.-J. Zimmermann, L.A. Zadeh and B.R.Gaines, Eds., *Fuzzy Sets and Decision Analysis*, North-Holland, New York, 133-145.

Zimmermann HJ (1985) *Fuzzy set theory and its applications*. Boston: Kluwer-Nijhoff.

Zimmermann HJ (1987) *Fuzzy Sets, Decision Making, and Expert Systems,* Kluwer Academic Publishers, Boston.

Zimmermann HJ (1991) *Fuzzy Set Theory and its Applications,* 2nd edn., Kluwer Academic Publishers, Boston.

Zanovello R and Budman H (1999) Model predictive control with soft constraints with application to lime kiln control. *Computers and Chemical Engineering*, *23*(6), 791-806.

Zhou YF, Li SJ, and Jin RC (2002) A new fuzzy neural network with fast learning algorithm and guaranteed stability for manufacturing process control. *Fuzzy Sets and Systems*, 132: 201-216.

APPENDIX 1

MATLAB Code for Hydraulic Reliability

- Random Number Generator
- Link MATLAB with EPANET
- Monte Carlo Simulation

```
function [x,t] = getwdsdata(wdsfile, code, id) %#ok<FNDEF>
% getwdsdata
%
% Get water distribution system data from an EPANET input file and run
% monte carlo tech.
% Initialise a few variables ...
wdsfile = 'wdsfile.inp';
errorcode = 0; %#ok<NASGU>

t= [];
code = ' ';  %#ok<NASGU>
L=[];

% Load the EPANET 2 dynamic link library ...
if ~libisloaded('epanet2')
    loadlibrary('epanet2', 'epanet2.h');
end

% Open the water distribution system ...
s = which(wdsfile);
if ~isempty(s)
    wdsfile = s;
end

[errorcode] = calllib('epanet2', 'ENopen', wdsfile, 'report', '');
if (errorcode)
     fprintf('Could not open network ''%s''.\nReturned empty array.\n',
wdsfile);
    return;
end

%read data from files
[T1,T2,T3,T4] = textread('tanklevel.txt','%q %q %f %f','headerlines',2);
[P1,P2,P3,P4] =
textread('piperoughness.txt','%q %q %f %f','headerlines',2);
[D1,D2,D3,D4] =
textread('jounctionbasedemand.txt','%q %q %f %f','headerlines',2);
[H1,H2] = textread('jounctionminhead.txt','%q %f','headerlines',2);


%count the number of tank, jounction and pipe
```

```
headcount=length(H1);
demandcount=length(D1);
tankcount=length(T1);
pipecount=length(P1);

%set zero metrix for x
x=zeros(1,headcount);

% Start Monte Carlo Simualtion
for m = 1:2000

    % Deal with the Tanks' data
    code = 'EN_TANKLEVEL';


    getindexfunc = ['ENget', 'node', 'index'];
    % Obtain correct epanet code for tanklevel
    epanetcode=8;

    setvaluefunc = ['ENset', 'node', 'value'];

    for n=1:tankcount

        %obtain random value
        if(strcmp(T2(n),'normal') )
        L(n)= random('normal',T3(n),T4(n));
        end

        if(strcmp(T2(n),'gamma') )
        L(n)= random('gam',T3(n),T4(n));
        end

        if(strcmp(T2(n),'binmial') )
        L(n)= random('bino',T3(n),T4(n));
        end

        if(strcmp(T2(n),'lognormal') )
        L(n)= random('logn',T3(n),T4(n));
        end

        if(strcmp(T2(n),'uniform') )
        L(n)= random('unif',T3(n),T4(n));
        end

        if(strcmp(T2(n),'poisson') )
        L(n)= random('poiss',T3(n),T4(n));
        end

       % Retrieve the indices for tanks...
        myvalue=0;
        [errorcode,T1{n}, myvalue] = calllib('epanet2', getindexfunc,
T1{n}, myvalue);
        if (errorcode)
            fprintf(['Problem retrieving index for ', 'Tank', ' ''',
```

```
T1{n}, '''.\n']);
            [errorcode] = calllib('epanet2', 'ENclose');
            unloadlibrary('epanet2');
            return;
        end
        Tankindex=double(myvalue);

        % Set Value to Tanklevels
        [errorcode] = calllib('epanet2', setvaluefunc, Tankindex,
epanetcode, L(n));
        if (errorcode)
            fprintf(['Problem set value for ', 'Tank', ' ''', T1{n},
''' (index).\n'])
            [errorcode] = calllib('epanet2', 'ENclose');
            unloadlibrary('epanet2');
            return;
        end
    end



     % Deal with the Pipes' data
    code = 'EN_ROUGHNESS';

    getindexfunc = ['ENget', 'link', 'index'];
    % Obtain correct epanet code for piperoughness
    epanetcode=2;
    % Set Value to Piperoughs
    setvaluefunc = ['ENset', 'link', 'value']; %#ok<NASGU>


    for n=1:pipecount

        %obtain random value
        if(strcmp(P2(n),'normal') )
        L(n)= random('normal',P3(n),P4(n));
        end

        if(strcmp(P2(n),'gamma') )
        L(n)= random('gam',P3(n),P4(n));
        end

        if(strcmp(P2(n),'binmial') )
        L(n)= random('bino',P3(n),P4(n));
        end

        if(strcmp(P2(n),'lognormal') )
        L(n)= random('logn',P3(n),P4(n));
        end

        if(strcmp(P2(n),'uniform') )
        L(n)= random('unif',P3(n),P4(n));
        end
```

```
        if(strcmp(P2(n),'poisson') )
        L(n)= random('poiss',P3(n),P4(n));
        end

      % Retrieve the indices for Pipes
       myvalue=0;
        [errorcode,P1{n}, myvalue] = calllib('epanet2', getindexfunc,
P1{n}, myvalue);
        if (errorcode)
            fprintf(['Problem retrieving index for ', 'link', ' ''',
P1{n}, '''.\n']);
            [errorcode] = calllib('epanet2', 'ENclose');
            unloadlibrary('epanet2');
            return;
        end
        Linkindex(n)=double(myvalue);

        % Set Value to Piperoughs
        [errorcode] = calllib('epanet2', setvaluefunc, Linkindex(n),
epanetcode, L(n));
        if (errorcode)
            fprintf(['Problem set value for ', 'Link', ' ''', P1{n},
''' (index).\n'])
            [errorcode] = calllib('epanet2', 'ENclose');
            unloadlibrary('epanet2');
            return;
        end
    end



 % Deal with the Nodes' data
    code = 'EN_BASEDEMAND';
    getindexfunc = ['ENget', 'node', 'index'];
    setvaluefunc = ['ENset', 'node', 'value'];
    % Obtain correct epanet code for nodedemand
    epanetcode=1;

    for n=1:demandcount

        %obtain random value
        if(strcmp(D2(n),'normal') )
        L(n)= random('normal',D3(n),D4(n));
        end

        if(strcmp(D2(n),'gamma') )
        L(n)= random('gam',D3(n),D4(n));
        end

        if(strcmp(D2(n),'binmial') )
        L(n)= random('bino',D3(n),D4(n));
        end

        if(strcmp(D2(n),'lognormal') )
        L(n)= random('logn',D3(n),D4(n));
```

```
        end

        if(strcmp(D2(n),'uniform') )
        L(n)= random('unif',D3(n),D4(n));
        end

        if(strcmp(D2(n),'poisson') )
        L(n)= random('poiss',D3(n),D4(n));
        end


        % Retrieve the indices for nodes..
         myvalue=0;
        [errorcode,D1{n}, myvalue] = calllib('epanet2', getindexfunc,
D1{n}, myvalue);
        if (errorcode)
            fprintf(['Problem retrieving index for ', 'Node', ' ''',
D1{n}, '''.\n']);
            [errorcode] = calllib('epanet2', 'ENclose');
            unloadlibrary('epanet2');
            return;
        end
        Nodeindex(n)=double(myvalue);

        % Set Value to nodedemand
        [errorcode] = calllib('epanet2', setvaluefunc, Nodeindex(n),
epanetcode, L(n));
        if (errorcode)
            fprintf(['Problem set value for ', 'Node', ' ''', D1{n},
''' (index).\n'])
            [errorcode] = calllib('epanet2', 'ENclose');
            unloadlibrary('epanet2');
            return;
        end
    end




     % Obtain correct epanet code for nodehead
     epanetcode=10;

    %  Run simulation ...
    nextfunc = 'ENnextH';
    initflag = 0;
    enflag = 'H';


    % Assign function calls ( Hydraulic) ...
    initfunc  = ['ENinit', enflag];
    openfunc  = ['ENopen', enflag];
    runfunc   = ['ENrun', enflag];
    closefunc = ['ENclose', enflag];
```

```
    % Open and initialise the Hydraulic solver ...
    [errorcode] = calllib('epanet2', openfunc);
    if (errorcode)
    fprintf('Could not open ENopenH.\n');
    return;
    end

    getvaluefunc = ['ENget', 'node', 'value'];

    [errorcode] = calllib('epanet2', initfunc, initflag);
    if (errorcode)
    fprintf('Could not open ENinitH.\n');
    return;
    end

    % Initialise some variables ...
    tval = 0; tstep = 1; value = 0.0; pt = 0;elevation_value=0;

    % Loop through simulation ...
    while tstep && ~errorcode
        [errorcode, tval] = calllib('epanet2', runfunc, tval);
        if (errorcode)
           fprintf('Could not run ENrunH.\n');
           return;
        end
        pt = pt + 1;

        t(pt)=double(tval)/3600; %#ok<AGROW>
        % Continue to the next time step ...
        [errorcode, tstep] = calllib('epanet2', nextfunc, tstep);
        if (errorcode)
           fprintf('Could not run ENnextH.\n');
           return;
        end
    end

    %obtain head and calculate reliabilty...
    for n = 1:headcount

        % Retrieve the indices for nodeheads..
         myvalue=0;
        [errorcode,H1{n}, myvalue] = calllib('epanet2', getindexfunc,
H1{n}, myvalue);
        if (errorcode)
            fprintf(['Problem retrieving index for ', 'Node', ' ''',
H1{n}, '''.\n']);
            [errorcode] = calllib('epanet2', 'ENclose');
            unloadlibrary('epanet2');
            return;
        end
        Nodeheadindex(n)=double(myvalue);
        %obtain nodeheadvalue
        [errorcode, value] = calllib('epanet2', getvaluefunc,
Nodeheadindex(n), epanetcode, value);
        if (errorcode)
```

```
            fprintf(['Problem retrieving value for ', 'nodehead', ' ''',
H1{n}, '''.\n']);
            return;
        end
        %obtain nodeelevation...
        [errorcode, elevation_value] = calllib('epanet2', getvaluefunc,
Nodeheadindex(n), 0, elevation_value);
        if (errorcode)
            fprintf(['Problem retrieving value for ', 'nodehead', ' ''',
H1{n}, '''.\n']);
            return;
        end

        if ((value-elevation_value)>=H2(n))
            x(n)=x(n)+1;
        end;
    end

    % Close the solver
    [errorcode] = calllib('epanet2', closefunc);
     if (errorcode)
           fprintf('Could not run ENcloseH.\n');
     return;
     end
end

for n = 1:headcount
    x(n)=x(n)/m;
end

% Close EPANET ...
[errorcode] = calllib('epanet2', 'ENclose');
if (errorcode)
    fprintf('EPANET error occurred. Code %g\n', num2str(errorcode));
end

% Convert to double precision ...
x = double(x);

if libisloaded('epanet2')
    unloadlibrary('epanet2');
end
```

APPENDIX 2

MATLAB Code for Repair Schedule

```
function[total_cost, breakrate,parallel] =
repair_optim(reliability,pipe_id,pipe_length,pipe_diameter,init_breakra
te)
%Find an optimal repair schedule for WDSs
     %Step 1.  calculate each pipeline's break rate break_rate(i, j) ;
                %and  compute each pipeline's Brkth and then obtain
their replace year break_year(j) .
                %where i represent time of year, and j is the pipe index.
     %Step 2. Set i=0;
     %Step 3. i= i+1;
     %Step 4. Run the hydraulic reliability model the calculate nodal
hydraulic reliability
              %hydra_relia(i, j)for all studying nodes in a WDS in the
ith year;
     %Step 5. Compare the predicted hydraulic reliability with the
minimum allowable
              %hydraulic reliability min_relia(i, j)at the ith year, to
find the pipes to be upgraded pipe_upgra(i, j);
     %Step 6. If the replace year break_year(j) of the upgraded pipe is
equal to or more than the
              %planning term PN. Then, no paralleling considered;
     %Step 7. Run Optimization Code (GA) to find optimal diameter pipe
pipe_upgra(i, j, m)(where m is
              %the index of pipe diameter, both replacement and
paralleling use this diameter
              %index), with the objective of minimizing total cost, and
subject to
              %the constraint that the hydra_relia(i, j) should be
greater than the maximum of min_relia(i, j)
              %during the whole planning period PN. The computation of
hydra_relia(i, j), of course, need
              %run hydraulic reliability prediction model;
     %Step 8. If i < PN, Then go to Step 3;
     %Step 9. Calculate the total cost and record the optimal
rehabilitation and upgrading schedule.

%read pipe data from files
[pipe_id,pipe_length,pipe_diameter,init_breakrate,
growthrate_A,new_breakrate] =
textread('pipe_information.txt','%q %f %f %f %f %f','headerlines',2);
[diameter_type,repair_cost,replacement_cost,paralleling_cost,discount_r
ate,inflation_rate] =
textread('pipe_cost.txt','%q %f %f %f %f %f','headerlines',2);

% Initialise a few variables ...
period=15;
pipenumber=length(pipe_id);
replacepoint=zeros(pipenumber,1);
```

```
breakrate=zeros(pipenumber,period);
replaceparam=zeros(pipenumber,period);

%count the number of pipe
 for n=1:pipenumber

        %obtain Threshold break rate value
        if(pipe_diameter(n)==6 )

Brk(n)=log(1+discount_rate(1))/log(repair_cost(1)*(1+inflation_rate(1))
/(1000*replacement_cost(1))+1+inflation_rate(1));
        end

        if(pipe_diameter(n)==8 )

Brk(n)=log(1+discount_rate(2))/log(repair_cost(2)*(1+inflation_rate(2))
/(1000*replacement_cost(2))+1+inflation_rate(2));
        end

        if(pipe_diameter(n)==10 )

Brk(n)=log(1+discount_rate(3))/log(repair_cost(3)*(1+inflation_rate(3))
/(1000*replacement_cost(3))+1+inflation_rate(3));
        end

        if(pipe_diameter(n)==12 )

Brk(n)=log(1+discount_rate(4))/log(repair_cost(4)*(1+inflation_rate(4))
/(1000*replacement_cost(4))+1+inflation_rate(4));
        end

        %obtain break rate for each pipe

        for m=1:period
            breakrate(n,m)=init_breakrate(n)*exp(growthrate_A(n)*m);
            if (breakrate(n,m)<=Brk(n))

breakrate(n,m)=(pipe_length(n)/1000)*init_breakrate(n)*exp(growthrate_A
(n)*m);
            end

            if (replacepoint(n)~=0)

breakrate(n,m)=(pipe_length(n)/1000)*new_breakrate(n)*exp(growthrate_A(
n)*(m-replacepoint(n)));
            end

            if (replacepoint(n)==0)&&(breakrate(n,m)>Brk(n))
                breakrate(n,m)=0;
                replaceparam(n,m)=1;
                replacepoint(n)=m;
            end
        end

 end
```

```
 breakrate=round(breakrate);



 % Get reliabilites from an EPANET input file and run
% monte carlo tech.

% Initialise a few variables ...
wdsfile = 'wdsfile.inp';
errorcode = 0; %#ok<NASGU>

t= [];
code = ' ';  %#ok<NASGU>
L=[];

% Load the EPANET 2 dynamic link library ...
if ~libisloaded('epanet2')
    loadlibrary('epanet2', 'epanet2.h');
end

% Open the water distribution system ...
s = which(wdsfile);
if ~isempty(s)
    wdsfile = s;
end

[errorcode] = calllib('epanet2', 'ENopen', wdsfile, 'report', '');
if (errorcode)
     fprintf('Could not open network ''%s''.\nReturned empty array.\n',
wdsfile);
    return;
end


%read data from files
[T1,T2,T3,T4] = textread('tanklevel.txt','%q %q %f %f','headerlines',2);
[P1,P2,P3,P4] =
textread('piperoughness.txt','%q %q %f %f','headerlines',2);
[D1,D2,D3,D4,D5] =
textread('jounctionbasedemand.txt','%q %q %f %f %f','headerlines',2);
[H1,H2,H3] =
textread('jounctionminhead.txt','%q %f %f','headerlines',2);

%count the number of tank, jounction and pipe
headcount=length(H1);
demandcount=length(D1);
tankcount=length(T1);
pipecount=length(P1);

%set zero metrix for reliability
reliability=zeros(headcount,period);
nodetopipe=ones(pipenumber,period);
%calculate reliability for whole period (15yrs in this case)
```

```
for i=1:period
    for n=1:demandcount
        D3(n)=D3(n)*(1+D5(n))^(i-1);
    end
    for n=1:headcount
        H2(n)=H2(n)*(1+H3(n))^(i-1);
    end

    % Start Monte Carlo Simualtion
    for m = 1:500

        % Deal with the Tanks' data
        code = 'EN_TANKLEVEL';


        getindexfunc = ['ENget', 'node', 'index'];
        % Obtain correct epanet code for tanklevel
        epanetcode=8;

        setvaluefunc = ['ENset', 'node', 'value'];

        for n=1:tankcount

             %obtain random value
             if(strcmp(T2(n),'normal') )
             L(n)= random('normal',T3(n),T4(n));
             end

             if(strcmp(T2(n),'gamma') )
             L(n)= random('gam',T3(n),T4(n));
             end

             if(strcmp(T2(n),'binmial') )
             L(n)= random('bino',T3(n),T4(n));
             end

            if(strcmp(T2(n),'lognormal') )
            L(n)= random('logn',T3(n),T4(n));
            end

            if(strcmp(T2(n),'uniform') )
            L(n)= random('unif',T3(n),T4(n));
            end

            if(strcmp(T2(n),'poisson') )
            L(n)= random('poiss',T3(n),T4(n));
            end

            % Retrieve the indices for tanks...
             myvalue=0;
             [errorcode,T1{n}, myvalue] = calllib('epanet2',
getindexfunc, T1{n}, myvalue);
             if (errorcode)
                 fprintf(['Problem retrieving index for ', 'Tank', '
```

```
''', T1{n}, '''.\n']);
                [errorcode] = calllib('epanet2', 'ENclose');
                unloadlibrary('epanet2');
                return;
            end
            Tankindex=double(myvalue);

            % Set Value to Tanklevels
             [errorcode] = calllib('epanet2', setvaluefunc, Tankindex,
epanetcode, L(n));
             if (errorcode)
                 fprintf(['Problem set value for ', 'Tank', ' ''',
T1{n}, ''' (index).\n'])
                 [errorcode] = calllib('epanet2', 'ENclose');
                 unloadlibrary('epanet2');
                 return;
             end
        end


          % Deal with the Pipes' data
          code = 'EN_ROUGHNESS';

         getindexfunc = ['ENget', 'link', 'index'];
         % Obtain correct epanet code for piperoughness
         epanetcode=2;
         % Set Value to Piperoughs
         setvaluefunc = ['ENset', 'link', 'value']; %#ok<NASGU>


        for n=1:pipecount

            %obtain random value
            if(strcmp(P2(n),'normal') )
            L(n)= random('normal',P3(n),P4(n));
            end

            if(strcmp(P2(n),'gamma') )
            L(n)= random('gam',P3(n),P4(n));
            end

            if(strcmp(P2(n),'binmial') )
            L(n)= random('bino',P3(n),P4(n));
            end

            if(strcmp(P2(n),'lognormal') )
            L(n)= random('logn',P3(n),P4(n));
            end

            if(strcmp(P2(n),'uniform') )
            L(n)= random('unif',P3(n),P4(n));
            end

            if(strcmp(P2(n),'poisson') )
```

```
                L(n)= random('poiss',P3(n),P4(n));
                end

              % Retrieve the indices for Pipes
               myvalue=0;
                [errorcode,P1{n}, myvalue] = calllib('epanet2',
getindexfunc, P1{n}, myvalue);
                if (errorcode)
                    fprintf(['Problem retrieving index for ', 'link', '
''', P1{n}, '''.\n']);
                    [errorcode] = calllib('epanet2', 'ENclose');
                    unloadlibrary('epanet2');
                    return;
                end
                Linkindex(n)=double(myvalue);

                % Set Value to Piperoughs
                [errorcode] = calllib('epanet2', setvaluefunc,
Linkindex(n), epanetcode, L(n));
                if (errorcode)
                    fprintf(['Problem set value for ', 'Link', ' ''',
P1{n}, ''' (index).\n'])
                    [errorcode] = calllib('epanet2', 'ENclose');
                    unloadlibrary('epanet2');
                    return;
                end
          end



        % Deal with the Nodes' data
           code = 'EN_BASEDEMAND';
           getindexfunc = ['ENget', 'node', 'index'];
           setvaluefunc = ['ENset', 'node', 'value'];
          % Obtain correct epanet code for nodedemand
          epanetcode=1;

          for n=1:demandcount

              %obtain random value
              if(strcmp(D2(n),'normal') )
              L(n)= random('normal',D3(n),D4(n));
              end

               if(strcmp(D2(n),'gamma') )
               L(n)= random('gam',D3(n),D4(n));
               end

               if(strcmp(D2(n),'binmial') )
               L(n)= random('bino',D3(n),D4(n));
               end

              if(strcmp(D2(n),'lognormal') )
              L(n)= random('logn',D3(n),D4(n));
              end
```

```
            if(strcmp(D2(n),'uniform') )
            L(n)= random('unif',D3(n),D4(n));
            end

            if(strcmp(D2(n),'poisson') )
            L(n)= random('poiss',D3(n),D4(n));
            end


             % Retrieve the indices for nodes..
              myvalue=0;
             [errorcode,D1{n}, myvalue] = calllib('epanet2',
getindexfunc, D1{n}, myvalue);
             if (errorcode)
                 fprintf(['Problem retrieving index for ', 'Node', '
''', D1{n}, '''.\n']);
                 [errorcode] = calllib('epanet2', 'ENclose');
                 unloadlibrary('epanet2');
                 return;
             end
             Nodeindex(n)=double(myvalue);

             % Set Value to nodedemand
             [errorcode] = calllib('epanet2', setvaluefunc,
Nodeindex(n), epanetcode, L(n));
             if (errorcode)
                 fprintf(['Problem set value for ', 'Node', ' ''',
D1{n}, ''' (index).\n'])
                 [errorcode] = calllib('epanet2', 'ENclose');
                 unloadlibrary('epanet2');
                 return;
             end
         end




          % Obtain correct epanet code for nodehead
          epanetcode=10;

         %  Run simulation ...
         nextfunc = 'ENnextH';
         initflag = 0;
         enflag = 'H';


        % Assign function calls ( Hydraulic) ...
         initfunc  = ['ENinit', enflag];
         openfunc  = ['ENopen', enflag];
         runfunc   = ['ENrun', enflag];
         closefunc = ['ENclose', enflag];

        % Open and initialise the Hydraulic solver ...
```

```
            [errorcode] = calllib('epanet2', openfunc);
            if (errorcode)
               fprintf('Could not open ENopenH.\n');
                return;
            end

            getvaluefunc = ['ENget', 'node', 'value'];

            [errorcode] = calllib('epanet2', initfunc, initflag);
            if (errorcode)
                fprintf('Could not open ENinitH.\n');
                return;
            end

            % Initialise some variables ...
            tval = 0; tstep = 1; value = 0.0; pt = 0;elevation_value=0;

            % Loop through simulation ...
            while tstep && ~errorcode
                [errorcode, tval] = calllib('epanet2', runfunc, tval);
                if (errorcode)
                   fprintf('Could not run ENrunH.\n');
                   return;
                end
                pt = pt + 1;

                t(pt)=double(tval)/3600; %#ok<AGROW>
                % Continue to the next time step ...
                [errorcode, tstep] = calllib('epanet2', nextfunc, tstep);
                if (errorcode)
                   fprintf('Could not run ENnextH.\n');
                   return;
                end
            end

            %obtain head and calculate reliabilty...
            for n = 1:headcount

                % Retrieve the indices for nodeheads..
                 myvalue=0;
                [errorcode,H1{n}, myvalue] = calllib('epanet2',
getindexfunc, H1{n}, myvalue);
                if (errorcode)
                    fprintf(['Problem retrieving index for ', 'Node', '
''', H1{n}, '''.\n']);
                    [errorcode] = calllib('epanet2', 'ENclose');
                    unloadlibrary('epanet2');
                    return;
                end
                Nodeheadindex(n)=double(myvalue);
                %obtain nodeheadvalue
                [errorcode, value] = calllib('epanet2', getvaluefunc,
Nodeheadindex(n), epanetcode, value);
                if (errorcode)
                    fprintf(['Problem retrieving value for ', 'nodehead',
```

```
' ''', H1{n}, '''.\n']);
                    return;
                end
                %obtain nodeelevation...
                [errorcode, elevation_value] = calllib('epanet2',
getvaluefunc, Nodeheadindex(n), 0, elevation_value);
                if (errorcode)
                    fprintf(['Problem retrieving value for ', 'nodehead',
' ''', H1{n}, '''.\n']);
                   return;
                end

                if ((value-elevation_value)>=H2(n))
                    reliability(n,i)=reliability(n,i)+1;
                end;
            end

            % Close the solver
            [errorcode] = calllib('epanet2', closefunc);
             if (errorcode)
                  fprintf('Could not run ENcloseH.\n');
                  return;
             end

    end

    for n = 1:headcount
        reliability(n,i)=reliability(n,i)/m;
    end

end

% Close EPANET ...
[errorcode] = calllib('epanet2', 'ENclose');
if (errorcode)
    fprintf('EPANET error occurred. Code %g\n', num2str(errorcode));
end

if libisloaded('epanet2')
    unloadlibrary('epanet2');
end
% Convert to double precision ...
reliability=double(reliability);

nodetopipe(2,:)=reliability(2,:);
    nodetopipe(4,:)=reliability(3,:);
    nodetopipe(6,:)=reliability(4,:);
    nodetopipe(9,:)=reliability(5,:);
    nodetopipe(11,:)=reliability(6,:);
    nodetopipe(13,:)=reliability(7,:);
    nodetopipe(1,:)=reliability(8,:);
    nodetopipe(14,:)=reliability(9,:);
    nodetopipe(16,:)=reliability(10,:);

%count hydraulic upgrade of pipe
```

```
updatepoint=zeros(pipenumber,1);
updateparam=zeros(pipenumber,period);

 for n=1:pipenumber

        for m=1:period

            if (updatepoint(n)~=0)
                updateparam(n,m)=0;
                breakrate(n,m)=0;
            end

            if (updatepoint(n)==0)&&(nodetopipe(n,m)<0.99)
                breakrate(n,m)=0;
                updateparam(n,m)=1;
                updatepoint(n)=m;
            end
        end

 end

 %count combo upgrade of pipe
combopoint=zeros(pipenumber,1);
for n=1:pipenumber
    for m=1:period
        if (updatepoint(n)>=replacepoint(n))&&(replacepoint(n)>0)
            updateparam(n,m)=0;
            combopoint(n)=replacepoint(n);
        end
        if (replacepoint(n)>updatepoint(n))&&(updatepoint(n)>0)
            replaceparam(n,m)=0;
            combopoint(n)=updatepoint(n);
        end
        if (updatepoint(n)>0)&&(replacepoint(n)==0)
            combopoint(n)=updatepoint(n);
        end
        if (updatepoint(n)==0)&&(replacepoint(n)==0)
            combopoint(n)=0;
        end
        if (updatepoint(n)==0)&&(replacepoint(n)>0)
            combopoint(n)=replacepoint(n);
        end
    end
end

 comboparam=zeros(pipenumber,period);
 comboparam=updateparam+replaceparam;

 %count global min cost of repair
 global_min = 0;
 total_cost = zeros(1,period);
for m=1:period
    for n=1:pipenumber
```

```
total_cost(1,m)=total_cost(1,m)+breakrate(n,m)*(repair_cost(2)*(1+infla
tion_rate(2))^m)+comboparam(n,m)*pipe_length(n)*replacement_cost(2)*(1+
inflation_rate(2))^m;
    end
    global_min=global_min+total_cost(1,m)/((1+discount_rate(2))^m);
end
```